CHALMERS

Internal Report 01/8

On Two-equation Eddy-Viscosity Models

JONAS BREDBERG

Department of Thermo and Fluid Dynamics
CHALMERS UNIVERSITY OF TECHNOLOGY
Göteborg, Sweden, 2001

On Two-equation Eddy-Viscosity Models

JONAS BREDBERG
Department of Thermo and Fluid Dynamics
Chalmers University of Technology

ABSTRACT

This report makes a thoroughly analysis of the two-equation eddy-viscosity models (EVMs). A short presentation of other types of CFD-models is also included. The fundamentals for the eddy-viscosity models are discussed, including the Boussinesq hypothesis, the derivation of the 'law-of-the-wall' and references to simple algebraic EVMs, such as Prandtls mixing-length model. Both the exact k- and ε-equations are discerned using DNS-data (Direct Numerical Simulation) for fully developed channel flow. In connection to this a discussion of the benefits and disadvantegous of the various two-equation models ($k-\varepsilon$, $k-\omega$, and $k-\tau$) is included.
Through-out the report special attention is made to the close connection between the various secondary equations. It is demonstrated that through some basic transformation rules, it is possible to re-cast eg. a $k-\varepsilon$ into a $k-\omega$ model. The additive terms from such a re-formulation is discussed at length and the possible connections to both the pressure-diffusion process and the Yap-correction are mentioned.
The report distinguish between EVMs that are developed with the aid of DNS-data or TSDIA (Two-scale Direct Integration Approximation) and those which are not. Within each group, the turbulence models are compared term by term. The chosen coefficients, damping functions, boundary condition etc. are discussed. The additive terms for the DNS tuned models are compared and criticized.
In a lengthy summary some thoughts and advices are given for the development of a two-equation. Apart from a discussion on the type of EVM attention is given to the turbulence model coefficients, Schmidt numbers and the possibilty to include cross-diffusion terms.
In the appendices a number of turbulence models are tabulated and compared with both DNS-data and experimental data for fully devloped channel flow, a backward-facing step flow and a rib-roughened channel flow. Particularly interest is given to how newer (DNS-tuned) turbulence models compare to the older, non-optimized EVMs.

Keywords: turbulence model, eddy-viscosity model, $k-\varepsilon$, $k-\omega$, $k-\tau$, cross-diffusion, TSDIA, DNS

Contents

Nomenclature

Latin Symbols

B	Turbulence model constant	$[-]$
C	Various constants	$[-]$
C_l	Length-scale constant	$[-]$
C_μ	Turbulence model coefficient	$[-]$
C_f	Skin friction coefficient, $2\tau_w/\rho U_b^2$	$[-]$
D	Hydrualic diameter	$[m]$
D	Diffusion term	$[*]$
$D()/Dt$	Material derivate, $\partial\rho\phi/\partial t + U_j\partial\rho\phi/\partial x_j$	$[s^{-1}]$
E	Turbulence model term	$[*]$
e	Rib-size	$[m]$
f	Damping function	$[-]$
H	Channel height	$[m]$
h	Step height	$[m]$
i, j	Tensor indices: streamwise: 1,U,u wall normal: 2,V,v spanwise: 3,W,w	$[-]$
k	Turbulent kinetic energy	$[m^2/s^2]$
L	Integral length scale	$[m]$
l	Length scale	$[m]$
Nu	Nusselt number	$[-]$
P	Static pressure	$[N/m^2]$
P	Rib-pitch	$[m]$
p	Fluctuating pressure	$[N/m^2]$
P_k	Turbulent production, $\overline{u_i'u_j'}\partial U_i/\partial x_j$	$[m^2/s^3]$
Pr	Prandtl number	$[-]$
Re	Reynolds number, UH/ν	$[-]$
R_t	Turbulent Reynolds number, ν_t/ν, $k/(\omega\nu)$, $k^2/(\varepsilon\nu)$	$[-]$
Re_τ	U_τ based Reynolds number, $yU_\tau\nu$	$[-]$
S	Turbulence model source term	[*]
S_{ij}	Strain-rate tensor, $1/2(\partial U_i/\partial x_j + \partial U_j/\partial x_i)$	$[s^{-1}]$
T	Turbulent transport term	[*]
T_t	Turbulent time scale	[s]
U_i	Velocity	$[m/s]$
u_i'	Fluctuating velocity	$[m/s]$
$\overline{u_i'u_j'}$	Reynolds stresses	$[m^2/s^2]$
U_τ	Friction velocity, $\sqrt{\tau_w/\rho}$	$[m/s]$
U_τ^*	Normalized value: $1000 \times U_\tau/U_b$	$[-]$
x	Streamwise coordinate	$[m]$
y	Wall normal coordinate	$[m]$
z	Spanwise coordinate	$[m]$

Greek Symbols

α	Turbulence model coefficients	$[-]$
β	Turbulence model coefficients	$[-]$
δ	Boundary layer thickness	$[m]$
ε	Dissipation rate	$[m^2/s^3]$
$\tilde{\varepsilon}$	Reduced dissipation rate $= \varepsilon - \hat{\varepsilon}$	$[m^2/s^3]$
$\hat{\varepsilon}$	Wall dissipation rate	$[m^2/s^3]$
η	Kolmogorov length scale	$[m]$
κ	Van Karman constant	$[-]$
ν	Kinematic viscosity	$[m^2/s]$
ρ	Density	$[kg/m^3]$
Π	Pressure-diffusion term	$[*]$
Φ	Destruction term	$[*]$
ϕ	Free variable	$[*]$
Ω_{ij}	Rotation tensor	$[s^{-1}]$
ω	Specific dissipation rate	$[s^{-1}]$
σ	Turbulent Schmidt number	$[-]$
τ	Turbulent time scale	$[s]$
τ	Shear stress	$[N/m^2]$
τ_w	Wall shear, ρU_τ^2	$[N/m^2]$

Superscripts

ν	Viscous value
ϕ^+	Normalized value using U_τ:
U^+	$= U/U_\tau$
y^+	$= yU_\tau/\nu$
k^+	$= k/U_\tau^2$
ε^+	$= \varepsilon\nu/U_\tau^4$
$*$	Normalized value
$*$	Alternative value

Subscripts

b	Bulk value
D	Hydraulic diameter
h	Step heigth
K	Quantity based on Kolmogorov scales
k	Quantity in k-equation
r	Re-attachment poin
t	Turbulent quantity
w	Wall value
y	Normalized using wall distance
ε	Quantity in ε-equation
λ	Quantity based on Taylor micro-scale
ω	Quantity in ω-equation
ϕ	Free variable
τ	Quantity based on the friction velocity
∞	Freestream value

1 Introduction

In both engineering and academia the most frequent employed turbulence models are the Eddy-Viscosity-Models (EVMs). Although the rapidly increasing computer power in the last decades, the simplistic EVMs still dominate the CFD community.

The landmark model is the $k-\varepsilon$ model of Jones and Launder [19] which appeared in 1972. This model has been followed by numerous EVMs, most of them based on the k-equation and an additional transport equation, such as the $k-\omega$ [52], the $k-\tau$ [47] and the $k-\nu_t$ [37] models. With the emerging Direct Numerical Simulations (DNSs), it has now been possible to improve the EVMs, especially their near-wall accuracy, to a level not achievable using only experimental data. The first accurate DNS was made by Kim *et al.* [20] albeit at a low Reynolds number $Re_\tau = 180$ and for a simple fully developed channel flow testcase. Today however, DNS's are made at both interesting high Reynolds numbers, and of more complex flows, enabling accurate and advanced EVMs to appear.

This paper will try to explain these newly developed EVMs which are based on DNS-data. A number of turbulence models are compared with both DNS-data and experimental data for different flows. Particularly interesting is how these newer models compare to the older, non-DNS-tuned EVMs. The majorities of the different ideas when modifying/tuning turbulence models, such as damping functions, boundary conditions, etc. are included. A special section deals with the difference between the secondary transported quantities $(\varepsilon, \omega, \tau)$. Although there is neither any hope nor intention to including all two-equation EVMs, quite a number of them are tabulated and referenced.

	ES	Time	3D	Aniso	Trans
DNS	Y	Y	Y	Y	Y
LES	Y*	Y	Y	Y	Y
RANS-RSM	N	N	N	Y	Y
RANS-EVM	N	N	N	N	Y
RANS-Algebraic	N	N	N	N	N

Table 1: Turbulence models and physics. ES: The ability to predict the Energy-Spectrum, Time: whether or not the computation is time accurate, 3D: if a 3D solution is required, Aniso: if the model predicts anisotropic Reynolds stresses, Trans: if turbulence is a transported or local quantity.

2 CFD Models for Turbulence

An important question, however less appropriate in this paper, is: whether or not a turbulence **model** should be used at all? With the progress of DNS there is no need of any modelling of the turbulence field or is it?

The question is answered through the study of the different approaches used in numerical simulations for turbulent flows, via Computation Fluid Dynamics (CFD) codes. Turbulence models could be conceptionally distinguished from physical accuracy, or computational resources point of view. However irrespectively of the basis for the evaluation, DNSs are located on the higher end of the spectrum. DNSs don't include any modelling at all, apart from numerical approximation and grid resolution, and hence are treated as accurate, or even more accurate than experiments. They may also be referred to as numerical experiments made in virtual windtunnels, ie. computers. On the opposite end are the algebraic EVM models, which compute the turbulent viscosity (eddy viscosity) using some algebraic relation[1]

Table 1 lists some of the modelling approaches to turbulence ordered by physical accuracy.

Substituting physical accuracy with computational demands, the same order is repeated, with DNS consuming most CPU-time, and algebraic models the least. Below are the different approaches briefly discussed.

2.1 DNS

The main reason why DNS is not used more frequently when computing turbulent flows is due to the fact that DNS is a VERY resource demanding computation:

- DNS is a time accurate simulation.
- DNS's need to solve the full 3D problem, becuase turbulence is always 3D.
- All length scales are resolved with a DNS.

If the length scale ratio is defined as L/η_K, where L is the integral length scale, and η is the Kolmogorov length scale, then using definitions it is easy to show that:

$$\frac{L}{\eta} \sim R_t^{3/4} \tag{1}$$

Assuming that $(L/\eta)^3$ is proportional to the number of grid points, the computational mesh increases as: $R_t^{9/4}$. Additionally the timestep decreases with increasing Reynolds number and thus the computational time increases rapidly with Reynolds number as seen in Leschziner [28]:

Re	6 600	20 000	100 000	10^6
N	2×10^6	40×10^6	3×10^9	15×10^{12}
Time	37h	740h	6.5y	3000y

[1] Here it is inferred that an algebraic relation, contrary to a differential relation can be explicitly solved, without the need for an iterative solution. It should be noted that real world differential equations rarely have an analytic solution.

where N is the number of grid-points, and time is the amount of time spent on a 150MFlops machine.

Evidently from the this table DNS will not be of engineering practise in the foreseeable future. The usefulness of DNSs in respect to research on turbulence, and as an aid when developing turbulence models, should however be recognized.

2.2 Large-Eddy-Simulation (LES)

The benefit of LES, and also its drawback, is the modelling of the sub-grid scales. The cut-off in wave-number space, enables higher Reynolds number flows to be simulated, however at the expenses of accuracy, especially in the near-wall regions. The fundamental principal behind LES is sound, because small scale turbulence is isotropic, and thus a simple model could be substitutes for the full resolution of a DNS in this region. For bluff-body flows this approximation is good as these flows are goven by large scale turbulent structures. In wall-bounded flows, simulations have however shown that the accuracy diminish if the cut-off wave-number is not positioned in the viscous sub-layer. Thus the requirements for LES is similar to those of DNSs which need to resolve all length scale down to the Kolmogorov wave-number.

2.3 Reynolds-Averaged-Navier-Stokes (RANS)

With a RANS approach the computer demands decrease substantially, however at the expense of excluding the multitude of length scales involved in turbulence. Whatever the complexity of a RANS-model, it could only compute a single point in the wave-number - energy spectrum, and thus it is questionable that such a model could be of much interest. Surprisingly RANS-models still perform reasonable in many flows – even though its non-physical foundations. Consequently these models are used extensively in CFD programs. RANS-models can be divided into two major categories, the EVMs and the Reynolds Stress Models (RSM).

2.3.1 Eddy-Viscosity Models

Two-equation relations: The eddy-viscosity models (EVMs) include the commonly used and well-known two-equation models, such as the $k-\varepsilon$ model. The concept behind the eddy-viscosity models are that the unknown Reynolds stresses, a consequence from the averaging-procedure, are modelled using flow parameters (S_{ij}, Ω_{ij}) and an eddy-viscosity. EVMs are sub-divided dependent on the way the eddy-viscosity is modelled. Obviously the two-equation models use two equations to describe the eddy-viscosity, while the algebraic or zero-equation models use, normally, a geometrical relation to compute the eddy-viscosity.

Non-linear relations: Based on the popularity of the two-equation models, several different extensions have been proposed, which attempts to improve upon the deficiencies of these models. The non-linear EVMs extend the description of the eddy-viscosity, with one or more terms that involve higher order flow parameters. Non-linear EVMs can, as opposed to the standard EVMs, predict anisotropicy, which is of importance for eg. rotating flows. There also exists three- and four-equations models, which use the two-equation model concept as a basis. The latter class includes models such as the $k-\varepsilon-v^2-f$ model of Durbin [13] and the $k-\varepsilon-A_2$ model of Suga *et al.* [48].

2.3.2 Reynolds-Stress-Models

Differential Models: The DSM (Differential-Stress-Models), RSTM (Reynolds-Transport-Stress-Models), or simply RSM solve one equation for each Reynolds stress and hence don't need any modelling of the turbulence to the first order. These model are therefore referred to as second-moment closures, since they only model terms in the transport equations for the Reynolds stress (third or higher moments). RSMs are numerically more demanding, and generally more difficult to converge, compared to EVMs.

Algebraic Models: The ARSMs (Algebraic-Reynolds-Stress-Models) or ASMs (Algebraic-Stress-Models) simplify the description of the Reynolds stress transport equations, so that they can be reduced to an algebraic relation. These relations are then solved iteratively, due to its implicit construction. ARSMs are even more numerically unstable then the RSM and hence are rarely used.

Explicit Algebraic Models: In the EARSMs (Explicit-Algebraic-Reynolds-Stress-Models) or EASMs (Explicit-Algebraic-Stress-Models) the Reynolds stresses are described in an explicit formulation, and are thus more easily solved. Several different approaches have been postulated which involve varies approximations on the way to the explicit formulation of the Reynolds stress, though they are essential similar to the non-linear EVMs, although with more sound theoretical foundations.

3 Eddy-Viscosity Models (EVMs)

3.1 Boussinesq Hypothesis

The eddy-viscosity concept is based on similarity reasoning, with turbulence being a physical concept connected to the viscosity. In the Navier-Stokes equation the viscous term is:

$$D_v = \frac{\partial}{\partial x_j}\left[\nu\left(\frac{\partial U_i}{\partial x_j} + \frac{\partial U_j}{\partial x_i}\right)\right] \tag{2}$$

It can be argued that similarly to viscosity, turbulence affects the dissipation, diffusion and mixing processes. Thus it is reasonable to model the Reynolds stresses in a fashion closely related to the viscous term. The Reynolds stress term produced by the Reynolds-averaging is:

$$D_R = \frac{\partial R_{ij}}{\partial x_j} = \frac{\partial}{\partial x_j}\left(-\overline{u_i' u_j'}\right) \tag{3}$$

A turbulent flow will, compared to a laminar flow, enhance the above properties, and thus a model for the Reynolds stress could be:

$$-\overline{u_i' u_j'} = \alpha_{ijkl}(x,y,z,t)\left(\frac{\partial U_k}{\partial x_l} + \frac{\partial U_l}{\partial x_k}\right) \tag{4}$$

where α_{ijkl}, is a fourth rank tensor that could have both spatial and temporal variations, as well as directional properties (anisotropic). In the EVM concept this coefficient looses the directional properties, and hence turbulence becomes isotropic, the spatial variation is modeled using some algebraic relation, while the temporal variation is in most cases dropped. Thus the eddy-viscosity, ν_t, using the EVM concept is incorporated in the RANS equation as:

$$-\overline{u_i' u_j'} = \nu_t(x,y,z)\left(\frac{\partial U_i}{\partial x_j} + \frac{\partial U_j}{\partial x_i}\right) \tag{5}$$

This method was first postulated by Boussinesq [4] and consequently denoted the Boussinesq hypothesis.

3.2 The Mixing-length Model and the Logarithmic Velocity Law

If one accepts the Boussinesq hypothesis, then it depends on the description of the eddy-viscosity, how the turbulence model will perform. Naturally the eddy-viscosity should depend on turbulence quantities somehow. The turbulence modelling community still debates regarding which parameters, are the most appropriate. By noting that the eddy-viscosity has the dimension of $[m^2/s]$, the most obvious choice is to model the eddy-viscosity using a velocity scale, and a length scale, as:

$$\nu_t = u \cdot l \tag{6}$$

3.2.1 Prandtl's mixing-length model

One of the first turbulence model to appear, the mixing-length model by Prandtl [39], used the turbulent mixing length scale, l_{mix}, as the length scale. The velocity scale is computed using the mixing length and the velocity gradient as:

$$u \sim l_{mix}\frac{dU}{dy} \tag{7}$$

The mixing-length model thus becomes:

$$\nu_t \sim l_{mix}^2\frac{dU}{dy} \qquad \text{Mixing-length model}$$

with the Reynolds stresses given by the Boussinesq hypothesis, Eq. 5. The mixing-length is closely connected to the idea of a turbulent eddy or a vortex. Such an eddy would be restricted by the presence of a wall, and hence the length scale should be damped close to a wall. The idea by Prandtl that the turbulent length scale varies linearly with the distance to the wall may be used as an initial condition for the turbulent mixing length scale:

$$l_{mix} = \kappa y \qquad \text{Prandtl}$$

The proportionality factor, κ (the van Karman constant) is determined through comparison with experiment, with $\kappa = 0.41$ and y is the wall normal distance.

The mixing-length model makes the eddy-viscosity local, in the meaning that the turbulence is only directly affected by the surrounding flow, through the local value of dU/dy.

The accuracy of this model is only reasonable for simple flows, and only in the logarithmic region, see Fig. 1.

3.2.2 Modified mixing-length models

Attempts to extend the validity of this model have been made several times, where the most notable are the damping close to the wall by van Driest [50], the cut-off by Escudier [14], and the freestream modification by Klebanoff [21]:

$$l = l_{mix}(1 - \exp(-y^+/26)) \qquad \text{van Driest}$$

$$l = \min(l_{mix}, 0.09\delta) \qquad \text{Escudier}$$

$$l = \frac{l_{mix}}{\sqrt{1 + 5.5(y/\delta)^6}} \qquad \text{Klebanoff}$$

The van Driest modification is an empirical damping function that fits experimental data, and also changes the near-wall asymptotic behaviour of ν_t, from y^2 to y^4. Although neither of them are correct (DNS-data gives $\nu_t \sim y^3$), the van Driest damping generally improves the predictions. It has, since its first appearance, repeatedly been used in turbulence models to introduce viscous effects in the near-wall region.

The cut-off to the turbulent length scale is based on similarity to the defect layer modification by Clauser [10]. Escudier however found that for boundary-layer flows a different and lower coefficient, as given above, was more appropriate than the one used for wake flows.

The Klebanoff modification originates from the experimental studies of intermittency, where it was found that the flow approaching the freestream (from within the boundary layer) is not always turbulent, but rather

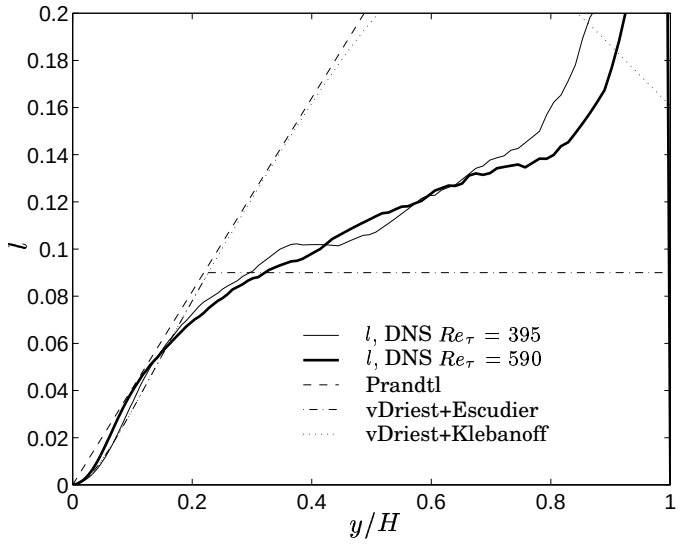

Figure 1: Turbulent length-scale in fully developed channel flow. DNS-data, Kim *et al.* [33], $Re_\tau = 395$ and $Re_\tau = 590$, and mixing-length models.

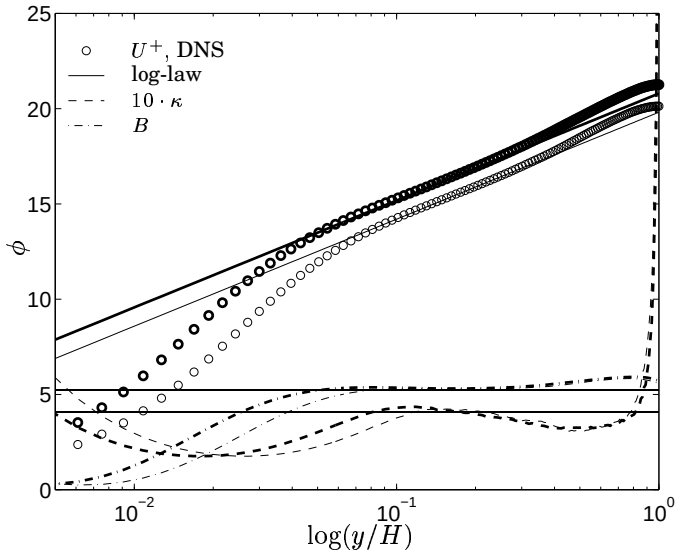

Figure 2: Log-law. DNS-data, Kim *et al.* [33], $Re_\tau = 395$ (thin lines) and $Re_\tau = 590$ (thick lines)

changing from laminar to turbulent intermittently. Klebanoff introduced a factor, F_{kleb}, which reduced the eddy-viscosity to model this effect. Here however for clarity, the modification is applied to the turbulent length scale, instead of, as devised, the turbulent viscosity.

Invoking the Boussinesq hypothesis, Eq. 5, and the Prandtl model, then in a fully developed channel flow, where only dU/dy and $\overline{u'v'}$ is of any importance, the turbulent mixing-length scale is computed as:

$$l = \frac{\sqrt{\overline{u'v'}}}{dU/dy} \tag{8}$$

In Fig. 1, the turbulent length-scale computed using this relation with *a priori* DNS-data of Kim *et al.* [33], $Re_\tau = 395$ and $Re_\tau = 590$, is compared with the standard (Prandtl's) mixing-length model, and the modified versions.

As notable from the figure the turbulent length scale models are very inaccurate beyond $y/H = 0.2$. The van Driest damping function improves the result for $y/H < 0.1$. Prandtl's mixing-length model is only reasonable accurate within $0.1 < y/H < 0.2$, which is not a very attractive situation. Although its limitations this model forms the basis for all eddy-viscosity models, and also gives the well-known logarithmic law for the velocity profile.

3.2.3 Law-of-the-wall

Assuming that we have fully developed channel flow with:

i The convective terms are negligible.

ii The total shear is constant (and equal to the wall shear).

iii The viscous shear is negligible compared to the turbulent shear.

Then the following is true:

$$-\overline{u'v'} \approx \frac{\tau_w}{\rho} \equiv U_\tau^2 \tag{9}$$

Using the mixing-length model for $-\overline{u'v'}$ an expression for the velocity profile could be find as:

$$\begin{aligned} (\kappa y)^2 \left(\frac{dU}{dy}\right)^2 = U_\tau^2 \qquad &\Rightarrow \\ \frac{U}{U_\tau} = U^+ = \frac{1}{\kappa}\ln(y^+) + B \end{aligned} \tag{10}$$

where $B \approx 5$, based on experimental data. The accuracy of this law, as can be seen in Fig. 2, is – not surprisingly – only acceptable in the logarithmic region. The standard practise of plotting the velocity in a linear-logarithmic graph (as done here) hides the discrepancies of the log-law very well. In the figure the validity of the van Karman constant, κ, and the constant, B, using the DNS-data are also shown.

In the figure κ is plotted as $10 \cdot \kappa$. The two horizontal lines show the commonly accepted values of 0.41 and 5.25 for κ and B, respectively. As noted B is well represented, although the value appears to be on the low side. The van Karman constant is however not a constant at all, and for these two DNS-data sets ($Re_\tau = 395$ and $Re_\tau = 590$), $\kappa = 0.41$ is within 5% error only between $43 < y^+ < 97$ and $43 < y^+ < 126$ respectively.

3.3 Algebraic or Zero-equation EVMs

Although its erroneous predictions and non-generality, the mixing-length model has formed the basis for other turbulence models, even recent one. The Cebeci and Smith [8], and Baldwin and Lomax [3] have had some success, especially in airfoil design. The accurate prediction of these model is however more contributed to the introduced *ad hoc* (or empirical) functions and constants, rather than any additional physics included in the models. Since the zero equation models don't have

any transport of turbulence, they cannot be expected to accurately predict any flows which have non-local mechanisms. The most important of these mechanisms is the history effect, ie. the influence of flow processes downstream the event. Numerical simulations with the zero-length models are thus usually restricted to attached boundary-layer flows, which can be modelled using only local relations. See however Wilcox [54] for a thorough discussion on the algebraic models and their performance.

3.4 One-equation EVMs

In order to avoid the local behaviour of the mixing-length turbulence models, a transport equation is needed for some turbulent quantity. A model that could conserve turbulence should improve the predictions in flows that depends on both the streamwise position and the wall-normal (cross-stream) position.

A most interesting turbulent quantity is the trace of the Reynolds stresses: $0.5R_{ii} = 0.5(\overline{u'u'} + \overline{v'v'} + \overline{w'w'})$, which is denoted the turbulent kinetic energy, k. It is reasonable to believe that for increasing normal stresses, the shear stresses would also increase, and hence k can be used to determine ν_t in the Boussinesq relation. As previously shown, Eq. 6, the eddy-viscosity is generally described as the product of a velocity scale and a length scale. Using the turbulent kinetic energy as the transported quantity, the eddy-viscosity is modelled as:

$$\nu_t \sim \sqrt{k} \cdot l \tag{11}$$

Such a scheme is used in the model by Wolfshtein [55], where the turbulent length scale is pre-described using an algebraic expression, based on geometrical conditions. Although the soundness of including a transport equation, the one-equation models do not improve the predictions greatly compared with the zero-equation models, mainly due to the required *a priori* knowledge of the length scale. Thus apart from the Wolfshtein model there exist rather few one-equation models. The recent Spalart-Allmaras model [46] which solves a transport equation for the turbulent viscosity itself, has however had some success. See Wilcox [54] for further information.

3.5 Turbulent Kinetic Energy Equation

The turbulent kinetic energy appears in almost every EVM and hence it is of interest to study this quantity in depth. The profile of k and the wall-distance dependency of k, (ie. the exponent in the relation, $k \sim y^C$), for fully developed channel flow (DNS-data) are shown in Fig. 3.

The transport equation for k, as derived in Bredberg [5] is:

$$\frac{Dk}{Dt} = P_k - \varepsilon + \Pi_k + T_k + D_k^\nu \tag{12}$$

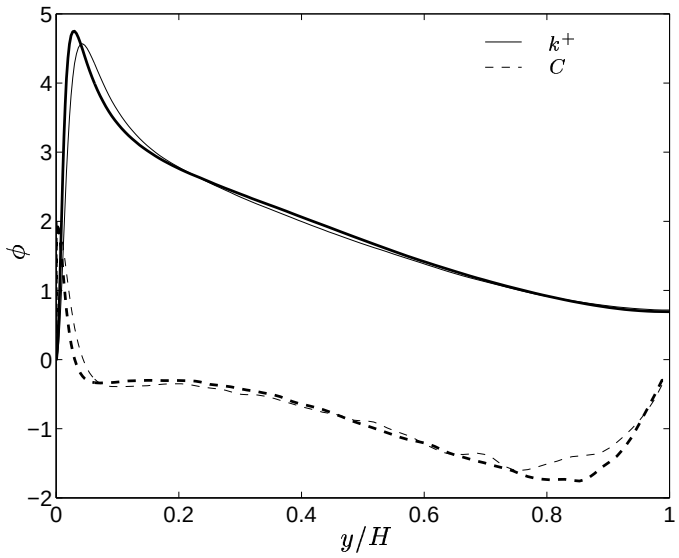

Figure 3: Profile of k and its exponential, C, y-dependency. DNS-data, Kim *et al.* [33], $Re_\tau = 395$ (thin lines) and $Re_\tau = 590$ (thick lines).

with,

$$P_k = -\overline{u_i'u_j'}\frac{\partial U_i}{\partial x_j}$$
$$\varepsilon = \nu\overline{\left(\frac{\partial u_i'}{\partial x_j}\right)^2}$$
$$\Pi_k = -\frac{\partial}{\partial x_j}\left(\overline{\frac{u_j'p'}{\rho}}\right)$$
$$T_k = -\frac{\partial}{\partial x_j}\left(\frac{1}{2}\overline{u_j'u_i'u_i'}\right)$$
$$D_k^\nu = \frac{\partial}{\partial x_j}\left(\nu\frac{\partial k}{\partial x_j}\right)$$

where P_k is the production, ε the dissipation, Π_k the pressure-diffusion, T_k the turbulent diffusion and D_k^ν the viscous diffusion term.

The importance of the individual terms are shown in Fig. 4, where each term is plotted as a fraction of the **absolute** sum of all terms. This was done because the sum of the terms is zero for fully developed flow, where the convective term is negligible.

In the near-wall region, the dissipation is balanced by the viscous diffusion (barely notable on this scale), while in the off-wall region although still close to the wall (the buffer layer) the dissipation plus the turbulent-diffusion term balance the production term. In the region from $y/H = 0.1$ to $y/H = 0.5$ the dominant terms are the production and dissipation terms. The commonly accepted production equals dissipation in the logarithmic region is a good approximation. Towards the centre of the channel the production gradually decreases, while the turbulent diffusion increases. In the middle of the channel ($y/H \approx 1$) the dissipation equals the turbulent diffusion term. As noted, nowhere is the pressure-diffusion term crucial for the balance which is also reflected in the included turbulence models where this term is seldom modeled.

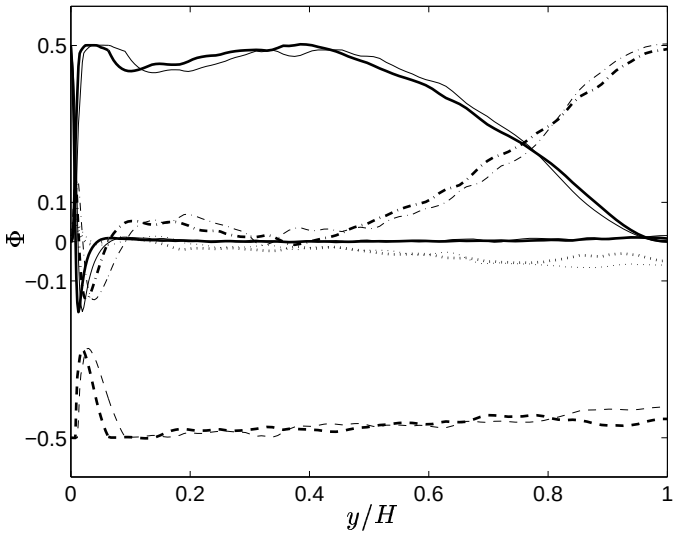

Figure 4: P_k, $-$, ε, $--$, T_k, $-.$, Π_k, $:$, D^ν, $-$ DNS-data, Kim *et al.* [33], $Re_\tau = 395$ (thin lines) and $Re_\tau = 590$ (thick lines).

3.6 Two-equation EVMs

In this report, as previously stated, the main focus will be on two-equation EVMs, which all use the turbulent kinetic energy as one of the solved turbulent quantities. Apart from the transport equation for k, the models add another transport equation for a second turbulent quantity. The main difference between these models is the choice of this quantity.

The commonly accepted idea is that the eddy-viscosity may be expressed as the product of a velocity scale and a length scale. Thus the obvious choice would be, as used in the Wolfshtein model, Eq. 11, to combine $\sqrt{k}$, with l. Although its logical construction this combination has not been used with any two-equation turbulence model.

Instead of a velocity-length scale model the overwhelmingly majority of the used two-equation EVMs are based on the $k-\varepsilon$ concept, which uses the dissipation, ε, in the k-equation to construct the eddy-viscosity. The subsequent relation is based on dimensional reasoning, and as such is no improvement compared to a $k-l$ model. However using the $k-\varepsilon$ concept one avoids the additional complication of how to model the dissipation rate in the k-equation.

Another version is the $k-\tau$ model, which uses the turbulent time scale to construct the eddy-viscosity. This type have an advantageous boundary condition as compared to the $k-\varepsilon$-type. The only model using this concept, the Speziale, Anderson and Abid, [47], is however numerical unstable and have not been a success.

The $k-\omega$ models originally developed by Kolmogorov [23], however more recently promoted by Wilcox [52], uses the reciprocal to the time scale or vorticity. This secondary quantity is however more commonly referred to as the specific dissipation rate of turbulent kinetic energy.

The major differences and also benefits of using either of the above mentioned types of two-equation EVMs are:

1. The used secondary turbulent quantity, and its boundary condition.
2. The way the turbulent viscosity is modelled.
3. Modelling of the exact terms in the ε-equation.

3.7 Secondary Quantity

Four different types of two-equation model were mention above, of these only two, the $k-\varepsilon$ and the $k-\omega$ are used frequently. However at this stage, for completeness, all four will be assessed. Noting the dimension of the eddy-viscosity, $[m^2/s]$, it is a matter of dimensional analysis to combine the correct powers of the turbulent kinetic energy and the secondary quantity to establish a relation for ν_t as:

$$\nu_t = k^a \phi^b \tag{13}$$

where the following two expressions need to be fulfilled:

$$\begin{aligned} [m]: &\qquad 2 = 2a + [m_\phi]b \\ [s]: &\qquad -1 = -2a + [s_\phi]b \end{aligned}$$

The different secondary turbulent quantities have the following dimensions; $l:\ [m]$, $\varepsilon:\ [m^2/s^3]$, $\tau:\ [s]$, and $\omega:\ [s^{-1}]$, respectively, and hence the turbulent viscosity need to be modelled according to:

$$\begin{aligned} k-l: &\qquad \nu_t \sim \sqrt{k}l \\ k-\varepsilon: &\qquad \nu_t \sim \frac{k^2}{\varepsilon} \\ k-\tau: &\qquad \nu_t \sim k\tau \\ k-\omega: &\qquad \nu_t \sim \frac{k}{\omega} \end{aligned}$$

In order to give some idea about the likelihood of success when employing any of the above combinations, the secondary quantities are discussed below in regards to both their wall dependency and boundary condition.

3.7.1 Wall dependency

The secondary quantities using the above relation for the turbulent viscosity are plotted in fully developed channel flow, using *a priori* DNS-data. Fig. 5 gives the profiles in the channel while Fig. 6 shows a close-up of the near-wall region.

The behaviour of the secondary quantities are subdivided into three different areas:

1. the core of the channel, spanning from roughly $y/H = 0.1 \rightarrow y/H = 1$ (the logarithmic layer and defect layer),
2. the near-wall region, although away from the wall (buffer layer), and
3. the immediate wall region (viscous sub-layer).

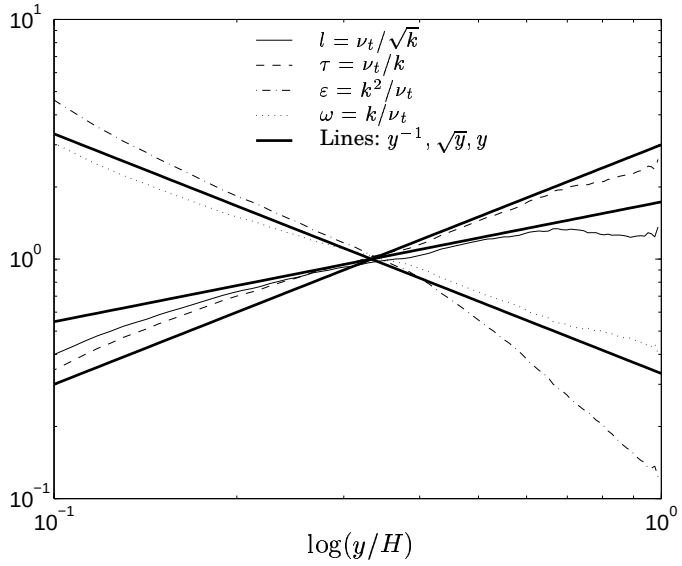

Figure 5: Variation of secondary quantity, whole region. DNS-data, Kim *et al.* [33], $Re_\tau = 590$.

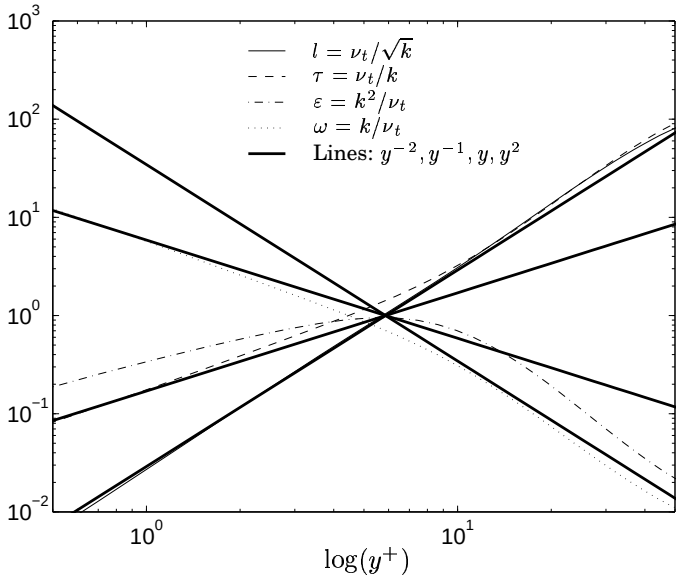

Figure 6: Variation of secondary quantity, near-wall region. DNS-data, Kim *et al.* [33], $Re_\tau = 590$.

ϕ	$0 < y^+ < 5$	$5 < y^+ < 30$	$y/H > 0.1$
l	y^2	y^2	$\sqrt{y}$
ε	y	const	y^{-1}
τ	y	y^2	y
ω	y^{-1}	y^{-2}	y^{-1}

Table 2: Secondary quantities computed from DNS-data. $l = \nu_t/\sqrt{k}, \varepsilon = k^2/\nu_t, \omega = k/\nu_t, \tau = \nu_t/k$.

An approximate wall-dependency is given by table 2. Note that the variables smoothly changes from one region to another, and not in the discontinuous way indicated by the table. Observe also that the secondary quantities are calculated using the indicated relations with DNS-data for ν_t and k. The asymptotic behaviour does hence not need to match the physical correct boundary conditions of Eq. 14. The discrepancies between these two relations are normally corrected using van Driest type of damping functions in turbulence models.

In order to visualize the accuracy of the different secondary quantities they are approximated using powers of y in the figures. The $k-\varepsilon$ model is the worst case as indicated. ε in the core region seems to decrease slightly more than the y^{-1} tendency given by the table, see Fig. 5. In addition it is impossible to curve-fit ε in the near-wall region with either a y-line or a constant approach, Fig. 6.

The $k-\tau$ and $k-\omega$ models are a mirror image of each other. These models are best fitted using a linear approach in the viscous sub-layer, and then smoothly changing to a quadratic variation. In the core of the channel the linear wall dependency is only approximative, however on a slightly more accurate level than for the ε.

The simplest type to curve-fit is the $k-l$ model which follows a quadratic behaviour from the wall outwards to a rapid change to $\sqrt{y}$ around the start of the logarithmic region. l however behave spuriously in the centre of the channel as seen in Fig. 5.

3.7.2 Boundary condition

The physically correct boundary condition for the respectively secondary quantities are:

$$\begin{aligned} l_w &= 0 \\ \varepsilon_w &\to \text{constant} \\ \tau_w &= 0 \\ \omega_w &\to \infty \end{aligned} \tag{14}$$

The l_w and τ_w is straightforward and non disputable, however for both ε_w and ω_w there are a number of different choices in the specification of the boundary condition.

ε : Using DNS-data [33] it has been shown that ε is finite and non-zero, at the wall, however it might not be a constant, since DNS-data appear to indicate a Reynolds number dependencies. The two most adopted models for the ε boundary conditions are:

$$\varepsilon_w = 2\nu \left(\frac{\partial \sqrt{k}}{\partial y} \right)^2 \tag{15}$$

$$\varepsilon_w = 2\nu \frac{k}{y^2} \tag{16}$$

which becomes identical if $k \sim y^2$. The dissipation rate, ε, can either be modelled as the true dissipation rate, ε or a reduced version, $\tilde{\varepsilon}$. The reduced and the true dissipation rate are connected according to:

$$\tilde{\varepsilon} = \varepsilon - \hat{\varepsilon} \tag{17}$$

where $\hat{\varepsilon}$ is the boundary value for ε. If $\tilde{\varepsilon}$ is solved, a zero boundary condition is imposed in the code, and an additional term is necessary in the k-equation.

ω : The boundary condition for ω is a consequence of both its definition and the construction of the ω-equation. Following Wilcox, the ω_w is given through

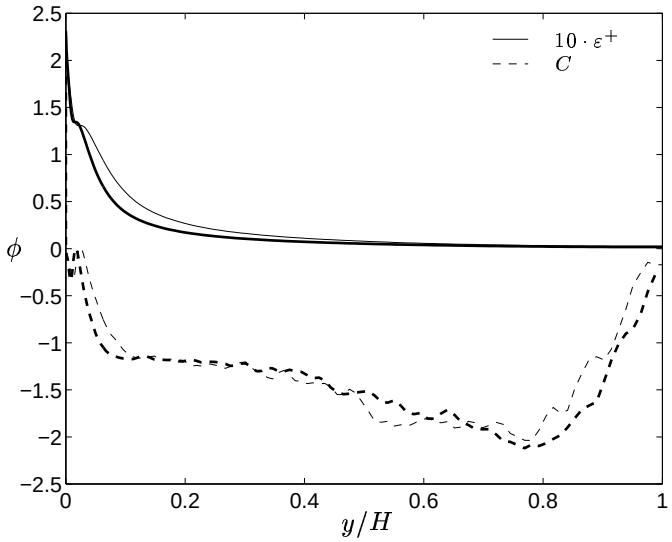

Figure 7: Profile of ε and its exponential, C, y-dependency. DNS-data, Kim *et al.* [33], $Re_\tau = 395$ (thin lines) and $Re_\tau = 590$ (thick lines).

equating the destruction and viscous term in the ω-equation[2]. The resulting boundary condition becomes:

$$\omega_w = \frac{6\nu}{\beta y^2} \tag{18}$$

This value is not entirely compatible with the definition of $\omega = \varepsilon/(\beta k)$ and the above boundary condition for ε, although there is only a constant which separates them: $\omega_{k-\omega} = 6/\beta = 80$ vs $\omega_{k-\varepsilon} = 2/\beta^* = 22$. Furthermore Menter [32] included, an additional factor of 10, hence the exact value of ω at the wall seems to be of little importance.

In the $k-\omega$ model of Bredberg *et al.*, [7], through the use of a viscous cross-diffusion term, a slightly different boundary condition is obtained:

$$\omega_w = \frac{2\nu}{C_k y^2} \tag{19}$$

This is identical to the boundary condition of ε in the Chien $k-\varepsilon$ model [9] if the definition of ω is used to translate ε into ω.

3.8 Dissipation Rate of Turbulent Kinetic Energy

Of the above secondary quantities (l, ε, ω and τ) there exists only an exact equation for one of them, namely the dissipation rate of turbulent kinetic energy, ε. Choosing another turbulent quantity as a secondary variable, the resulting modelled equation is necessarily derived on reasoning from the ε-equation.

Figure 7 shows the distribution of the dissipation rate in fully developed channel flow for the two sets of DNS-data available. Using the definition of ε:

$$\varepsilon = \nu \overline{\frac{\partial u_i'}{\partial x_j}\frac{\partial u_i'}{\partial x_j}} \tag{20}$$

[2]The other terms in the ω-equation being negligible in the viscous sub-layer.

it is possible, although a bit tedious, to derive the exact ε-equation, see Bredberg [5]:

$$\frac{D\varepsilon}{Dt} = P_\varepsilon^1 + P_\varepsilon^2 + P_\varepsilon^3 + P_\varepsilon^4 + T_\varepsilon + \Pi_\varepsilon + D_\varepsilon^\nu - \Phi_\varepsilon \tag{21}$$

where

$$P_\varepsilon^1 = -2\nu \overline{\frac{\partial u_i'}{\partial x_k}\frac{\partial u_j'}{\partial x_k}}\frac{\partial U_i}{\partial x_j} \qquad \text{Mixed production}$$

$$P_\varepsilon^2 = -2\nu \overline{\frac{\partial u_i'}{\partial x_k}\frac{\partial u_i'}{\partial x_j}}\frac{\partial U_j}{\partial x_k} \qquad \text{Mean production}$$

$$P_\varepsilon^3 = -2\nu \overline{u_j'\frac{\partial u_i'}{\partial x_k}}\frac{\partial^2 U_i}{\partial x_j \partial x_k} \qquad \text{Gradient production}$$

$$P_\varepsilon^4 = -2\nu \overline{\frac{\partial u_i'}{\partial x_k}\frac{\partial u_j'}{\partial x_k}\frac{\partial u_i'}{\partial x_j}} \qquad \text{Turbulent production}$$

$$T_\varepsilon = -\nu\frac{\partial}{\partial x_j}\left(\overline{u_j'\varepsilon}\right) \qquad \text{Turbulent diffusion}$$

$$\Pi_\varepsilon = -2\frac{\nu}{\rho}\frac{\partial}{\partial x_i}\left(\overline{\frac{\partial u_i'}{\partial x_k}\frac{\partial p'}{\partial x_k}}\right) \qquad \text{Pressure diffusion}$$

$$D_\varepsilon^\nu = \nu\frac{\partial^2 \varepsilon}{\partial x_k \partial x_k} \qquad \text{Viscous diffusion}$$

$$\Phi_\varepsilon = 2\overline{\left(\nu\frac{\partial^2 u_i'}{\partial x_k \partial x_m}\right)^2} \qquad \text{Destruction}$$

Comparing the ε-equation with the k-equation, Eq. 12, the equations include the same type of terms, although the ε-equation have several production terms.

For turbulence modelling purpose, the ε-equation is a severe obstacle as only a single term, as opposed to all but one in the k-equation, can be implemented exactly. Even employing a RSM type of model the situation does not improve, as all terms, apart from the viscous dissipation term, include fluctuating velocities which are not solved using a turbulence model. The other terms are not normally modelled using various simplifications. In EVMs these terms are lumped together either as production, destruction or diffusion terms, without much physical background, apart from that the exact terms mainly are a source, a sink or enhancing diffusivity to the equation.

Unfortunately the individual terms are not available in the open literature, and hence an importancy control of the different terms, similar to Fig. 4 can not be included here.

Based on the complexity of each term in the ε-equation, and also the number of unknown involved, it is quite understandable that their exist a magnitude of different approaches to the modelling of this equation. One requirement for these models are that the near-wall behaviour of the individual terms in ε-equation, given by the following table, are truthfully obeyed.

$P_\varepsilon^1 \sim y$	$P_\varepsilon^2 \sim y^2$	$P_\varepsilon^3 \sim y^2$	$P_\varepsilon^4 \sim y$
$T_\varepsilon \sim y$	$\Pi_\varepsilon \sim y^0$	$D_\varepsilon^\nu \sim y^0$	$\Phi_\varepsilon \sim y^0$

As the table indicates, in the near-wall region the most important terms to model are the pressure-diffusion, viscous diffusion and destruction (dissipation) terms. See Rodi and Mansour [43] for further information on the exact ε-equation.

3.9 EVMs Treated in this Report

There exists a number of two-equation EVMs today, with an ever increasing number, as these models are fairly easy to modify, tune and improve. It is thus not possible, not even necessary to include all models in a report like this. Choosing models with different secondary quantities, and of different complexity (number of terms/damping functions etc.) a limited number of models is sufficient to exemplify and compare nearly all existing two-equation EVMs, at least at a theoretical level.

Thus similar to previous papers on this subject, such as Patel *et al.* [36], Sarkar and So [44], and Wilcox [53] around ten models have been chosen. These are:

- $k-\varepsilon$ models:
  - Yang and Shih, 1993 [56] (YS)
  - Abe, Kondoh and Nagano, 1994 [1] (AKN)
  - Yoon and Chung, 1995 [58] (YC)
- $k-\tilde{\varepsilon}$ models:
  - Jones and Launder, 1972 [19] (JL)
  - Chien, 1982 [9] (C)
  - Launder and Sharma, 1974 [25]
    - with Yap-correction, 1987 [57] (LSY)
  - Nagano and Shimada, 1995 [34] (NS)
  - Hwang and Lin, 1998 [17] (HL)
  - Rahman and Siikonen, 2000 [40] (RS)
- $k-\omega$ models:
  - Wilcox, 1988 [52] (WHR)
  - Wilcox, 1993 [53] (WLR)
  - Peng, Davidson and Holmberg, 1997 [38] (PDH)
  - Bredberg, Davidson and Peng, 2001 [7] (BDP)
- $k-\tau$ model:
  - Speziale, Abid and Anderson, 1992 [47] (SAA)

The models are henceforth referred to with the abbreviation indicated above.

4 The Classic Two-equation EVMs

In the present paper, classic models is defined as models which have not used DNS-data to fundamentally alter the modelled equations, but rather base the modelling on comparisons with experiments and through more or less heuristic theoretical explanations and simplifications. Into this group falls naturally all models which dates prior to the first DNSs: JL, C, LSY, but also some of the later models which either have not used DNS data bases at all: WHR, or merely used them to tune constants and damping functions: YS, AKN, WLR, SAA. The other models: YC, NS, HL, RS, PDH, BPD, have used either DNS data or TSDIA results as the foundation for their theory. Yoshizawas [59] TSDIA (Two-Scale Direct-Interaction Approximation) analysis is here treated, similarly to DNS, as a numerical advancement rather than an improvement in physical understanding.

4.1 Turbulent Viscosity, ν_t

Of the four different types of two-equations EVMs discussed earlier, only three types are used for the turbulence models listed above. The $k-l$ version has so far not been used as a basis for an EVM. The turbulent viscosity for these three types is computed according to one of the following notations:

$$\begin{aligned} k-\varepsilon: &\qquad \nu_t = C_\mu \frac{k^2}{\varepsilon} \\ k-\omega: &\qquad \nu_t = C_\mu \frac{k}{\omega} \\ k-\tau: &\qquad \nu_t = C_\mu k\tau \end{aligned}$$

C_μ in the above formula can be established from equilibrium flow, where in the logarithmic region $C_\mu \approx 0.09$. However both DNS-data, Moser *et al.* [33], and experiments indicates a reduction of C_μ in the near-wall region.

The 'correct' C_μ, or effective C_μ^e can be computed as:

$$C_\mu^e \equiv \frac{-\overline{u'v'}/(dU/dy)}{k\phi} \tag{22}$$

where ϕ is either k/ε, τ or $1/\omega$ for the $k-\varepsilon$, $k-\tau$ and $k-\omega$ type respectively. The effective C_μ for the different turbulence models is compared with DNS-data in Fig. 8. Note that for EVMs, which do not compute the Reynolds stresses, the Boussinesq hypothesis, Eq. 5, is substituted into the above equation as: $C_\mu^e = \nu_t\varepsilon/k^2$ ($k-\varepsilon$ model).

4.1.1 Near-wall damping

The agreement between DNS and the constant C_μ is very poor in the near-wall region. The inclusion of a function which reduces (damps) ν_t in the near-wall region can significantly improve the result as notable. Models which employ damping function, are commonly referred to as Low-Reynolds-Number (LRN) turbulence models, and differs from their High-Reynolds-Number (HRN)

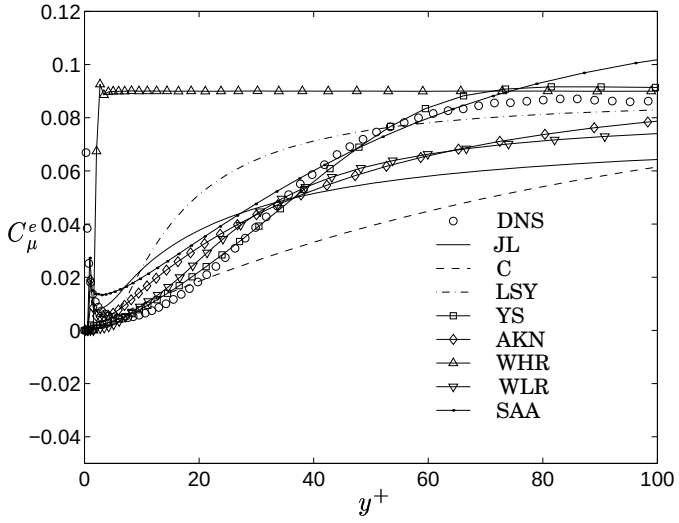

Figure 8: C_μ^e in the near wall region.

counterparts in that they can (and need to) be resolved down to the wall.

The HRN-models use wall functions to bridge the near wall region, and hence only concern about the value of C_μ in the inertial sub-layer, where C_μ is fairly accurate approximated by $C_\mu = 0.09$. See also the complementary paper on wall boundary condition [6].

There are mainly two effects of adding a damping function to ν_t:

- Reduce C_μ near a wall.
- Correct the asymptotic behaviour of $\overline{u'v'}$.

For the LRN-models, as seen in Fig. 8, the effective C_μ is reduced, through the damping function, f_μ.

DNS-data show that the near-wall asymptotic behaviour of the involved variables in the definition of ν_t are: $k \sim y^2$, $\varepsilon \sim y^0$, $\omega \sim y^{-2}$ and $\tau \sim y^0$. Thus the damping function should vary either as: y^{-1} ($k-\varepsilon$, $k-\omega$) or y ($k-\tau$) to impose the correct near-wall behaviour of the turbulent shear stress as $\nu_t \sim y^3$.

4.1.2 Wall-distance relations

Nearly all LRN EVMs use an exponential function and a variable somehow related to the wall distance, in their definition of the damping function. The following wall-distance functions are frequently used:

$$R_t = \frac{k^2}{\nu\varepsilon}\ (k-\varepsilon \text{ type}) \qquad R_t = \frac{k}{\nu\omega}\ (k-\omega \text{ type})$$

$$R_y = \frac{\sqrt{k}y}{\nu}$$

$$R_\varepsilon = \frac{y}{(\nu^3/\varepsilon)^{1/4}}$$

$$R_\lambda = \frac{y}{\sqrt{\nu\tau}}$$

$$y_\lambda = \frac{y}{\sqrt{\nu k/\varepsilon}}$$

$$y^* = \frac{U_\varepsilon y}{\nu}, \qquad U_\varepsilon = (\varepsilon\nu)^{1/4}$$

$$y^+ = \frac{U_\tau y}{\nu}, \qquad U_\tau = \sqrt{\tau_w/\rho}$$

Fig. 9 shows their near-wall variation using DNS-data for fully developed channel flow. The most appreciated version is the first, because it doesn't depend on the wall distance at all, and hence simplifies the treatment in complex geometries. The last variant should be avoided, because it uses U_τ, which becomes zero in separation and re-attachment points. Employing a U_τ-based damping function for re-circulating flows is thus highly questionable, with spurious results as a consequence, see the predictions using eg. the Chien $k-\varepsilon$ model for the backward-facing-step and the rib-roughened case in Appendix B. Consult also Launder [24].

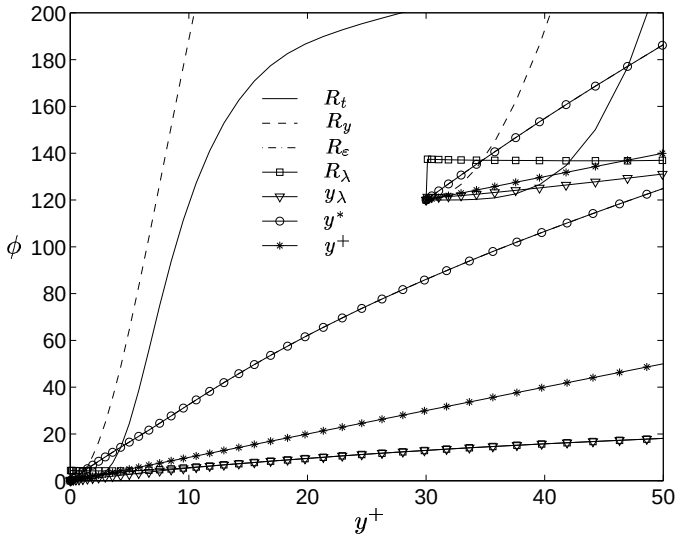

Figure 9: Wall-distance variation of damping function parameters. The immediate near-wall region is inserted in the upper-right corner of the figure.

4.1.3 Damping function, f_μ

The used damping functions for the turbulent viscosity by the turbulence models are listed below:

$k-\varepsilon$ **models:**

$$\nu_t = C_\mu f_\mu \frac{k^2}{\varepsilon}$$

$$f_\mu = \exp\left[\frac{-2.5}{(1+R_t/50)}\right] \quad \text{JL}$$

$$f_\mu = 1-\exp(-0.0115y^+) \quad \text{C}$$

$$f_\mu = \exp\left[\frac{-3.4}{(1+R_t/50)^2}\right] \quad \text{LSY}$$

$$f_\mu = [1-\exp(-1.5\times10^{-4}R_y - 5\times10^{-7}R_y^3 - 1\times10^{-10}R_y^5)]^{0.5} \quad \text{YS}$$

$$f_\mu = \left[1-\exp\left(-\frac{y^*}{14}\right)\right]^2 \times\left[1+\frac{5}{R_t^{3/4}}\exp\left\{-\left(\frac{R_t}{200}\right)^2\right\}\right] \quad \text{AKN}$$

$k-\omega$ **models:**

$$\nu_t = C_\mu f_\mu \frac{k}{\omega}$$

$$f_\mu = 1 \quad \text{WHR}$$

$$f_\mu = \frac{0.025+10/27R_t}{1+10/27R_t} \quad \text{WLR}$$

$k-\tau$ **model:**

$$\nu_t = C_\mu f_\mu k\tau$$

$$f_\mu = \left(1+\frac{3.45}{\sqrt{R_t}}\right)\tanh\left(\frac{y^+}{70}\right) \quad \text{SAA}$$

with the models abbreviated as defined earlier.

The computed f_μ with these models are shown in Fig. 10. The relevant f_μ for DNS-data is computed by normalizing Eq. 22 with the standard value of $C_\mu = 0.09$. It should be noted that f_μ never reaches unity using DNS-data, hence the value of $C_\mu = 0.09$ is slightly too high.

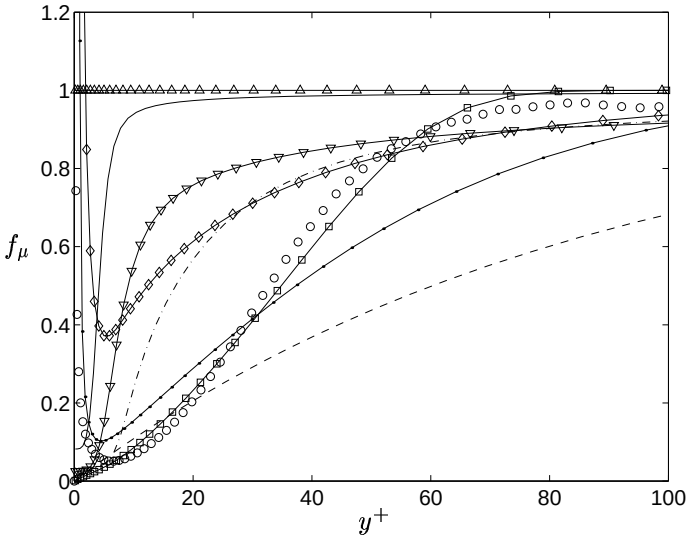

Figure 10: f_μ in the near wall region. For legend, see Fig. 8

4.2 Modelling Turbulent Kinetic Energy, k-equation

The exact turbulent kinetic energy, Eq. 12, repeated here for clarity, is:

$$\frac{Dk}{Dt} = \underbrace{-\overline{u_i'u_j'}\frac{\partial U_i}{\partial x_j}}_{P_k} \underbrace{-\nu\overline{\left(\frac{\partial u_i'}{\partial x_j}\right)^2}}_{\varepsilon} + \underbrace{\left[-\frac{\partial}{\partial x_j}\left(\overline{\frac{u_j'p'}{\rho}}\right)\right]}_{\Pi_k} + \underbrace{\left[-\frac{\partial}{\partial x_j}\left(\frac{1}{2}\overline{u_j'u_i'u_i'}\right)\right]}_{T_k} + \underbrace{\frac{\partial}{\partial x_j}\left(\nu\frac{\partial k}{\partial x_j}\right)}_{D_k} \tag{23}$$

Note that the turbulent diffusion (T_k) and the pressure-diffusion (Π_k) terms are normally combined into one term, see Eq. 27.

In the standard $k-\varepsilon$ model, the viscous term is the only exact term on the right-hand side, while the other are modelled using, in some case rather questionable assumptions. Below the terms are treated individually.

4.2.1 Production

The production term in an EVM is:

$$P_k = -\overline{u_i'u_j'}\frac{\partial U_i}{\partial x_j} \approx \nu_t\left(\frac{\partial U_i}{\partial x_j}+\frac{\partial U_j}{\partial x_i}\right)\frac{\partial U_i}{\partial x_j} \tag{24}$$

For fully developed channel flow with only one velocity gradient component (in the wall normal direction, dU/dy) most turbulence models predict an accurate level of turbulent production. However in flows with a high degree of anisotropy, the linear EVMs ($k-\varepsilon$ etc.) fails through their use of the isotropic eddy-viscosity, ν_t. In order to rectify this an extension to the Boussinesq hypothesis is needed. In non-linear EVMs the introduction of higher order terms in the relation for the Reynolds stresses improves the predictions in flows involving eg. rotation, curvature and re-circulating regions.

4.2.2 Dissipation

The dissipation term is either modeled using its own transport equation, as in the $k-\varepsilon$ models or via some relation with k and the secondary turbulent quantity ($k-\omega$ and $k-\tau$ models).

In the case of the $k-\varepsilon$ models there is a choice for the dissipation rate: either the true, ε, or the reduced, $\tilde{\varepsilon}$. If the reduced $\tilde{\varepsilon}$ is used, then there is a modification, an extra term, E_k, in the k-equation, since the true ε always appear in the k-equation.

The reduced dissipation rate method is employed in the JL, C and LSY models, with E_k taking two different forms:

$$E_k = -\hat{\varepsilon} = -2\nu\frac{y}{k^2} \quad \text{C}$$

$$E_k = -\hat{\varepsilon} = -2\nu\left(\frac{\partial\sqrt{k}}{\partial y}\right)^2 \quad \text{JL, LSY}$$

When the true ε is solved (YS and AKN models), there is no additional term in the k-equation.

In the $k-\omega$ models, the dissipation term is model as $\varepsilon = k\omega$. Dependent on the definition of ω, it may be necessary to introduce an additional coefficient. In the Wilcox models, ε is modelled as:

$$\varepsilon = \beta^* k\omega \tag{25}$$

with

$$\beta^* = 0.09 \qquad \text{WHR}$$

$$\beta^* = 0.09\frac{5/18+(R_t/8)^4}{1+(R_t/8)^4} \qquad \text{WLR}$$

In the $k-\tau$ model (SAA) the dissipation rate is modelled as

$$\varepsilon = \frac{k}{\tau} \tag{26}$$

4.2.3 Diffusion

Pressure-diffusion and turbulent-diffusion: In the standard $k-\varepsilon$, as well as for other classic models, the two diffusion terms are lumped together and modelled through a gradient model, known as the simple gradient diffusion hypothesis (SGDH):

$$\begin{aligned}\Pi_k + T_k &= -\frac{\partial}{\partial x_j}\left(\overline{\frac{u_j' p'}{\rho}} + \frac{1}{2}\overline{u_j' u_i' u_i'}\right) \\ &\approx \frac{\partial}{\partial x_j}\left(\frac{\nu_t}{\sigma_k}\frac{\partial k}{\partial x_j}\right)\end{aligned} \tag{27}$$

Viscous diffusion:

$$D_k^\nu = \frac{\partial}{\partial x_j}\left(\nu\frac{\partial k}{\partial x_j}\right) \tag{28}$$

Since this term can be implemented exactly there is no need for a model.

4.2.4 The modelled k-equation

Summing up, the classic modelled k-equation is:

$$\begin{aligned}\frac{Dk}{Dt} = \nu_t\left(\frac{\partial U_i}{\partial x_j}+\frac{\partial U_j}{\partial x_i}\right)\frac{\partial U_i}{\partial x_j} - \varepsilon + E_k + \\ + \frac{\partial}{\partial x_j}\left[\left(\nu+\frac{\nu_t}{\sigma_k}\right)\frac{\partial k}{\partial x_j}\right]\end{aligned} \tag{29}$$

where ε, in the case of the $k-\omega$ and $k-\tau$ models is substituted according to Eqs. 25 or 26.

The additional term E_k represents the difference between the true ε – always used in the k-equation – and the reduced $\tilde{\varepsilon}$. If the latter is used in the dissipation rate equation, E_k takes the value of $\hat{\varepsilon}$, defined above.

Apart from the treatment of the dissipation rate the difference between the 'classic' turbulence models, is restricted to the Schmidt number, σ_k, which adopts the following values:

$k-\varepsilon$				$k-\omega$		$k-\tau$
JL	LSY	YS	AKN	WHR	WLR	SAA
1.0	1.0	1.0	1.4	2.0	2.0	1.36

The performance of the k-equation for the different turbulence models in fully developed channel flow are compared with DNS-data in Figs. 14 and 15, Appendix B.

4.3 Modelling the Secondary Turbulent Equation

In the case of the numerous $k-\varepsilon$ models, the standard praxis for the modelling of the ε-equation is to use the modelled k-equation as a basis, and then dimensionally map ε onto it, with added constants and damping functions.

The ω- and τ-equation in the $k-\omega$- and $k-\tau$- models, could similarly be a direct dimensional transformation of the k-equation. Another possibility would be to use the modelled k- and ε-equations to construct either a ω- or a τ-equation. In all cases, the secondary transport equation would be essentially identical, and could schematically be displayed as:

$$\begin{aligned}\frac{D\phi}{Dt} = \underbrace{C_{\phi 1} f_1 \frac{\phi}{k}\nu_t\left(\frac{\partial U_i}{\partial x_j}+\frac{\partial U_j}{\partial x_i}\right)\frac{\partial U_i}{\partial x_j}}_{P_\phi} - \underbrace{C_{\phi 2} f_2 \frac{\phi}{k}}_{\Phi_\phi}\varepsilon + \\ + \Pi_\phi + E_\phi + \underbrace{\frac{\partial}{\partial x_j}\left[\left(\nu+\frac{\nu_t}{\sigma_\phi}\right)\frac{\partial \phi}{\partial x_j}\right]}_{D_\phi}\end{aligned} \tag{30}$$

where P_ϕ is the production term, Φ_ϕ the destruction term, Π_ϕ the pressure-diffusion term, D_ϕ the diffusion term and E_ϕ an additional term. ϕ is one of the secondary turbulent quantity, ε, ω or τ.

4.4 The Jones-Launder $k-\varepsilon$ model and the Dissipation Rate of Turbulent Kinetic Energy, ε-equation

All the classic modeled ε-equations are developed by simply multiplying each term in the modelled k-equation by ε/k and adding a number of coefficients.

Thus these ε-equations consists of a production, a destruction term, a viscous diffusion term (which is exact) and a turbulent diffusion term.

4.4.1 Production term

The production terms in the exact dissipation rate equation, should according to Rodi and Mansour [43], be distributed into both the production and the destruction term in the modelled equation.

In the classic model, this is of course of less importance, because the modelling is more based on dimensionality reasoning than actually capture the physics term by term. Of the production terms in Eq. 21, P_ε^1 and P_ε^2 should be included in the destruction term, while P_ε^4 is modelled as a production term:

$$P_\varepsilon^4 = \ldots \approx C_{\varepsilon 1} f_1 \frac{\varepsilon}{k}\nu_t\left(\frac{\partial U_i}{\partial x_j}+\frac{\partial U_j}{\partial x_i}\right)\frac{\partial U_i}{\partial x_j} \tag{31}$$

where f_1 is a tunable damping function, which has been set to 1 in all of the described models. The constant $C_{\varepsilon 1}$ is set to:

JL	C	LSY	YS	AKN
1.55	1.35	1.44	1.44	1.5

The term P_ε^3, see Eq. 21, could be argued to be negligibly small in comparison to the other production terms, however it could still influence the results, Rodi and Mansour [43]. Thus in some models, (JL and LSY), an additional term is included to simulate its effect:

$$P_\varepsilon^3 = \ldots \approx 2\nu\nu_t \left(\frac{\partial^2 U_i}{\partial x_j^2}\right)^2 \tag{32}$$

Note however that this term imposes numerical problems due to its second derivate and is only used in models by Launder *et al.* [19], [25].

4.4.2 Destruction term

The destruction term is the sum of the P_1^ε, P_2^ε and $-\Phi_\varepsilon$ terms, and is modelled as:

$$P_\varepsilon^1 + P_\varepsilon^2 - \Phi_\varepsilon = \ldots \approx C_{\varepsilon 2} f_2 \frac{\varepsilon^2}{k} \tag{33}$$

with a damping function, f_2 as follows:

$$f_2 = 1 - 0.3\exp\left(-R_t^2\right) \qquad \text{JL}$$

$$f_2 = 1 - 0.22\exp\left(-\frac{R_t}{6}\right)^2 \qquad \text{C}$$

$$f_2 = 1 - 0.3\exp(-R_t^2) \qquad \text{LSY}$$

$$f_2 = 1 \qquad \text{YS}$$

$$f_2 = \left[1 - \exp\left(-\frac{y^*}{3.1}\right)\right]^2 \left[1 - 0.3\exp\left\{-\left(\frac{R_t}{6.5}\right)^2\right\}\right] \qquad \text{AKN}$$

The constant, $C_{\varepsilon 2}$, has the following values:

JL	C	LSY	YS	AKN
2.0	1.8	1.92	1.92	1.9

The reason behind the damping function is argued from the process of decaying turbulence. Townsend [49] gives the decay as:

$$k \sim t^{-n} \tag{34}$$

where $n = 1.25$ initially, but increases to $n = 2.5$ in the final period, for which $R_t \to 0$. In decaying turbulence, the only terms that are of importance are the destruction, and time derivate terms:

$$\frac{dk}{dt} = -\varepsilon \tag{35}$$

$$\frac{d\varepsilon}{dt} = -C_{\varepsilon 2} f_2 \frac{\varepsilon^2}{k} \tag{36}$$

Solving the equation system for n, with $k \sim t^{-n}$ gives:

$$n = \frac{1}{C_{\varepsilon 2} f_2 - 1} \tag{37}$$

For the two extremes, $R_t \to \infty$ and $R_t \to 0$ the following relations holds:

$$\begin{aligned} f_2 C_{\varepsilon 2} &\to 1.4, \qquad R_t \to 0 \\ f_2 C_{\varepsilon 2} &\to 1.8, \qquad R_t \to \infty \end{aligned} \tag{38}$$

The Chien $k-\varepsilon$ model simulates this behaviour very accurately using its relation for f_2.

4.4.3 Diffusion

Pressure and turbulent diffusion terms: Similar to the k-equation a simple gradient term is used to model the diffusion effect:

$$\Pi_\varepsilon + T_\varepsilon = \ldots \approx \frac{\partial}{\partial x_j}\left(\frac{\nu_t}{\sigma_\varepsilon}\frac{\partial \varepsilon}{\partial x_j}\right) \tag{39}$$

The involved Schmidt numbers are:

JL	C	LSY	YS	AKN
1.3	1.3	1.3	1.3	1.4

Viscous diffusion term: As noted above this term can be implemented exactly as:

$$D_\varepsilon^\nu = \frac{\partial}{\partial x_j}\left(\nu \frac{\partial \varepsilon}{\partial x_j}\right) \tag{40}$$

4.4.4 The modelled ε-equation

The modelled ε-equation is the summation of the above terms, with the resulting equation similar to the modelled k-equation, Eq. 30 as:

$$\begin{aligned} \frac{D\varepsilon}{Dt} = C_{\varepsilon 1}\nu_t \frac{\varepsilon}{k}\left(\frac{\partial U_i}{\partial x_j} + \frac{\partial U_j}{\partial x_i}\right)\frac{\partial U_i}{\partial x_j} - C_{\varepsilon 2} f_2 \frac{\varepsilon^2}{k} + \\ + E_\varepsilon + \frac{\partial}{\partial x_j}\left[\left(\nu + \frac{\nu_t}{\sigma_\varepsilon}\right)\frac{\partial \varepsilon}{\partial x_j}\right] \end{aligned} \tag{41}$$

E_ε is an additional term simulating the extra production in the JL and LSY models. The predicted ε for fully developed channel flow using the different turbulence models are displayed in Figs 16 and 17, in Appendix B.

4.5 Transforming the ε-equation

Contrary to the dissipation rate, ε, there exists no exact equation for the ω- and τ-equations, as previously disclosed. Thus in order to model these quantities, the equations need to be constructed. This can be done in two different ways are:

1. Similarly to the modelled ε-equation, the k-equation is dimensionally changed through a multiplication of either ω/k or τ/k to yield a new secondary transport equation.

2. The ω- or τ-equation can be constructed from a transformation of the modelled k- and ε-equations, by substituting ω or τ with either ε/k or k/ε.

The first method is straight forward and it is not further discussed here. The second choice is much more complicated and also adds a number of new terms to the secondary equation. Using this technique the new turbulence model will be identical to the original $k-\varepsilon$ model, however expressed in a new secondary variable with a different, and improved, near-wall behaviour. The transformation to a ω- and τ-equation is treated separately below.

4.5.1 The ω-equation

The transport equation for the specific dissipation rate (ω) obtained from the k- and ε-equations reads:

$$\begin{aligned}\frac{D\omega}{Dt} =&\frac{D}{Dt}\left(\frac{\varepsilon}{C_k k}\right) = \frac{1}{C_k k}\frac{D\varepsilon}{Dt} - \frac{\varepsilon}{k^2}\frac{Dk}{Dt} = \\ =&\frac{1}{C_k k}\left[P_\varepsilon - \Phi_\varepsilon + \Pi_\varepsilon + T_\varepsilon + D_\varepsilon^\nu\right] - \\ &- \frac{\omega}{k}\left[P_k - \varepsilon + \Pi_k + T_k + D_k^\nu\right]\end{aligned} \tag{42}$$

Dependent on the complexity of the modelled k- and ε-equations there will be different versions of the resulting ω-equation. Using the standard $k-\varepsilon$ model as a basis (Eqs. 29 and 41), the resulting transport equation for ω becomes[3] (see Appendix C for a thorough derivation):

$$\begin{aligned}\frac{D\omega}{Dt} =&(C_{\varepsilon 1}-1)\frac{\omega}{k}P_k - (C_{\varepsilon 2}f_2 - 1)\omega^2 + \\ &+ \frac{2}{k}\left(\nu + \frac{\nu_t}{\sigma_\varepsilon}\right)\frac{\partial k}{\partial x_j}\frac{\partial \omega}{\partial x_j} + \\ &+ \frac{\omega}{k}\left(\frac{\nu_t}{\sigma_\varepsilon} - \frac{\nu_t}{\sigma_k}\right)\frac{\partial^2 k}{\partial x_j^2} + \frac{\partial}{\partial x_j}\left[\left(\nu + \frac{\nu_t}{\sigma_\varepsilon}\right)\frac{\partial \omega}{\partial x_j}\right]\end{aligned} \tag{43}$$

The term which includes the second order derivate of k could normally be neglected since the Schmidt numbers of k and ε (σ_k and σ_ε) are fairly similar. With identical Schmidt numbers (as in the Wilcox $k-\omega$ model) the term is identical zero.

4.5.2 The τ-equation

Performing similar operations on the τ-equation as for the ω-equation gives:

$$\begin{aligned}\frac{D\tau}{Dt} =&\frac{D}{Dt}\left(\frac{\varepsilon}{k}\right) = \frac{1}{\varepsilon}\frac{Dk}{Dt} - \frac{k}{\varepsilon^2}\frac{D\varepsilon}{Dt} = \\ =&\frac{\tau}{k}\left[P_k - \varepsilon + \Pi_k + T_k + D_k^\nu\right] - \\ &- \frac{\tau^2}{k}\left[P_\varepsilon - \Phi_\varepsilon + \Pi_\varepsilon + T_\varepsilon + D_\varepsilon^\nu\right]\end{aligned} \tag{44}$$

[3] As the transformation only applies to the ω-equation, the k-equation in the $k-\omega$ model identical to original equation in the $k-\varepsilon$ model.

Using the standard k- and ε-equation the τ-equation becomes:

$$\begin{aligned}\frac{D\tau}{Dt} =&(1-C_{\varepsilon 1})\frac{\tau}{k}P_k - (1-C_{\varepsilon 2}f_2) + \\ &+ \frac{2}{k}\left(\nu + \frac{\nu_t}{\sigma_\varepsilon}\right)\frac{\partial k}{\partial x_j}\frac{\partial \tau}{\partial x_j} - \frac{2}{\tau}\left(\nu + \frac{\nu_t}{\sigma_\varepsilon}\right)\left(\frac{\partial \tau}{\partial x_j}\right)^2 \\ &+ \frac{\tau}{k}\left(\frac{\nu_t}{\sigma_\varepsilon} - \frac{\nu_t}{\sigma_k}\right)\frac{\partial^2 k}{\partial x_j^2} + \frac{\partial}{\partial x_j}\left[\left(\nu + \frac{\nu_t}{\sigma_\varepsilon}\right)\frac{\partial \tau}{\partial x_j}\right]\end{aligned} \tag{45}$$

Note that there are some peculiar effects in the modelled τ- equation:

- The production and destruction term using standard values for the coefficients, gives that the production term decreases τ, while the destruction term increases τ.
- The destruction term is constant, and set according to the used coefficient ($C_{\varepsilon 2}$). This makes the equation numerically stiff which is a disadvantagous feature of the τ-equation.
- Compared with the ω-equation an additional term appears, namely the square of the derivate of τ.

4.6 Wilcox and the $k-\omega$ model

It can be claimed that the ω-equation in the standard $k-\omega$ [52] was derived using the more complex method of transforming a $k-\varepsilon$ model to a $k-\omega$. It is however more likely that the simpler route of dimensionally modify the k-equation was used, since the ω-model only composes of a production term, a destruction term and the two standard diffusion terms (turbulent- and viscous- respectively).

Thus using method 1, the k-equation is multiplied with ω/k to yield the ω-equation as:

$$\frac{D\omega}{Dt} = \underbrace{C_{\omega 1}f_\omega}_{\alpha}\frac{\omega}{k}P_k - \underbrace{C_{\omega 2}}_{\beta}\omega^2 + \frac{\partial}{\partial x_j}\left[\left(\nu + \frac{\nu_t}{\sigma_\omega}\right)\frac{\partial \omega}{\partial x_j}\right] \tag{46}$$

The Wilcox $k-\omega$ models use a slightly different nomenclature for both coefficients and Schmidt numbers, than shown above; here however, for clarity, a more general nomenclature is used. The Wilcox nomenclature (α, β) is also noted above.

The difference between the ω-equation of the few $k-\omega$ models is restricted to, as in the case of the ε-equation: the values of the Schmidt number (σ_ω), coefficients and damping functions.

There is however, an additional (unnecessary) complexity connected to $k-\omega$ models, which is the definition of ω. There exist two different versions:

$$\begin{aligned}\omega \equiv&\frac{\varepsilon}{k} \\ \omega \equiv&\frac{\varepsilon}{\beta^* k}\end{aligned} \qquad \begin{matrix}\\ \text{Wilcox}\end{matrix}$$

with $\beta^* = 0.09$.

There is no particular modelling reason for either of them, and hence the author thinks that the first version should be used in order the minimize confusion, as well as showing the clear similarity between the ε- and ω-equation. Unfortunately, Wilcox when designing the standard $k-\omega$ model, used the second formulation, and since then that version has prevailed. There is only a few modelers that use the alternative version, eg. Abid *et al.* [2].

Due to the additional constant in the definition of ω for the Wilcox models the turbulent viscosity is modeled as:

$$\nu_t = \alpha^* \frac{k}{\omega} \tag{47}$$

with $\alpha^* \rightarrow 1$ in order to predict the same level of turbulence. For the WLR α^*, is damped close to the wall, while in the WHR it is unity, see Section 4.1.

The Schmidt numbers[4] for the Wilcox $k-\omega$ models are:

WHR	WLR
2.0	2.0

with the coefficients $C_{\omega 1}(\alpha)$ and $C_{\omega 2}(\beta)$ as:

	WHR	WLR
$C_{\omega 1}$	0.55	0.55
$C_{\omega 2}$	0.075	0.075

As can be seen the ω-equation of the WHR and WLR models are identical apart from an added damping function to the production term of the latter. $C_{\omega 1}$ is in the WLR-model multiplied with the following relation:

$$f_\omega = \frac{0.1 + 10R_t/27}{1 + 10R_t/27} \tag{48}$$

The two models are usually referred to as the HRN version (WHR) and LRN version (WLR) of the standard $k-\omega$.

4.7 Speziale and the $k-\tau$ model

The only two-equation EVM that utilizes the τ-equation is the model by Speziale *et al.* [47]. Speziale, contrary to Wilcox, took almost certainly the more complicated road toward the construction of a secondary transport equation, since all the additional terms, as presented in Eq. 45, are present in the SAA-model:

$$\begin{aligned}\frac{D\tau}{Dt} =& (1-C_{\varepsilon 1})\frac{\tau}{k}P_k - (1-C_{\varepsilon 2}f_2) + \\ &+ \frac{2}{k}\left(\nu + \frac{\nu_t}{\sigma_{\tau 1}}\right)\frac{\partial k}{\partial x_j}\frac{\partial \tau}{\partial x_j} - \\ &- \frac{2}{\tau}\left(\nu + \frac{\nu_t}{\sigma_{\tau 2}}\right)\left(\frac{\partial \tau}{\partial x_j}\right)^2 + \\ &+ \frac{\partial}{\partial x_j}\left[\left(\nu + \frac{\nu_t}{\sigma_{\tau 2}}\right)\frac{\partial \tau}{\partial x_j}\right]\end{aligned} \tag{49}$$

with the $\partial^2 k/\partial x_j^2$-term zero due to identical Schmidt numbers. The coefficients used in the model are:

[4]Note that Wilcox use the reciprocal denotation for the Schmidt number, here however for clarity the standard praxis is used.

$C_{\varepsilon 1}$	$C_{\varepsilon 2}$	$\sigma_{\tau 1}$	$\sigma_{\tau 2}$
1.44	1.83	1.36	1.36

with the damping function defined as:

$$f_2 = \left[1 - \frac{2}{9}\exp\left(-\frac{R_t^2}{36}\right)\right]\left[1 - \exp\left(-\frac{y^+}{4.9}\right)\right]^2 \tag{50}$$

Note that the first part of the damping function is included in $C_{\varepsilon 2}$ in the Speziale *et al.* paper.

5 The TSDIA and DNS Revolution

In this section models which have been developed using DNS-data or TSDIA, either directly or indirect will be treated.

With the appearance of DNS-data for fully developed flow, Kim *et al.* [20], $Re_\tau = 180$, Kim [18], $Re_\tau = 395$ and Moser *et al.* [33], $Re_\tau = 590$, the modelling of turbulence models, and especially the dissipation rate equation, has been improved. Several papers have analyzed the computed DNS-data, eg. Mansour *et al.* [29], and Rodi and Mansour [43], which have resulted in new proposals to the modelling of the individual terms in the exact equations.

Yoshizawa [59] used a different approach to improve the turbulence models. Based on the two-scale direct-interaction approximation (TSDIA), he came up with new modelling strategies, which introduces cross-diffusion terms in both the $k-$ and ε-equations.

In the paper these diffusion terms are, in the k-equation:

$$D_k = \underbrace{\frac{\partial}{\partial x_j}\left(C_{kk}\frac{k^2}{\varepsilon}\frac{\partial k}{\partial x_j}\right)}_{T_k} + \frac{\partial}{\partial x_j}\left(C_{k\varepsilon}\frac{k^3}{\varepsilon^2}\frac{\partial \varepsilon}{\partial x_j}\right) \tag{51}$$

and in the ε-equation:

$$D_\varepsilon = \underbrace{\frac{\partial}{\partial x_j}\left(C_{\varepsilon\varepsilon}\frac{k^2}{\varepsilon}\frac{\partial \varepsilon}{\partial x_j}\right)}_{T_\varepsilon} + \frac{\partial}{\partial x_j}\left(C_{kk}k\frac{\partial k}{\partial x_j}\right) + \\ + C_{k^2}\left(\frac{\partial k}{\partial x_j}\right)^2 + C_{k\varepsilon}\frac{k}{\varepsilon}\frac{\partial k}{\partial x_j}\frac{\partial \varepsilon}{\partial x_j} + C_{\varepsilon^2}\frac{k^2}{\varepsilon^2}\left(\frac{\partial \varepsilon}{\partial x_j}\right)^2 \tag{52}$$

Note that the standard turbulent diffusion terms, T_k and T_ε, respectively, are included and note also that the denotation of the coefficient have been changed compared with the paper.

Using these new findings a number of models have seen the light which mimick DNS-data for both k^+- and ε^+- profiles, and in some cases even their budgets. Rodi and Mansour [43] (RM), Nagano and Shimada [34] (NS) and Peng *et al.* [38] (PDH) used results from DNS analysis, while Yoon and Chung [58] (YC), Hwang and Lin [17] (HL), Rahman and Siikonen [40] (RS) and Bredberg *et al.* [7] (BPD) used TSDIA results.

5.1 Turbulent Time Scales?

Although the idea of a specific turbulent time scale does not originate from either DNS-data or TSDIA, it is questionable that it would have evolved in such a way without the aid of DNS-databases.

Similar to the $k-\tau$ model, several $k-\varepsilon$ models use the turbulent time scale, τ, as a substitute for the ratio, k/ε. Little is however gained through only a nomenclature change and hence these models also included modifications to the turbulent time scale.

The standard argument to introduce a specific time scale is that near a wall the flow is not turbulent anymore, and hence using turbulent quantities to define the time scale is not appropriate. Employing $\tau = k/\varepsilon$ results in that the time scale vanishes when approaching a wall, where k is zero, and ε non-zero. Instead the common praxis is to invoke the Kolmogorov time scale which is based on the molecular viscosity and the dissipation as $\tau_K = \sqrt{\nu/\varepsilon}$. Near a wall this relation is preferable as both quantities are valid and non-zero.

Durbin [13] in his $k-\varepsilon-v^2-f$ model, was one of the first to introduce a Kolmogorov time scale, in the definition of the time scale:

$$\tau = \max\left(\frac{k}{\varepsilon}, C_T\sqrt{\frac{\nu}{\varepsilon}}\right) \tag{53}$$

with $C_T = 6.0$. This relation is substituted with k/ε in both the formulation of the turbulent viscosity, and in the ε-equation.

The idea of a specific time scale is also used by the YS- and RS-models, however with slightly different definitions:

$$\tau = \frac{k}{\varepsilon} + \sqrt{\frac{\nu}{\varepsilon}} \qquad \text{YS}$$

$$\tau = \max\left(\frac{k}{\tilde{\varepsilon}}, \sqrt{2\frac{\nu}{\varepsilon}}\right) \qquad \text{RS}$$

The reduced dissipation rate, $\tilde{\varepsilon}$, in the RS-model is computed as $\tilde{\varepsilon} = \varepsilon - \hat{\varepsilon}$ with the boundary condition for ε given by $\varepsilon_w \equiv \hat{\varepsilon} = 2\nu k/y^2$.

5.2 Turbulent Viscosity

DNS/TSDIA-models use the same structure as the classic model in the formulation of the turbulent viscosity. However the time scale modified EVMs (YS and RS) uses the following relation:

$$\nu_t = C_\mu f_\mu k\tau \tag{54}$$

Note that the YS-model is classified as a classic model here, and is thus described in Section 4. The damping functions for the other models are:

$k-\varepsilon$ models:

$$\nu_t = C_\mu f_\mu \frac{k^2}{\varepsilon}$$

$$f_\mu = ? \qquad \text{YC}$$

$$f_\mu = \left(1-\exp(-0.002R_\varepsilon^2)\right) \times \left[1+\frac{80}{R_t}\exp\left\{-\left(\frac{R_t}{40}\right)\right\}\right] \qquad \text{NS}$$

$$f_\mu = 1-\exp(-0.01y_\lambda - 0.008y_\lambda^3) \qquad \text{HL}$$

$$f_\mu = 1-\exp(-0.01R_\lambda - 0.0068R_\lambda^3) \qquad \text{RS}$$

Note that the RS-model use the turbulent time scale, τ instead of k/ε in the definition of ν_t.

$k-\omega$ **models:**

$$\nu_t = C_\mu f_\mu \frac{k}{\varepsilon}$$

$$f_\mu = 0.025 + \left[1 - \exp\left(\frac{R_t}{10}\right)^{3/4}\right] \times \left[0.975 + \frac{0.001}{R_t}\exp\left\{-\left(\frac{R_t}{200}\right)^2\right\}\right] \quad \text{PDH}$$

$$f_\mu = 0.09 + \left(0.91 + \frac{1}{R_t^3}\right) \times \left[1 - \exp\left\{-\left(\frac{R_t}{25}\right)^{2.75}\right\}\right] \quad \text{BPD}$$

Strangely enough the YC-models damping function was not described in the paper, and since near-wall results are presented, it is unlikely that f_μ is unity, as for HRN-models. The model is anyhow included here, since it is one of few models that uses TSDIA results. The effect of the various damping functions are shown in Fig. 11. Note that for the DNS-data, f_μ is computed using, Eq. 22, normalized with $C_\mu = 0.09$. As indicated by the figure this value is slightly too high, as f_μ does not reach unity.

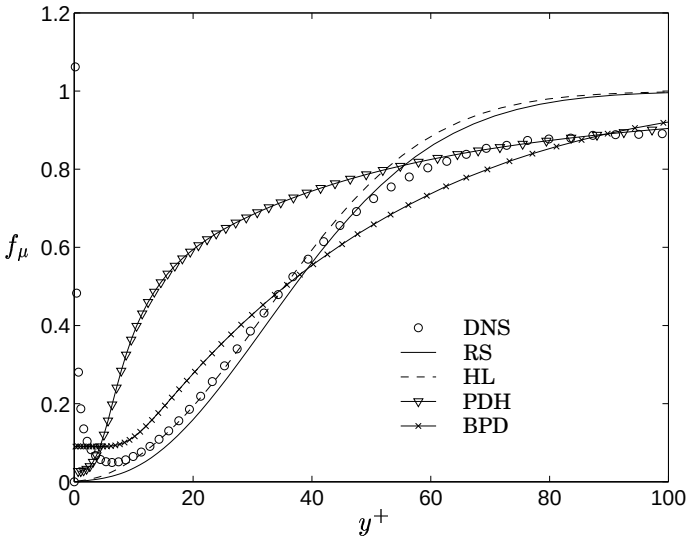

Figure 11: f_μ in the near wall region. $Re_\tau = 590$

5.3 Coupled Gradient and the Pressure-diffusion Process

Based on the Two-Scale Direct-Interaction Approximation (TSDIA) of Yoshizawa [59] there appear a number of coupled gradient terms in the k- and ε-equation. These are usually referred to as cross-diffusion terms. By cross-diffusion it is meant that the term is a product of gradient of both turbulent quantities, ie. eg. $\partial k/\partial x_j \partial \varepsilon/\partial x_j$.

It is argued in several models that the cross-diffusion terms are beneficial to the accuracy of the model, and that they have a similar effect on the equations as the pressure-diffusion term in the exact equations.

The inclusion of cross-diffusion terms in the secondary equation could also be the results of the transformation from the ε-equation to either a ω- or a τ-equation. In both cases there appear cross-diffusion terms (as well as other terms) in the transformed equation. Through wisely chosen Schmidt numbers (they need to be identical, see Appendix D) the cross-diffusion terms may be the only failing link between a transformed $k-\varepsilon$ model and a $k-\omega$ model. Thus by adding a cross-diffusion term to the ω-equation, the behaviour of the $k-\omega$ model would be similar to the $k-\varepsilon$ model; further information is given in the next section.

A well documented discrepancy of the $k-\omega$ models is the sensitivity of the predictions to the freestream value of ω, see eg. Menter [31]. Thus by adding a cross-diffusion term to the ω-equation the $k-\omega$ model could become more universal. $k-\omega$ models which include a cross-diffusion term are eg. Menter [32] Peng *et al.* [38], Kok [22], Wilcox [54], Bredberg *et al.* [7].

Another reason for the inclusion of these additional terms is numerical. The classic versions of both the k- and ε-equation are not well balanced close to a wall because there is a missing term: the pressure-diffusion. Since the classic models were mostly based on 1) experiments – which are unable to measure the pressure-diffusion, and 2) theory – which shows its relatively small importance, the pressure-diffusion term was with good arguments neglected.

The appearance of DNSs have however improved the understanding of the near-wall behaviour of turbulent quantities, and also supplied a valuable data base. Using both near-wall asymptotic analysis of the individual term and the budgets of the transport equations, the importance of the pressure-diffusion term close to a wall can be established.

This is graphically shown for the k-equation in Fig. 4, while an asymptotic analysis of the terms in the ε-equation is given by the table on page 8. Although hardly discernible in Fig. 4 the dissipation, ε, in the k-equation is balanced by the viscous diffusion, D_k, and the pressure-diffusion, Π_k in the near-wall region. Simiarly the non-zero ($\sim y^0$) (thus important) terms at the wall in the ε-equation are the destruction, Φ_ε, the viscous diffusion, D_ε^ν and the pressure-diffusion, Π_ε.

Especially the classic ε-equation benefits from the addition of a pressure-diffusion term, since in these models the wall value for the dissipation is set using either a fixed ε_w, as in the ε-models (YS, AKN) or by adding a term, E, as in the $\tilde{\varepsilon}$-models (JL, C, LSY, RS, HL, NS).

5.3.1 The k-equation

The result of the TSDIA operation of the k-equation, is two diffusion terms. The first term is the standard diffusion term (SGDH), while the second term is a cross-diffusion term.

Of the newer model included in this paper, three use an additional diffusion term in the k-equation. These are the NS-, HL- and RS-models. Only Rahman-Siikonen cite the TSDIA results as the main origin for this term. Nagano-Shimada and Hwang-Lin argue the

inclusion of an additional term from near-wall asymptotic analysis.

NS and HL state that this additional diffusion term gives similar effect to the k-equation as the exact pressure-diffusion term, even though their dissimilarities, and hence denote it Π_k. Rahman and Siikonen on the other hand don't give any physical reasoning behind the term, and simple denote it E_k:

$$
\begin{aligned}
E_k &= \frac{1}{2}\nu_t \min\left[\frac{\partial(k/\varepsilon)}{\partial x_j}\frac{\partial\tilde{\varepsilon}}{\partial x_j}, 0\right] && \text{RS}\\
\Pi_k &= \max\left[\frac{\partial}{\partial x_j}\left\{\nu\frac{\partial k}{\partial x_j} - \exp\left(-\frac{R_\varepsilon}{8}\right)\varepsilon \right.\right.\\
&\qquad \left.\left. \times\frac{\sqrt{2k}}{2}\left(\sqrt{\frac{\nu}{\varepsilon}} + \sqrt{\frac{\nu}{\varepsilon_w}}\right)\right\}, 0.\right] && \text{NS}\\
\Pi_k &= -\frac{1}{2}\frac{\partial}{\partial x_j}\left(\nu\frac{k}{\varepsilon}\frac{\partial\hat{\epsilon}}{\partial x_j}\right) && \text{HL}
\end{aligned}
$$

The main difference between the three models are that the RS-model is purely a turbulent term, similar to the TSDIA-result. The two others models include viscous effects, through the usage of the molecular viscosity. The latter is more plausible, if a comparison is made to the pressure-diffusion term, since a turbulent term become zero close to a wall where the pressure-diffusion term is most important.

Because there is no reference to the pressure-diffusion process in the RS-model, it is of more interest to compare it with the TSDIA result, Eq. 51. Although the formulations are similar, they are not identical, which can be shown by expanding them and including the stated coefficients:

RS-formulation:

$$0.045\left[\frac{k^2}{\varepsilon^2}\frac{\partial k}{\partial x_j}\frac{\partial\varepsilon}{\partial x_j} - \frac{k^3}{\varepsilon^3}\left(\frac{\partial\varepsilon}{\partial x_j}\right)^2\right]$$

TSDIA-formulation (Eq. 51):

$$-0.72\left[3\frac{k^2}{\varepsilon^2}\frac{\partial k}{\partial x_j}\frac{\partial\varepsilon}{\partial x_j} - 2\frac{k^3}{\varepsilon^3}\left(\frac{\partial\varepsilon}{\partial x_j}\right)^2 + \frac{k^3}{\varepsilon^2}\frac{\partial^2\varepsilon}{\partial x_j^2}\right]$$

As can be seen there is one term missing in the RS-formulation, but worse is that the terms have opposite sign. The coefficients in the RS-model are also markedly lower.

This latter fact is however of minor importance as coefficient are normally based more on numerical tuning than theoretical foundations. As a comparison the coefficient for the SGDH term is also markedly different: $1.27k^2/\varepsilon$ in TSDIA, compared with: $0.09k^2/\varepsilon$, in the standard $k-\varepsilon$ model.

Although the HL-model is a viscous term, its construction is very similar to the TSDIA model. If k^2/ε in the TSDIA formulation is exchanged with ν, the two models becomes identical, with only the coefficients different. Naturally the behaviour of the molecular and turbulent viscosity are very different, and hence such a comparison is really not appropriate.

The main argument for the term in the HL-model is however the need for a well balanced k-equation near the wall, for which the above model is well suited.

The NS-model differs remarkebly from the HL-model, and its formulation is rather questionable. The first term, $\nu\partial^2 k/\partial x_j^2$, is identical to the viscous diffusion, while the second term is very similar to the square-root of the boundary condition for ε used in the JL- and LSY-models, see Eq. 15:

$$
\begin{aligned}
\sqrt{\varepsilon_w} &= \sqrt{2\nu}\frac{\partial\sqrt{k}}{\partial x_j} && \text{JL, LSY}\\
&\stackrel{?}{=} \exp\left(-\frac{R_\varepsilon}{8}\right)\sqrt{2\nu}\frac{\partial}{\partial x_j}\left(\sqrt{k}\sqrt{\varepsilon}\right) && \text{NS}
\end{aligned}
$$

Note that ε_w has been substituted with ε in the NS-formulation to simplify the comparison. In the limit of $y \to 0$ these are identical, and hence it is a valid substitution.

The only difference between the two models is the addition of $\sqrt{\varepsilon}$ inside the gradient and the exponential function in the NS-model. The addition of $\sqrt{\varepsilon}$ is of course necessary to ensure the correct dimension. Assuming a constant gradient of ε close to the wall it is fair to state that the NS-model adds $\varepsilon_w - C\sqrt{\varepsilon_w}$ to the k-equation through the Π_k term.

5.3.2 The ε-equation

Compared to the k-equation, the TSDIA result for the ε-equation includes a wealth of different terms. In fact all the possible combination of gradients of ε and k is represented and of course no EVM utilizes all these forms. Models that explicitly state that the origins for the cross-diffusion terms are from the TSDIA are the YC- and RS-models, while the other two models (NS and HL) argue from a balancing point of view.

As for the k-equation, the additional term is simply denoted E_ε for the TSDIA models (YC, RS), while the NS- and HL-models states that they are adding a pressure-diffusion term, and hence denote the term, Π_ε:

$$
\begin{aligned}
E_\varepsilon &= -0.1134\frac{k^3}{\varepsilon}\frac{\partial(\varepsilon/k)}{\partial x_j}\frac{\partial k}{\partial x_j} && \text{YC}\\
\Pi_\varepsilon &= -\max\left[\nu\frac{\partial}{\partial x_j}\left(\frac{\tilde{\varepsilon}}{k}\frac{\partial k}{\partial x_j}\right), 0.\right] && \text{NS}\\
\Pi_\varepsilon &= -\nu\frac{\partial}{\partial x_j}\left(\frac{\tilde{\varepsilon}}{k}\frac{\partial k}{\partial x_j}\right) && \text{HL}\\
E_\varepsilon &= -\frac{\nu_t}{\tau^2}\frac{\partial(k/\varepsilon)}{\partial x_j}\frac{\partial k}{\partial x_j} && \text{RS}
\end{aligned}
$$

Note that the expression for the YC-model is most probably erroneous, since the dimension is not correct. In the following the multiplier k^3/ε has been changed to k^2/ε to yield the correct dimension.

Note also that τ in the RS-model, is defined according to what was stated in the above Section 5.1.

The NS and HL models are almost identical, while the YC (the corrected version) and RS are similar. RS uses the gradient of the turbulent time, while the YC-model uses its reciprocal, ω. Both models combine this with the

gradient of k. The expression in front of the gradients are merely to correct the dimension using a combination of k, ε and ν, for all models.

A noteworthy reflection is that similar to the added term in the k-equation, the HL- and NS-models use a viscous term, while the YC- and RS-models use a turbulent term.

The connection to the full derived expression of Yoshizawa (Eq. 52) is loose, however at least the YC- and RS-model retains some of the terms in the TSDIA expression, which can be visualized through a simplification of the expressions:

$$\frac{k^2}{\varepsilon}\frac{\partial(\varepsilon/k)}{\partial x_j}\frac{\partial k}{\partial x_j} = \frac{k}{\varepsilon}\frac{\partial k}{\partial x_j}\frac{\partial \varepsilon}{\partial x_j} - \left(\frac{\partial k}{\partial x_j}\right)^2 \quad \text{YC}$$

$$\frac{\partial}{\partial x_j}\left(\nu\frac{\varepsilon}{k}\frac{\partial k}{\partial x_j}\right) = \frac{\nu}{k}\frac{\partial k}{\partial x_j}\frac{\partial \varepsilon}{\partial x_j} - \frac{\nu\varepsilon}{k^2}\left(\frac{\partial k}{\partial x_j}\right)^2 - \frac{\nu\varepsilon}{k}\frac{\partial^2 k}{\partial x_j^2} \quad \text{HL, NS}$$

$$\frac{\nu_t}{T_t^2}\frac{\partial(k/\varepsilon)}{\partial x_j}\frac{\partial k}{\partial x_j} = -\frac{\nu_t}{k}\frac{\partial k}{\partial x_j}\frac{\partial \varepsilon}{\partial x_j} + \frac{\nu_t \varepsilon}{k^2}\left(\frac{\partial k}{\partial x_j}\right)^2 \quad \text{RS}$$

All three models include the cross-diffusion term, $\partial\varepsilon/\partial x_j \partial k/\partial x_j$, and the square of the derivate of k. The NS- and HL-models also include the second derivate of k.

Which of the different terms that are most important is not reported in the Yoshizawa paper. From a numerical standpoint it is however disadvantageous to include any second derivate in the modelling, similarly to the NS- and HL-models.

It should also be noted that any term which is constructed with the molecular viscosity may be numerically unstable. In particular when ν is multiplied with gradients of quantities which are unrestricted. There is always a risk that during the iterative process such a term may become un-proportionally large. A code running with either the NS- and HL-models would thus most probably be less numerical stable than the other formulations.

5.3.3 The ω-equation

There exists, at least to the best knowledge of the author, no $k-\omega$ models that are directly based on results from either TSDIA or DNS-data.

In order to get DNS-data for an ω-equation it is necessary to derive an exact ω-equation, which is a function of primitive quantities, such as u', p' etc. Using DNS-data it would then be possible to compute the individual terms in the ω-equation and then use this as a modelling basis for the $k-\omega$ model. However as the accuracy of the budget in the ε-equation is rather questionable, and seldom directly used, the (possible) marginal gains of such a derivation is not in balance with the arduous workload needed.

In addition it is questionable how to formulate the exact ω-equation, even to exactly define ω. The reciprocal time scale, or the specific dissipation rate? It is most possible that the exact ω-equation will be quite different dependent on the concept of ω.

Thus the common praxis, also used here, is to either make a direct substitution of ε to ω or do a proper transformation of a $k-\varepsilon$ model to a $k-\omega$ model, as was done in Section 4.6. Note however that already in the formulation of the ε-equation we are using modelled terms. Thus dependent on the original $k-\varepsilon$ model, there will exist a number of different ω-equations. A discussion regarding this is left to the next Section. Note also that the k-equation will always be unaffected by this transformation.

The result of transforming the classic $k-\varepsilon$ model was shown in Eq. 43. The two additional terms in the ω-equation as compared with the standard $k-\omega$ model of Wilcox are the cross-diffusion term:

$$\frac{2}{k}\left(\nu + \frac{\nu_t}{\sigma_\varepsilon}\right)\frac{\partial k}{\partial x_j}\frac{\partial \omega}{\partial x_j} \tag{55}$$

and the turbulent diffusion like term:

$$\frac{\omega}{k}\left(\frac{\nu_t}{\sigma_\varepsilon} - \frac{\nu_t}{\sigma_k}\right)\frac{\partial^2 k}{\partial x_j^2} \tag{56}$$

The two models which are based on this transformation, the PDH- and BPD-models, include only the cross-diffusion term, while the second gradient of k-term is dropped. In the case of the PDH-model only a turbulent part is retained, while the BPD-model includes both a viscous and turbulent part of the cross-diffusion term:

$$C_\omega \frac{\nu_t}{k}\frac{\partial k}{\partial x_j}\frac{\partial \omega}{\partial x_j} \quad \text{PDH}$$

$$C_\omega \left(\frac{\nu}{k} + \frac{\nu_t}{k}\right)\frac{\partial k}{\partial x_j}\frac{\partial \omega}{\partial x_j} \quad \text{BPD}$$

with C_ω numerically optimized to:

PDH	BPD
0.75	1.1

It should be noted that the addition of a viscous term necessitates a modification of the other terms in the ω-equation, since this term make the standard $k-\omega$ unbalanced in the near-wall, while a turbulent term only modifies the equation further out, and could be added to existing models.

The main argument for this cross-diffusion term varies, however several authors, including Menter [31], [32], Peng *et al.* [38], Kok [22], Wilcox [54], claim that it improves the prediction of flows with a freestream boundary, for which the Wilcox $k-\omega$ is less accurate. In the derivation of the BPD-model [7] the viscous term was however attributed to model a pressure-diffusion process.

5.4 Fine-tuning the Modelled Transport Equations

5.4.1 The k-equation

Apart from the addition of a cross-diffusion, some of the newer models also incorporate a variable Schmidt number, which, if the SGDH-model is used, is necessary to

simulate the near-wall reduction of the diffusion. The NS- and HL-model use such a scheme:

$$\sigma_k = \frac{1.2}{1+5\exp(-R_\varepsilon/8)} \qquad \text{NS}$$
$$\sigma_k = 1.4 - 1.1\exp\left(-\frac{y_\lambda}{10}\right) \qquad \text{HL}$$

Using *a priori* tests the HL-model faithfully reproduce DNS-data, however one should be careful to include too many flow dependent variables into a model, as those are more likely to introduce numerical problems.

The other models (YC, RS, PDH and BPD) use a standard constant Schmidt number:

$k-\varepsilon$		$k-\omega$	
YC	RS	PDH	BPD
1	1	0.8	1

Note that the PDH-model has chosen a slightly lower Schmidt number than the commonly used. However as the basis for choosing a unity value is rather vague, as the models above indicate, there should be nothing to deter modellers from change σ_k through numerical optimization.

In addition the PDH-model uses a variable coefficient for the dissipation term, through an additional damping function, f_k:

$$\begin{aligned} \varepsilon &= C_k f_k \omega k \\ f_k &= 1 - 0.722\exp\left[-\left(\frac{R_t}{10}\right)^4\right] \end{aligned} \tag{57}$$

5.4.2 The ε-equation

The sections below follow the presentation in the comprehensive paper on the modelling of the ε-equation by Rodi and Mansour, [43].

Modelling the production terms, P_ε^1 and P_ε^2: Because these terms give a negative source of ε, ie. being destruction terms, they are treated togther with the destruction term, below.

Modelling the production term, P_ε^3: In comparison to the other production terms, this term is very small, however relatively to the sum of $P_\varepsilon^1 + P_\varepsilon^2 + P_\varepsilon^4 - \Phi_\varepsilon$, it becomes significant. Rodi and Mansour [43] devised the following model for the P_ε^3-term:

$$P_\varepsilon^3 = C_{\varepsilon 3}\nu\nu_t\left(\frac{\partial^2 U}{\partial y^2}\right)^2 + C_{\varepsilon 4}\nu\frac{k}{\varepsilon}\frac{\partial k}{\partial y}\frac{\partial U}{\partial y}\frac{\partial^2 U}{\partial y^2} \tag{58}$$

where $C_{\varepsilon 3}$ and $C_{\varepsilon 4}$ are tunable constants.

The first term is identical to the term used in the models by Launder *et al.* (JL and LSY), (with $C_{\varepsilon 3} = 2$), while the second is a numerically cumbersome construction. The predictions when including both terms in the ε-equation are however improved, at least for channel flows.

The NS-model uses, similarly to Launder, only the first term, however with a different coefficient:

$$\begin{aligned} C_{\varepsilon 3} &= (1-f) \\ f &= 1 - \exp(-0.002R_\varepsilon^2) \end{aligned} \tag{59}$$

The models based on the TSDIA results (YC and RS) do not include a model for this term.

Modelling the production term, P_ε^4: The fourth production term is the main production and is modelled in the classic way:

$$P_\varepsilon^4 = C_{\varepsilon 1} f_1 \frac{\varepsilon}{k} P_k \tag{60}$$

where none of the models utilize the damping function, thus $f_1 = 1$. The coefficient, $C_{\varepsilon 1}$, is set to:

YC	NS	HL	RS
1.17	1.45	1.44	1.44

Note that the YS- and RS-models use the turbulent time scale, instead of k/ε, in the relation for the production term.

Modelling the destruction term, Φ_ε: As noted above the model for the destruction term, is the sum of the two first production terms and the destruction term. In these newer turbulence models the destruction term is modelled as in the classic model:

$$\Phi_\varepsilon = C_{\varepsilon 2} f_2 \frac{\varepsilon^2}{k} \tag{61}$$

f_2, the damping function, is used only in the NS-model:

$$f_2 = 1 - 0.3\exp\left[-\left(\frac{R_t}{6.5}\right)^2\right] \tag{62}$$

The coefficient $C_{\varepsilon 2}$ is given the following value:

YC	NS	HL	RS
1.92	1.9	1.92	1.92

Modelling turbulent diffusion: The turbulent diffusion is modelled as in the classic model using the standard gradient hypothesis (SGDH):

$$T_\varepsilon = \frac{\partial}{\partial x_j}\left(\frac{\nu_t}{\sigma_\varepsilon}\frac{\partial \varepsilon}{\partial x_j}\right) \tag{63}$$

The difference among the turbulence models is restricted to the Schmidt number:

$$\sigma_\varepsilon = 0.75 \qquad \text{YC}$$
$$\sigma_\varepsilon = \frac{1.4}{1+5\exp(-R_\varepsilon/8)} \qquad \text{NS}$$
$$\sigma_\varepsilon = 1.3 - \exp\left(-\frac{y_\lambda}{10}\right) \qquad \text{HL}$$
$$\sigma_\varepsilon = 1.3 \qquad \text{RS}$$

The NS- and HL-models adopt damping functions similar to that for the k-equation, see above. The other models use constant Schmidt numbers.

Viscous diffusion: Since this term is exact, it is not modelled:

$$D_{\varepsilon}^{\nu} = \frac{\partial}{\partial x_j}\left(\nu \frac{\partial \varepsilon}{\partial x_j}\right) \tag{64}$$

5.4.3 The ω-equation

Similar to the $k-\varepsilon$ models, the main change made to the $k-\omega$ models, due to DNS-data, has been to improve and add damping functions. However for the ω-equation, there exists no rigid analysis as the one made by Rodi and Mansour, and hence improvements are purely based on numerical optimization.

The PDH- and BPD-models introduce an additional cross-diffusion term, as noted previously, but are otherwise similar to the standard $k-\omega$ model.

Production: The PDH-model adds a damping function, in the modelling of the production term, whereas the BPD-model only differs through the coefficient, $C_{\omega 1}$:

PDH	BPD
0.42	0.49

with the damping function in the PDH given as:

$$f_{\omega} = 1 + 4.3 \exp\left[-\left(\frac{R_t}{1.5}\right)^{1/2}\right] \tag{65}$$

Destruction: The model for the destruction is the same as for the standard $k-\omega$ model $C_{\omega 2}\omega^2$, with only marginally different coefficients, $C_{\omega 2}$:

PDH	BPD
0.075	0.072

Turbulent diffusion: The SGDH-model is used with different Schmidt numbers compared to the Wilcox $k-\omega$ models:

PDH	BPD
1.35	1.8

In summation the DNS-data have, similarly to the $k-\varepsilon$ models, been used to improve the predictions for the $k-\omega$ models, however for the latter models the change is less fundamental and only apply to improved damping functions and coefficients. The only additional term, the cross-diffusion term in the ω-equation, appears more due to the transformation of the ε-equation than to DNS-data.

6 Enhancing the ω-equation?

Even though the emphasis of this report is general, ie. that all types of EVMs are discussed, this section will be entirely devoted to the $k-\omega$-type of models. In some way this reflects the good experience of the $k-\omega$ models by the author, however equally important is to produce a counter-balance to the wealth of information regarding the $k-\varepsilon$-type of models. In addition anyone who desires to develop a new $k-\varepsilon$ model, may consult both DNS-data and the TSDIA analysis to enhance the modelling. The basis for improving a $k-\omega$ model relays more on enhanced treatment of transformations and improved understanding of modelling theory, which is the purpose of the present report. It should however be recognized that in the end all turbulence models are numerically tuned using test-cases, with comparison to experiments and, if available, DNS-data. The performance of the model for basic flows, included in Appendix B, is a most important issue in the validation procedure.

There will be numerous references made to the Bredberg *et al.* [7] BPD-model as this report is partly the result of the work done during the development phase of the new model. The main focus in the following analysis will be the origin and connection of the cross-diffusion terms in various recent turbulence models.

6.1 Transforming the DNS/TSDIA $k-\varepsilon$ models

In the above sections, the modelling of the ω-equation in the PDH and BPD $k-\omega$ models was discussed in connection with the transformation of the standard $k-\varepsilon$-equation, using the relations shown in Eq. 43. It is however unnecessary to use the inaccurate classic $k-\varepsilon$ model as the basis for such a transformation when there exists newer and more accurate versions.

Below, instead of employing the classic $k-\varepsilon$ model, the TSDIA/DNS modified $k-\varepsilon$ models which include additional terms will be used. In the formulation of the ω-equation, as shown in Eq. 42, terms in the k-equation should be multiplied with $-\omega/k$ and those in the ε-equation with $1/(C_k k)$.

6.1.1 Turbulent approach, YC- and RS-models

If the additional terms in the k- and ε-equations are modelled using a turbulent approach, as in the YC- and RS-models, the extra terms appearing in the ω-equation are (RS-model):

from the k-equation:

$$\begin{aligned} -\frac{\omega}{k}E_k &= \frac{1}{2}\nu_t \frac{\omega}{k}\frac{\partial (k/\varepsilon)}{\partial x_j}\frac{\partial \varepsilon}{\partial x_j} = \\ &= -\frac{\nu_t}{2k}\left[\frac{\partial \omega}{\partial x_j}\frac{\partial k}{\partial x_j} + \frac{k}{\omega}\left(\frac{\partial \omega}{\partial x_j}\right)^2\right] \end{aligned} \tag{66}$$

from the ε-equation:

$$\begin{aligned}\frac{1}{C_k k}E_\varepsilon &= -\frac{\nu_t}{T_t^2}\frac{1}{C_k k}\frac{\partial (k/\varepsilon)}{\partial x_j}\frac{\partial k}{\partial x_j} = \\ &= \frac{\nu_t}{kC_k^2\omega^2 T_t^2}\left[\frac{\partial \omega}{\partial x_j}\frac{\partial k}{\partial x_j}\right] = \left\{T_t = \frac{1}{C_k\omega}\right\} = \\ &= \frac{\nu_t}{k}\left[\frac{\partial \omega}{\partial x_j}\frac{\partial k}{\partial x_j}\right]\end{aligned} \tag{67}$$

The sum of the above terms becomes:

$$\frac{3\nu_t}{2k}\left[\frac{\partial \omega}{\partial x_j}\frac{\partial k}{\partial x_j}\right] + \frac{\nu_t}{2\omega}\left(\frac{\partial \omega}{\partial x_j}\right)^2 \tag{68}$$

Thus the addition of terms 'a la' the RS-model gives two terms in the modelled ω-equation. The first is similar to what results from classic transformation, while the second is a new construction.

6.1.2 Viscous approach, NS- and HL-models

If one instead uses the models of NS or HL, which involve viscous terms, then the extra terms appearing in the ω-equation is (HL-model):

from the k-equation:

$$\begin{aligned}-\frac{\omega}{k}\Pi_k &= -\frac{\omega}{k}\frac{\partial}{\partial x_j}\left(\nu\frac{k}{\varepsilon}\frac{\partial \varepsilon}{\partial x_j}\right) = \\ &= \frac{\nu}{\omega}\left(\frac{\partial \omega}{\partial x_j}\right)^2 - \frac{\nu}{k}\frac{\partial \omega}{\partial x_j}\frac{\partial k}{\partial x_j} - \nu\frac{\omega}{k}\frac{\partial^2 k}{\partial x_j^2} - \nu\frac{\partial^2 \omega}{\partial x_j^2}\end{aligned} \tag{69}$$

from the ε-equation:

$$\begin{aligned}\frac{1}{C_k k}\Pi_\varepsilon &= \frac{1}{C_k k}\frac{\partial}{\partial x_j}\left(\nu\frac{\varepsilon}{k}\frac{\partial k}{\partial x_j}\right) = \\ &= \frac{\nu}{k}\frac{\partial \omega}{\partial x_j}\frac{\partial k}{\partial x_j} + \nu\frac{\omega}{k}\frac{\partial^2 k}{\partial x_j^2}\end{aligned} \tag{70}$$

Summing them up yields the following extra terms in the ω- equation:

$$\frac{\nu}{\omega}\left(\frac{\partial \omega}{\partial x_j}\right)^2 - \nu\frac{\partial^2 \omega}{\partial x_j^2} = -\omega\frac{\partial}{\partial x_j}\left(\frac{\nu}{\omega}\frac{\partial \omega}{\partial x_j}\right) \tag{71}$$

The first term of the LHS is similar to what was found in the RS-model, although here it is a viscous term.

The second term (LHS) cancels out the normal viscous diffusion in the ω-equation which is indeed very strange! It is questionable if the HL-model pressure-strain model is very reliable. Such a model should nonetheless not be used in the modelling of ω-equation.

6.2 Additivional Terms in the ω-equation

Although it is possible to add any term with a dimensionally correct combination of k and ω, to the ω-equation, it feels however more important to especially note those term appearing from the transformations of the different $k-\varepsilon$ models.

6.2.1 Cross-diffusion, $\partial k/\partial x_j \partial\omega/\partial x_j$

The most frequent term in the resulting ω-equation, is the cross-diffusion term, $\partial k/\partial x_j \partial\omega/\partial x_j$. It appears due to the standard terms in the classic formulation, and also due to terms similar to both the RS-models E_k and E_ε, and the HL-models Π_k and Π_ε. Dependent on the magnitude of the term, the back-transformation of a $k-\omega$ model, see later, will possibly give a more correct $k-\varepsilon$ model, with a pressure-diffusion like term. Thus it is not surprising that the addition of a cross-diffusion term to the ω-equation was one of the first major modifications to the standard $k-\omega$ model.

6.2.2 Turbulent diffusion, $\partial^2 k/\partial x_j^2$

Transforming the standard $k-\varepsilon$ model, the second-gradient of k also appears in the ω-equation. However as repeatedly stated the coefficient in front of this term could be made small through proper usage of the Schmidt numbers. In any case any second-gradient term is unwanted in CFD-codes, due to implementation and numerical stability reasons.

6.2.3 Other terms

The two final terms from the transformation of the DNS/TSDIA modified $k-\varepsilon$ models are both relations of only ω, either using a first or second derivate. The NS- and HL-model resulted in a viscous diffusion term that canceled the normal diffusion term, and hence such a model is rather questionable. It would be possible to introduce a term based on the square of the derivate of ω, as $(\partial\omega/\partial x_j)^2$ to the ω-equation. It should however be noted that such a term would be very large close to a wall, and hence a viscous term based on this idea, as given by the NS- and HL-models, would be very difficult to make numerically stable. A model including the turbulent viscosity (RS- and YC-models), could possibly be introduced with the same arguments as the cross-diffusion term, however again with a more delicate tuning, due to the tendency of such a term to become inaccessibly large.

6.3 Back-transforming the ω-equation

From a modeller's point of view, the critical secondary quantity is the dissipation rate, since this is the only variable for which there exists an exact equation. In addition the availability of DNS-data for terms in the ε-equation makes it possible to scrutinize an ε-model to levels unreachable using any other secondary quantity. Using a $k-\omega$ model it is thus of the outermost interest to see the resulting terms in a ε-equation when the model is re-casted into a $k-\varepsilon$ model using the previous transformation rules. Selecting the BPD $k-\omega$ model as the basis – since this model includes most terms – the ε-equation is transformed as:

$$\begin{aligned}\frac{D\varepsilon}{Dt} =& \frac{D(C_k k\omega)}{Dt} = C_k k\frac{D\omega}{Dt} + C_k\omega\frac{Dk}{Dt} = \\ =& C_k k\left[P_\omega - \Phi_\omega + \Pi_\omega + T_\omega + D_\omega^\nu\right] + \\ &+ C_k\omega\left[P_k - \varepsilon + \Pi_k + T_k + D_k^\nu\right]\end{aligned} \tag{72}$$

	Vis: $\nu/k\times$ $\partial\varepsilon/\partial x_j\partial k/\partial x_j$	Turb: $\nu_t/k\times$ $\partial\varepsilon/\partial x_j\partial k/\partial x_j$
WHR	-2	-1
PDH	-2	-1.24
BPD	-0.9	-0.67
YC	0	$-1.26/f_\mu$
RS	0	1
HL,NS	-1	0

Table 3: Cross-diffusion term, $\partial\varepsilon/\partial x_j\partial k/\partial x_j$, in the ε-equation

	Vis: $\nu\varepsilon/k^2\times$ $(\partial k/\partial x_j)^2$	Turb: $\nu_t\varepsilon/k^2\times$ $(\partial k/\partial x_j)^2$
WHR	2	1
PDH	2	1.24
BPD	0.9	0.67
YC	0	$1.26/f_\mu$
RS	0	-1
HL,NS	1	0

Table 4: Terms involving the first derivate of k, $(\partial k/\partial x_j)^2$, in the ε-equation

The result becomes, see Appendix C:

$$\begin{aligned}\frac{D\varepsilon}{Dt} &= (1+C_{\omega 1})\frac{\varepsilon}{k}P_k - \left(1+\frac{C_{\omega 2}}{C_k}\right)\frac{\varepsilon^2}{k} - \\ &- \left[(2-C_1)\frac{\nu}{k} + \left(\frac{1}{\sigma_\omega}+\frac{1}{\sigma_k}-C_2\right)\frac{\nu_t}{k}\right]\frac{\partial k}{\partial x_j}\frac{\partial \varepsilon}{\partial x_j} \\ &+ \frac{\varepsilon}{k}\left[(2-C_1)\frac{\nu}{k} + \left(\frac{1}{\sigma_\omega}+\frac{1}{\sigma_k}-C_2\right)\frac{\nu_t}{k}\right]\left(\frac{\partial k}{\partial x_j}\right)^2 \\ &+ \frac{\varepsilon}{k}\left(\frac{\nu_t}{\sigma_k}-\frac{\nu_t}{\sigma_\omega}\right)\frac{\partial^2 k}{\partial x_j^2} + \frac{\partial}{\partial x_j}\left[\left(\nu+\frac{\nu_t}{\sigma_\omega}\right)\frac{\partial \varepsilon}{\partial x_j}\right]\end{aligned} \tag{73}$$

The coefficients C_1 and C_2 are the constants connected to the viscous- and turbulent cross-diffusion terms respectively. Because coefficients and damping functions are tunable, and also differ considerably among the $k-\varepsilon$ models they are left-out of the analysis. Table 3 and 4 however list the coefficients for the relevant terms.

The additional terms in the back-transformed ε-equation ($k-\varepsilon$ model $\rightarrow$ transformed ω-equation $\rightarrow$ $k-\omega$ model $\rightarrow$ back-transformed ε-equation), compared with the standard ε-equation, are;

- The cross-diffusion term: $\partial\varepsilon/\partial x_j\partial k/\partial x_j$.
- The term including the square of the first derivate of k: $(\partial k/\partial x_j)^2$.
- The second derivate of k: $\partial^2 k/\partial x_j^2$.

Based on the coefficients connected to each term, it is reasonable to pay less attention to the last term. In the case of equal Schmidt number this term is also identical zero. Note also that neither of the two models (RS, YC) that add a purely turbulent term to ε-equation include this term.

The two other terms are closely connected, and always appear together, however here more emphasis is paid to the cross-diffusion term.

Transforming the standard $k-\omega$ model (WHR) results in a negative cross-diffusion in the ε-model. The introduction of a cross-diffusion term in the ω-equation (PDH, BPD), could dependent on the magnitude of the coefficient, C_2, change this according to:

$$\begin{aligned} C_2 &> \frac{1}{\sigma_k}+\frac{1}{\sigma_\omega} \Rightarrow \Pi_\varepsilon > 0 \\ C_2 &= \frac{1}{\sigma_k}+\frac{1}{\sigma_\omega} \Rightarrow \Pi_\varepsilon = 0 \\ C_2 &< \frac{1}{\sigma_k}+\frac{1}{\sigma_\omega} \Rightarrow \Pi_\varepsilon < 0 \end{aligned} \tag{74}$$

Based on the construction of the newer $k-\varepsilon$ models and DNS-data suggest that the cross-diffusion in the ε-equation should be negative; however read also the discussion on the Yap-correction below.

The term with the first derivate of k, is similarly affected by the inclusion of a cross-diffusion term in the ω-equation, with the resulting condition as above, Eq. 74.

The coefficients from the transformed ε-equation of the different $k-\omega$ models and the new DNS/TSDIA modified ε-equation are gathered in tables 3 and 4.

6.4 Cross-diffusion Terms in the ω-equation?

So should there be a cross-diffusion term in the modelled ω -equation? Based on the above comparison one can not simply due to the effect of the cross-diffusion term in the ω-equation on the transformed ε-equation include the term. Transforming the standard ω-equation, eg. the WHR or WLR model, would also result in a cross-diffusion term in the ε-equation, if this is the appreciated result. However one should bare in mind, that it is only through the questionably high Schmidt numbers of the Wilcox's models that the coefficients in-front of the $\partial k/\partial x_j\partial\varepsilon/\partial x_j$-term, and the $(\partial k/\partial x_j)^2$-term (in the back-transformed ε-equation) that the WHR/WLR-models becomes similar (actually identical) to those of the newer $k-\varepsilon$ models.

With a reduction of the Schmidt number, as in the PDH-model, there becomes a necessity to include a cross-diffusion term in the ω-equation, in order to keep the cross-diffusion term in the transformed ε-equation reasonable.

Stating that a cross-diffusion term should be included in the ω-equation because the transformation of the standard modelled ε-equation indicates this, is not good enough. Because the modelled ε-equation is simply what it says: a model. There is no reason to be mathematically correct when designing the ω-equation, especially when noting the theory behind the construction of the ε-equation in the first place.

Better arguments are those based on the predicted results using the different ε-equations. Dependent on which construction gives the overall most correct results, one could declare if cross-diffusion terms should

be included or not in the ω-equation. If these newer models (those which include cross-diffusion terms in the k- and ε-equations) only improve the predictions in wall-bounded flows, one should consider to still use the standard $k-\varepsilon$ as the transformation basis, and hence add cross-diffusion terms to the $k-\omega$ model. Even if the cross-diffusion modified $k-\varepsilon$ models prove to be more general applicable models, it is still possible to construct a $k-\omega$ model without any cross-diffusion terms. By carefully tuning the coefficients and Schmidt numbers one could still arrive at the desirable cross-diffusion modified $k-\varepsilon$ model, since the transformation will produce cross-diffusion terms.

Simulations using the BPD-model [7] however indicate that the cross-diffusion terms play an important role in reducing the inaccurate behaviour of the $k-\omega$ models for free shear layer flows. It is also considerably easier, although more time consuming, to develop a more general model through adding terms to the standard model.

7 Summary

In this section a short theoretical summary of the EVMs are included. The performance of the different models for three fundamental flows are presented in Appendix B.

7.1 The k-equation

The difference between the k-equations are generally rather small among the EVMs. It does not matter whether it is a $k-\varepsilon$ or $k-\omega$ model, they all use a production term, a destruction term, a turbulent- and a viscous-diffusion term. Some of the newer $k-\varepsilon$ models add a pressure-diffusion term, which improves the result marginally, although indisputable enhances the near-wall behaviour of the turbulent quantities. The gain is however marginal and cannot definitely be attributed to a pressure-diffusion process and hence such a term was not included in the BPD-model. It is believed that wisely constructed damping functions, as in the PDH-model, could perform a similar effect as a pressure-diffusion term, without the additional computational effort and the risk of deteriorate numerical stability. A variable Schmidt number could also be included with the same argument as a pressure-diffusion term, and also sharing some of its drawbacks. A further discussion on the Schmidt numbers follows below.

7.2 The Secondary Equation

The second transport equation in the formulation of a two-equation EVM differs a lot more than the k-equation. First there is the choice of the solved variable. The turbulence modelling community cannot agree, although strong arguments from all sides, which type of model performs the best. The two main candidates, the $k-\varepsilon$ and the $k-\omega$, both have their advantage and disadvantage.

The $k-\varepsilon$ model is thought as the more general model, with good predictions for both free shear flows (mixing layer, jets and wakes) and wall bounded flows. The $k-\omega$ model certainly perform better in wall-bounded flows, especially for adverse pressure flows, although its free-estream problem is notorious. The $k-\omega$ model is credited with a higher numerical stability.

The conclusion from this should maybe be that the EVMs are not the all-performing turbulence model which one desires, but rather case-dependent, although certainly less than an algebraic zero-equation model.

Within each group the difference between the models is, similarly to the k-equation, restricted to coefficients and damping functions. The magnitude of the coefficients in the ε-equation are tuned along the following lines:

- $C_{\varepsilon 1}$: Backward-facing step and re-attachment length, since $C_{\varepsilon 1}$ has a strong influence on separated flows.
- $C_{\varepsilon 2}$: Decaying turbulent which states: $n = 1/(C_{\varepsilon 2} - 1)$ where n is 1.25 to 2.5.

- σ_ε: Log-law: $C_{\varepsilon 1} = C_{\varepsilon 2} - \kappa^2/\sigma_\varepsilon\sqrt{C_\mu}$

Damping of $C_{\varepsilon 2}$: f_2, is introduced to improve the decaying turbulence predictions. Recent studies, [15] also indicate that there should be a case-dependency on $C_{\varepsilon 2}$. Dependent on the numerical optimization done, models use different sets of constants. This apply mainly for the σ_ε and $C_{\varepsilon 2}$.

Note that the above discussed was focused to the $k-\varepsilon$ model, however similar rules applies for the ω- and τ-equation.

7.3 Schmidt Numbers

Here only some comments on the magnitude of the Schmidt numbers are included. It should be emphasized that the common acceptable values ($\sigma_k = 1$ and $\sigma_\varepsilon = 1.3$) is as little founded as any other combination. Generally the Schmidt numbers should depend on the wall-distance, with a reduced value as the wall is approach, similarly to the models by HL and NS. These number can hence not be considered constants at all, and are open for numerical optimization.

Jones and Launder [19] simply concluded that Schmidt numbers close to unity accord with expectations. Launder and Spalding [26], through extensive examinations of free turbulent flows, specified the now well accepted standard values. They however stated that slightly different values may be necessary in wall-bounded flows, without giving any specific values.

Indeed Launder in a subsequent paper [16] opts for slightly different values. Although the model is a RSM, and as such does not employ Schmidt numbers, the model, in the limit of thin shear layers, gives a ratio of $11/12$ for turbulent diffusion of the k-equation to that of the ε-equation. Thus contrary to the standard values, this RSM uses a higher σ_k than σ_ε.

Nagano and Tagawa (NT) [35], citing both the Hanjalic-Launder [16] turbulent diffusion ratio as well as improved predictions of the k-profile in the core region, increase the Schmidt number in the k-equation to $\sigma_k = 1.4$. The NT-model retains the standard σ_ε value, which is connected through the log-law to the other coefficients. Several models have continue the usage of higher σ_k (AKN, HL).

In the case of the Wilcox $k-\omega$ models, one could really start to question what is a reasonable values for the diffusion coefficient of the turbulent kinetic energy. The WHR/WLR-models use twice as high σ_k, as the standard $k-\varepsilon$ models.

In addition should the diffusion coefficient of ω be similar to that of ε? Using the variable, $\phi = k^m/l^n$, Launder showed (see also Appendix D), that with the usage of the logarithmic law, the coefficients in the secondary transport equation should satisfy:

$$\frac{n^2}{\sigma_\phi} = \frac{\sqrt{C_\mu}}{\kappa}\left(C_{\phi 2} - C_{\phi 1}\right) \tag{75}$$

The Schmidt number using this equation with standard coefficients becomes, for a $k-\varepsilon$ model with $n = 1$ (LSY): $\sigma_\varepsilon = 1.17$, for a $k-\omega$ model with $n = 1$ (WHR): $\sigma_\omega = 2.02$, and for a $k-\tau$ model with $n = -1$ (SAA): $\sigma_\tau = 1.37$. The required Schmidt numbers naturally differ dependent on the used coefficients, and notably is that for the standard $k-\varepsilon$ model a value of $\kappa = 0.435$ is needed to give $\sigma_\varepsilon = 1.3$.

With a SGDH-model, the varying Schmidt number of the HL-model is a very accurate approximation for fully developed channel flow DNS-data. However as indicated by Launder, different flows, necessities different constants, and in reflection of that, the standard value may very well be as good as any DNS-data optimized values. In addition a variable Schmidt number imposes yet another worry for numerical problems, as well as increased implementation efforts.

7.4 Cross-diffusion vs Yap-correction

It has been argued [38], [7] that the cross-diffusion term appearing in the ε-equation could be connected to the Yap-correction term of the Launder-Sharma model. Whether the term is due to a cross-diffusion term in the ω-equation or due to modelling argument from DNS/TSDIA is of less importance.

Launder *et al.* [57], [24] found that when using a LRN $k-\varepsilon$ model the predicted heat transfer level in the vicinity of the re-attachment point could be several times too high. This discrepancy is the result of the excessive levels of near-wall length-scale that is generated in separated flows.

Yap [57] devised a term, which in non-equilibrium flows reduces the turbulent length-scale when added to the right-hand-side of the ε-equation:

$$S_\varepsilon = 0.83\left(\frac{\tilde{\varepsilon}^2}{k}\right)\left(\frac{k^{3/2}}{C_l y\tilde{\varepsilon}} - 1\right)\left(\frac{k^{3/2}}{C_l y\tilde{\varepsilon}}\right)^2 \tag{76}$$

The term has no effect in local equilibrium, for which near a wall, $k^{3/2}/\tilde{\varepsilon} = C_l y$ and hence the term vanishes. In re-circulating regions the Yap-correction term however increases the near-wall dissipation, and hence reduces the heat transfer to a more acceptable level.

The question is, whether or not a cross-diffusion term affects the flow in a similar manner? Using the LSY-model as the reference model, the wall-normal (the most influential) gradients of k and ε are positive close to the wall, while further out they both become negative. A (positive) cross-diffusion term thus affects most parts of a flow with an additional source term to the ε-equation, while the effects of a Yap-correction term, is confined to the near-wall region.

A direct comparison between the two terms is difficult to make, due to the influence the modified ε in the core of the flow could have on the near-wall heat transfer. Even more alarming is that nearly all models (not RS) use a coefficient in the cross-diffusion term that is negative, see table 3. The pressure-diffusion term is thus constructed to reduce the dissipation rate, contrary to the idea behind the Yap-correction term.

The addition of the cross-diffusion term to the ω-equation however reduces the negative source the cross-diffusion in the ε-equation. In Bredberg *et al.* [7] it was also noted that the Schmidt number has a strong impact

on the cross-diffusion term, which should be considered when comparing the Wilcox-, PDH- and BPD-models in table 3. Based on the values in this table, the predicted heat transfer using the $k-\omega$ models should result in levels from low to high: the BPD-, the WHR-, and with the PDH-model reaching the highest levels. Not surprisingly the simulations, Figs. 22 and 23 in Appendix B, indicates a rather more complex nature for the predicted heat transfer level. The Yap-correction term on the other hand reduces the Nusselt number markedly for the LSY-model, which can be noted in the same figures through a comparison with the similar, although not Yap corrected, JL-model.

The conclusion from this can thus only serve to show the futility of trying to adopt *posterior* discussions on the turbulence models, which are too coupled to single out the effect of a modified term, or coefficient.

Acknowledgments

Funding for the present work has been provided by STEM, Volvo Aero Corporation and ALSTOM Power via the Swedish Gas Turbine Center.

References

[1] K. Abe, T. Kondoh, and Y. Nagano. A new turbulence model for predicting fluid flow and heat transfer in separating and reattaching flows - I. flow field calculations. *Int. J. Heat and Mass Transfer*, 37:139–151, 1994.

[2] R. Abid, C. Rumsey, and T. Gatski. Prediction of nonequilibrium turbulent flows with explicit algebraic stress models. *AIAA Journal*, 33:2026–2031, 1995.

[3] B.S. Baldwin and H. Lomax. Thin-layer approximation and algebraic model for separated turbulent flows. AIAA Paper 78-257, Huntsville, AL, USA, 1978.

[4] T.V. Boussinesq. Mém. pres Acad. Sci.,3rd ed Paris XXIII p. 46, 1877.

[5] J. Bredberg. Prediction of flow and heat transfer inside turbine blades using EARSM, $k-\varepsilon$ and $k-\omega$ turbulence models. Thesis for the Degree of Licentiate of Engineering, Dept. of Thermo and Fluid Dynamics, Chalmers University of Technology, Gothenburg, 1999. Also available at www.tfd.chalmers.se/~bredberg.

[6] J. Bredberg. On the wall boundary condition for turbulence model. Report 00/4, Dept. of Thermo and Fluid Dynamics, Chalmers University of Technology, Gothenburg, 2000. Also available at www.tfd.chalmers.se/~bredberg.

[7] J. Bredberg, S-H. Peng, and L. Davidson. An improved $k-\omega$ turbulence model applied to recirculating flows. Accepted for publication in Int. J. Heat and Fluid Flow, 2002.

[8] T. Cebeci and A.M. Smith. Analysis of turbulent boundary layers. In *Series in Applied Mathematcis and Mechanics, Vol XV*, 1974.

[9] K.Y. Chien. Predictions of channel and boundary-layer flows with a low-Reynolds-number turbulence model. *AIAA Journal*, 20:33–38, 1982.

[10] F.H. Clauser. The turbulent boundary layer. *Advances in Applied Mechanics*, 6:1–51, 1956.

[11] L. Davidson and B. Farhanieh. CALC-BFC. Report 95/11, Dept. of Thermo and Fluid Dynamics, Chalmers University of Technology, Gothenburg, 1995.

[12] F.W. Dittus and L.M.K. Boelter. Heat transfer in automobile radiators of the tubular type. *Univ. of Calif. Pubs. Eng.*, 2:443–461, 1930.

[13] P.A. Durbin. Near-wall turbulence closure modeling without damping functions. *Theoretical Computational Fluid Dynamics*, 3:1–13, 1991.

[14] M.P. Escudier. The distribution of mixing-length in turbulent flows near walls. Report, twf/tn/12, Imperical College, Heat Transfer Section, 1966.

[15] W.B. George. Lecture notes, turbulence theory. Report, Dept. Thermo and Fluid Dynamics, Chalmers University of Technology, Gothenburg, 2001.

[16] K. Hanjalić and B.E. Launder. Contribution towards a Reynolds-stress closure for low-Reynolds-number turbulence. *J. Fluid Mechanics*, 74:593–610, 1976.

[17] C.B. Hwang and C.A. Lin. Improved low-Reynolds-number $k-\epsilon$ model based on direct numerical simulation data. *AIAA Journal*, 36:38–43, 1998.

[18] J.Kim. On the structure of pressure fluctuations in simulated turbulent channel flow. *J. Fluid Mechanics*, 205:421–451, 1989.

[19] W.P. Jones and B.E. Launder. The prediction of laminarization with a two-equation model of turbulence. *Int. J. Heat and Mass Transfer*, 15:301–314, 1972.

[20] J. Kim, P. Moin, and R. Moser. Turbulence statistics in fully developed channel flow at low Reynolds number. *J. Fluid Mechanics*, 177:133–166, 1987.

[21] P.S. Klebanoff. Characteristics of turbulence in a boundary layer with zero pressure gradient. Report, tn 3178, NACA, 1954.

[22] J.C. Kok. Resolving the dependence on freestream values for the $k-\omega$ turbulence model. *AIAA Journal*, 38:1292–1295, 2000.

[23] A.N. Kolomogorov. Equations of turbulent motion in incompressible viscous fluids for very large Reynolds numbers. *Izvestia Academy of Sciences, USSR, Physics*, 6:56–58, 1942.

[24] B.E. Launder. On the computation of convective heat transfer in complex turbulent flows. *J. Heat Transfer*, 110:1112–1128, 1988.

[25] B.E. Launder and B.I. Sharma. Application of the energy-dissipation model of turbulence to the calculation of flow near a spinning disc. *Letters in Heat and Mass Transfer*, 1:131–138, 1974.

[26] B.E. Launder and D.B. Spalding. The numerical computation of turbulent flows. *Computational Methods Appl. Mech. Eng.*, 3:269–289, 1974.

[27] H. Le, P. Moin, and J. Kim. Direct numerical simulation of turbulent flow over a backward-facing step. *J. Fluid Mechanics*, 330:349–374, 1997.

[28] M.A. Leschziner. Turbulence modelling for physically complex flows pertinent to turbomachinery aerodynamics. van Karman Lecture Series 1998-02, 1998.

[29] N.N. Mansour, J.Kim, and P. Moin. Reynolds-stress and dissipation-rate budgets in a turbulent channel flow. *J. Fluid Mechanics*, 194:15–44, 1988.

[30] W.H. McAdams. *Heat Transmission*. McGraw-Hill, New York, 2nd edition, 1942.

[31] F.R. Menter. Influence of freestream values on $k-\omega$ turbulence model prediction. *AIAA Journal*, 30:1657–1659, 1992.

[32] F.R. Menter. Two-equation eddy-viscosity turbulence models for engineering applications. *AIAA Journal*, 32:1598–1605, 1994.

[33] R.D. Moser, J. Kim, and N.N. Mansour. Direct numerical simulation of turbulent channel flow up to Re=590. *Physics of Fluids*, 11:943–945, 1999. Data available at www.tam.uiuc.edu/Faculty/Moser/.

[34] Y. Nagano and M. Shimada. Rigorous modeling of dissipation-rate equation using direct simulation. *JSME International Journal*, 38:51–59, 1995.

[35] Y. Nagano and M. Tagawa. An improved $k-\varepsilon$ model for boundary layer flows. *J. Fluids Engineering*, 112:33–39, 1990.

[36] V.C. Patel, W. Rodi, and G. Scheuerer. Turbulence models for near-wall and low Reynolds number flows: A review. *AIAA Journal*, 23:1308–1319, 1985.

[37] S-H. Peng and L. Davidson. New two-equation eddy viscosity transport model for turbulent flow computation. *AIAA Journal*, 38:1196–1205, 2000.

[38] S-H. Peng, L. Davidson, and S. Holmberg. A modified low-Reynolds-number $k-\omega$ model for recirculating flows. *J. Fluid Engineering*, 119:867–875, 1997.

[39] L. Prandtl. Bericht über die ausgebildete turbulenz. *ZAMM*, 5:136–139, 1925.

[40] M.M. Rahman and T. Siikonen. Improved low-Reynolds-number $k-\epsilon$ model. *AIAA Journal*, 38:1298–1300, 2000.

[41] G. Rau, M. Cakan, D. Moeller, and T. Arts. The effect of periodic ribs on the local aerodynamic and heat transfer performance of a straight cooling channel. *J. Turbomachinery*, 120:368–375, 1998.

[42] C.M. Rhie and W.L. Chow. Numerical study of the turbulent flow past an airfoil with trailing edge separation. *AIAA Journal*, 21:1525–1532, 1983.

[43] W. Rodi and N.N. Mansour. Low Reynolds number $k-\epsilon$ modelling with the aid of direct numerical simulation. *J. Fluid Mechanics*, 250:509–529, 1993.

[44] A. Sarkar and R.M.C So. A critical evaluation of bear-wall two-equation models against direct numerical simulation. *Int. J. Heat and Fluid Flow*, 18:197–207, 1997.

[45] P.R. Spalart. Direct simulation of a turbulent boundary layer up to $R_\theta = 1410$. *J. Fluid Mechanics*, 187:61–98, 1988.

[46] P.R. Spalart and S.R. Allmaras. A one-equation turbulence model for aerodynamic flows. AIAA Paper 92-439, Reno, NV, USA, 1992.

[47] C.G. Speziale, R. Abid, and E.C. Anderson. Critical evaluation of two-equation models for near-wall turbulence. *AIAA Journal*, 30:324–331, 1992.

[48] K. Suga, M. Nagaoka, N. Horinouchi, K. Abe, and Y. Kondo. Application of a three equation cubic eddy viscosity model to 3-D turbulent flow by the unstructed grid method. In K. Hanjalić Y. Nagano and T. Tsuji, editors, *3:rd Int. Symp. on Turbulence, Heat and Mass Transfer*, pages 373–381, Nagoya, 2000. Aichi Shuppan.

[49] A.A. Townsend. *The structure of turbulent shear flow*. Cambridge University Press, Cambridge, 1976.

[50] E.R. van Driest. On turbulent flow near a wall. *Aeronautical Sciences*, 23:1007–, 1956.

[51] B. van Leer. Towards the ultimate conservative difference monotonicity and conservation combined in a second-order scheme. *J. Computational Physics*, 14:361–370, 1974.

[52] D.C. Wilcox. Reassessment of the scale-determining equation for advanced turbulence models. *AIAA Journal*, 26:1299–1310, 1988.

[53] D.C. Wilcox. Comparison of two-equation turbulence models for boundary layers with pressure gradient. *AIAA Journal*, 31:1414–1421, 1993.

[54] D.C. Wilcox. *Turbulence Modeling for CFD*. DCW Industries, Inc., 1998.

[55] M. Wolfshtein. The velocity and temperature distribution in one-dimensional flow with turbulence augmentation and pressure gradient. *Int. J. Heat and Mass Transfer*, 12:301–318, 1969.

[56] Z. Yang and T.H. Shih. New time scale based $k - \epsilon$ model for near-wall turbulence. *AIAA Journal*, 31:1191–1198, 1993.

[57] C.R. Yap. *Turbulent heat and momentum transfer in recirculation and impinging flows*. PhD thesis, Dept. of Mech. Eng., Faculty of Technology, Univ. of Manchester, 1987.

[58] B.K. Yoon and M.K. Chung. Computation of compression ramp flow with a cross-diffusion modified $k - \epsilon$ model. *AIAA Journal*, 33:1518–1520, 1995.

[59] A. Yoshizawa. Statistical modeling of a transport equation for the kinetic energy dissipation rate. *Physics of Fluids*, 30:628–631, 1987.

A Turbulence Models

Nearly all of the treated turbulence model in the report, listed on page 9, have been used to compute three different test-cases. Turbulence models not included below, were excluded due to: numerical problems (SAA), insufficient information (YC), or lack of time (NS). The remaining models are:

- $k-\varepsilon$ models:
  - Yang and Shih, 1993 [56] (YS)
  - Abe, Kondoh and Nagano, 1994 [1] (AKN)
- $k-\tilde{\varepsilon}$ models:
  - Jones and Launder, 1972 [19] (JL)
  - Chien, 1982 [9] (C)
  - Launder and Sharma, 1974 [25]
    - with Yap-correction, 1987 [57] (LSY)
  - Hwang and Lin, 1998 [17] (HL)
  - Rahman and Siikonen, 2000 [40] (RS)
- $k-\omega$ models:
  - Wilcox, 1988 [52] (WHR)
  - Wilcox, 1993 [53] (WLR)
  - Peng, Davidson and Holmberg, 1997 [38] (PDH)
  - Bredberg, Davidson and Peng, 2001 [7] (BDP)

The models are displayed below with constants tabulated. In addition an individual summary of their performance in the respectively test-case, is included. More detail information as well as comparisons are found in the following section, Appendix B.

The notation D/Dt is used for the material derivate, ie. the convective plus time derivate term. The production term is defined as:

$$P_k = \nu_t \left(\frac{\partial U_i}{\partial x_j} + \frac{\partial U_j}{\partial x_i} \right) \frac{\partial U_i}{\partial x_j} \tag{77}$$

The boundary conditions for k and $\tilde{\varepsilon}$ are both zero, while the boundary condition for ε or ω is displayed along with each turbulence model.

The definition of the variables in the damping function can be found on page 10.

A.1 Yang-Shih $k-\varepsilon$

$$\begin{aligned} \nu_t &= C_\mu f_\mu k T_t \\ f_\mu &= [1 - \exp(-1.5 \times 10^{-4} R_y - 5 \times 10^{-7} R_y^3 - \\ &\qquad - 1 \times 10^{-10} R_y^5)]^{0.5} \end{aligned} \tag{78}$$

where a specific definition for the time scale is used:

$$T_t = \frac{k}{\varepsilon} + \sqrt{\frac{\nu}{\varepsilon}} \tag{79}$$

$$\frac{Dk}{Dt} = P_k - \varepsilon + \frac{\partial}{\partial x_j} \left[\left(\nu + \frac{\nu_t}{\sigma_k} \right) \frac{\partial k}{\partial x_j} \right] \tag{80}$$

$$\begin{aligned} \frac{D\varepsilon}{Dt} &= \left(C_{\varepsilon 1} P_k - C_{\varepsilon 2} \varepsilon \right) / T_t + 2\nu\nu_t \left(\frac{\partial^2 U_i}{\partial x_j^2} \right) + \\ &\quad + \frac{\partial}{\partial x_j} \left[\left(\nu + \frac{\nu_t}{\sigma_\varepsilon} \right) \frac{\partial \varepsilon}{\partial x_j} \right] \end{aligned} \tag{81}$$

Boundary conditions for ε is:

$$\varepsilon_w = \nu \frac{\partial^2 k}{\partial x_j^2} \tag{82}$$

The coefficients are:

C_μ	$C_{\varepsilon 1}$	$C_{\varepsilon 2}$	σ_k	σ_ε
0.09	1.44	1.92	1.0	1.3

Pros/Cons:

+ Numerically stable

– Strange definition for the time scale.

– Awkward damping function for ν_t.

– Second-derivate of velocity in the ε-equation is numerically unsatisfying.

– Boundary condition for ε is numerically awkward to implement.

Model Performance:

Channel: Good performance.

BFS: Underestimated re-attachment length, erroneous C_f.

Rib: Slight overestimation of Nu.

A.2 Abe-Kondoh-Nagano $k-\varepsilon$

$$\begin{aligned} \nu_t &= C_\mu f_\mu \frac{k^2}{\varepsilon} \\ f_\mu &= \left[1 - \exp\left(-\frac{y^*}{14} \right) \right] \left[1 + \frac{5}{R_t^{3/4}} \exp\left\{ -\left(\frac{R_t}{200} \right)^2 \right\} \right] \end{aligned} \tag{83}$$

$$\frac{Dk}{Dt} = P_k - \varepsilon + \frac{\partial}{\partial x_j} \left[\left(\nu + \frac{\nu_t}{\sigma_k} \right) \frac{\partial k}{\partial x_j} \right] \tag{84}$$

$$\begin{aligned} \frac{D\varepsilon}{Dt} &= C_{\varepsilon 1} \frac{\varepsilon}{k} P_k - C_{\varepsilon 2} f_2 \frac{\varepsilon^2}{k} + \frac{\partial}{\partial x_j} \left[\left(\nu + \frac{\nu_t}{\sigma_\varepsilon} \right) \frac{\partial \varepsilon}{\partial x_j} \right] \\ f_2 &= \left[1 - \exp\left(-\frac{y^*}{3.1} \right) \right] \left[1 - 0.3 \exp\left\{ -\left(\frac{R_t}{6.5} \right)^2 \right\} \right] \end{aligned} \tag{85}$$

Boundary conditions for ε is:

$$\varepsilon_w = \frac{2\nu k}{y^2} \tag{86}$$

The coefficients are:

C_μ	$C_{\varepsilon 1}$	$C_{\varepsilon 2}$	σ_k	σ_ε
0.09	1.5	1.9	1.4	1.4

Pros/Cons:

+ Numerically stable

Model Performance:

Channel: Good performance.

BFS: Decent estimate of the re-attachment length, and C_f.

Rib: Good performance.

A.3 Jones-Launder, standard $k-\tilde{\varepsilon}$

$$\begin{aligned} \nu_t &= C_\mu f_\mu \frac{k^2}{\tilde{\varepsilon}} \\ f_\mu &= \exp\left(\frac{-2.5}{1+R_t/50}\right) \end{aligned} \tag{87}$$

$$\frac{Dk}{Dt} = P_k - \tilde{\varepsilon} - 2\nu\left(\frac{\partial\sqrt{k}}{\partial x_j}\right)^2 + \frac{\partial}{\partial x_j}\left[\left(\nu + \frac{\nu_t}{\sigma_k}\right)\frac{\partial k}{\partial x_j}\right] \tag{88}$$

$$\begin{aligned} \frac{D\tilde{\varepsilon}}{Dt} =& C_{\varepsilon 1}\frac{\tilde{\varepsilon}}{k}P_k - C_{\varepsilon 2}f_2\frac{\tilde{\varepsilon}^2}{k} + 2\mu\nu_t\left(\frac{\partial^2 U_i}{\partial x_j^2}\right) + \\ &+ \frac{\partial}{\partial x_j}\left[\left(\nu + \frac{\nu_t}{\sigma_\varepsilon}\right)\frac{\partial\tilde{\varepsilon}}{\partial x_j}\right] \\ f_2 =& 1 - 0.3\exp(-R_t^2) \end{aligned} \tag{89}$$

The coefficients are:

C_μ	$C_{\varepsilon 1}$	$C_{\varepsilon 2}$	σ_k	σ_ε
0.09	1.55	2.0	1.0	1.3

Pros/Cons:

+ Damping functions based on R_t

– Second-derivate of velocity in $\tilde{\varepsilon}$-equation is numerically unsatisfying.

– Boundary condition for ε is numerically awkward to implement.

– Model is poorly numerically optimized.

Model Performance:

Channel: Underestimated k and U_τ

BFS: Underestimated re-attachment length, and overestimated C_f

Rib: Overestimated Nu

A.4 Chien $k-\tilde{\varepsilon}$

$$\begin{aligned} \nu_t &= C_\mu f_\mu \frac{k^2}{\tilde{\varepsilon}} \\ f_\mu &= 1 - \exp\left(-0.115y^+\right) \end{aligned} \tag{90}$$

$$\frac{Dk}{Dt} = P_k - \tilde{\varepsilon} - 2\nu\frac{k}{y^2} + \frac{\partial}{\partial x_j}\left[\frac{\nu_t}{\sigma_k}\left(\frac{\partial k}{\partial x_j}\right)\right] \tag{91}$$

$$\begin{aligned} \frac{D\tilde{\varepsilon}}{Dt} =& C_{\varepsilon 1}\frac{\tilde{\varepsilon}}{k}P_k - C_{\varepsilon 2}f_2\frac{\tilde{\varepsilon}^2}{k} - 2\nu\frac{\tilde{\varepsilon}}{y^2}\exp(-0.5y^+) + \\ &+ \frac{\partial}{\partial x_j}\left[\frac{\nu_t}{\sigma_\varepsilon}\left(\frac{\partial\tilde{\varepsilon}}{\partial x_j}\right)\right] \\ f_2 =& 1 - 0.22\exp\left[(-R_t/6)^2\right] \end{aligned} \tag{92}$$

The coefficients are:

C_μ	$C_{\varepsilon 1}$	$C_{\varepsilon 2}$	σ_k	σ_ε
0.09	1.35	1.8	1.0	1.3

Pros/Cons:

+ Numerically stable.

– Damping functions based on y^+.

Model Performance:

Channel: Overestimation of k in the inertial sub-range.

BFS: Underestimated re-attachment length and erroneous C_f.

Rib: Terrible overestimation of Nu.

A.5 Launder-Sharma + Yap $k-\tilde{\varepsilon}$

$$\begin{aligned} \nu_t &= C_\mu f_\mu \frac{k^2}{\tilde{\varepsilon}} \\ f_\mu &= \exp\left[\frac{-3.4}{(1+R_t/50)^2}\right] \end{aligned} \tag{93}$$

$$\frac{Dk}{Dt} = P_k - \tilde{\varepsilon} - 2\nu\left(\frac{\partial\sqrt{k}}{\partial x_j}\right)^2 + \frac{\partial}{\partial x_j}\left[\left(\nu + \frac{\nu_t}{\sigma_k}\right)\frac{\partial k}{\partial x_j}\right] \tag{94}$$

$$\begin{aligned} \frac{D\tilde{\varepsilon}}{Dt} =& C_{\varepsilon 1}\frac{\tilde{\varepsilon}}{k}P_k - C_{\varepsilon 2}f_2\frac{\tilde{\varepsilon}^2}{k} + 2\nu\nu_t\left(\frac{\partial^2 U_i}{\partial x_j^2}\right) + \\ &+ 0.83\left(\frac{\tilde{\varepsilon}^2}{k}\right)\left(\frac{k^{3/2}}{C_l y\tilde{\varepsilon}} - 1\right)\left(\frac{k^{3/2}}{C_l y\tilde{\varepsilon}}\right)^2 + \\ &+ \frac{\partial}{\partial x_j}\left[\left(\nu + \frac{\nu_t}{\sigma_\varepsilon}\right)\frac{\partial\tilde{\varepsilon}}{\partial x_j}\right] \\ f_2 =& 1 - 0.3\exp(-R_t^2) \end{aligned} \tag{95}$$

C_μ	$C_{\varepsilon 1}$	$C_{\varepsilon 2}$	C_l	σ_k	σ_ε
0.09	1.44	1.92	2.55	1.0	1.3

Pros/Cons:

+ Damping functions based on R_t.
+ Greatly improved near-wall prediction with the Yap-correction.
– Second-derivate of velocity in $\tilde{\varepsilon}$-equation is numerically unsatisfying.
– Boundary condition for ε is numerically awkward to implement.

Model Performance:

Channel: Underestimated k, U_τ

BFS: Overestimation of the re-attachment length.

Rib: Fairly good estimation of Nu

Notes: Repeatedly used as a comparative model, thus a well established model with overall average prediction. Several models however give improved result, with simpler terms, and improved numerical stability.

A.6 Hwang-Lin $k - \tilde{\varepsilon}$

$$\begin{aligned} \nu_t &= C_\mu f_\mu \frac{k^2}{\tilde{\varepsilon}} \\ f_\mu &= 1 - \exp\left(-0.01 y_\lambda - 0.008 y_\lambda^3\right) \end{aligned} \tag{96}$$

$$\begin{aligned} \frac{Dk}{Dt} =& P_k - \tilde{\varepsilon} - \underbrace{2\nu \left(\frac{\partial \sqrt{k}}{\partial x_j}\right)^2}_{\varepsilon_w} - \frac{\nu}{2}\frac{\partial}{\partial x_j}\left(\frac{k}{\tilde{\varepsilon}}\frac{\partial \varepsilon_w}{\partial x_j}\right) + \\ &+ \frac{\partial}{\partial x_j}\left[\left(\nu + \frac{\nu_t}{\sigma_k}\right)\frac{\partial k}{\partial x_j}\right] \\ \sigma_k =& 1.4 - 1.1\exp\left(-y_\lambda/10\right) \end{aligned} \tag{97}$$

$$\begin{aligned} \frac{D\tilde{\varepsilon}}{Dt} =& C_{\varepsilon 1}\frac{\tilde{\varepsilon}}{k}P_k - C_{\varepsilon 2}\frac{\tilde{\varepsilon}^2}{k} + 2\nu\nu_t\left(\frac{\partial^2 U_i}{\partial x_j^2}\right) - \\ &- \nu\frac{\partial}{\partial x_j}\left(\frac{\tilde{\varepsilon}}{k}\frac{\partial k}{\partial x_j}\right) + \frac{\partial}{\partial x_j}\left[\left(\nu + \frac{\nu_t}{\sigma_\varepsilon}\right)\frac{\partial \tilde{\varepsilon}}{\partial x_j}\right] \\ \sigma_\varepsilon =& 1.3 - \exp\left(-y_\lambda/10\right) \end{aligned} \tag{98}$$

C_μ	$C_{\varepsilon 1}$	$C_{\varepsilon 2}$
0.09	1.44	1.92

Pros/Cons:

+ Variable Schmidt-numbers improve results for channel flow.
+ Extensively tuned using DNS-data.
– Several terms are awkward to implement.
– Numerically unstable model.
– Variable Schmidt numbers are numerically undesirable.

Model Performance:

Channel: Excellent estimation of k and U_τ, and even ε.

BFS: Underestimated re-attachment length.

Rib: Surprisingly bad estimation of Nu.

Notes: Based on the included test-cases it seems that the HL-model predicts too high level of turbulence for non-simple flows which might be a consequence of the variable Schmidt numbers. The theory is however sound, although one might try to use a different wall-dependent parameter. It seems that y_λ may be too insensitive for variating levels of turbulence.

A.7 Rahman-Siikonen $k - \tilde{\varepsilon}$

$$\begin{aligned} \nu_t &= C_\mu f_\mu k T_t \\ f_\mu &= 1 - \exp\left(-0.01 R_\lambda - 0.0068 R_\lambda^3\right) \end{aligned} \tag{99}$$

where the turbulent time scale is defined as:

$$T_t = \max\left(k/\tilde{\varepsilon}, \sqrt{2\nu/\varepsilon}\right) \tag{100}$$

$$\begin{aligned} \frac{Dk}{Dt} =& P_k - \tilde{\varepsilon} - 2\nu\left(\frac{\partial \sqrt{k}}{\partial x_j}\right)^2 + \\ &+ \frac{\nu_t}{2}\min\left[\frac{\partial (k/\tilde{\varepsilon})}{\partial x_j}\frac{\partial \tilde{\varepsilon}}{\partial x_j}, 0.\right] + \\ &+ \frac{\partial}{\partial x_j}\left[\left(\nu + \frac{\nu_t}{\sigma_k}\right)\frac{\partial k}{\partial x_j}\right] \end{aligned} \tag{101}$$

$$\begin{aligned} \frac{D\tilde{\varepsilon}}{Dt} =& \left(C_{\varepsilon 1}P_k - C_{\varepsilon 2}\tilde{\varepsilon} - 2\nu\frac{k}{y^2}\exp(-R_y/80)^2\right)/T_t - \\ &- \frac{\nu_t}{T_t^2}\left[\frac{\partial (k/\tilde{\varepsilon})}{\partial x_j}\frac{k}{\partial x_j}\right] + \frac{\partial}{\partial x_j}\left[\left(\nu + \frac{\nu_t}{\sigma_\varepsilon}\right)\frac{\partial \tilde{\varepsilon}}{\partial x_j}\right] \end{aligned} \tag{102}$$

C_μ	$C_{\varepsilon 1}$	$C_{\varepsilon 2}$	σ_k	σ_ε
0.09	1.44	1.92	1.0	1.3

Pros/Cons:

+ Improved representation of the turbulent time scale, with enhanced near-wall predictions.
– Unstable model.

Model Performance:

Channel: Severely underestimated U_τ.

BFS: Underestimated C_f, with a too slow recovery.

Rib: Qualitatively erroneous prediction of Nu.

Notes: This is a modified Chien $k - \varepsilon$ model with only marginally improved results. In addition this model is both more demanding when implementing, and also less numerically stable.

A.8 Wilcox HRN $k-\omega$

$$\nu_t = \frac{k}{\omega} \tag{103}$$

$$\frac{Dk}{Dt} = P_k - \beta^* k\omega + \frac{\partial}{\partial x_j}\left[\left(\nu + \sigma^* \nu_t\right)\frac{\partial k}{\partial x_j}\right] \tag{104}$$

$$\frac{D\omega}{Dt} = \gamma\frac{\omega}{k}P_k - \beta\omega^2 + \frac{\partial}{\partial x_j}\left[\left(\nu + \sigma\nu_t\right)\frac{\partial \omega}{\partial x_j}\right] \tag{105}$$

with the constants, using Wilcox nomenclature as:

β^*	γ	β	σ^*	σ
0.09	5/9	0.075	0.5	0.5

Boundary condition for ω is:

$$\omega = \frac{6\nu}{\beta y^2} \tag{106}$$

Pros/Cons:

+ No damping function.

Model Performance:

Channel: Underestimated k.

BFS: Overestimated the re-attachment length, and underestimated C_f.

Rib: Underestimation of Nu.

A.9 Wilcox LRN $k-\omega$

$$\begin{aligned}\nu_t =& \alpha^* \frac{k}{\omega} \\ \alpha^* =& \frac{0.025 + 10R_t/27}{1 + 10R_t/27}\end{aligned} \tag{107}$$

$$\begin{aligned}\frac{Dk}{Dt} =& P_k - \beta^* k\omega + \frac{\partial}{\partial x_j}\left[\left(\nu + \sigma^*\nu_t\right)\frac{\partial k}{\partial x_j}\right] \\ \beta^* =& \frac{9}{100}\frac{5/18 + (R_t/8)^4}{1 + (R_t/8)^4}\end{aligned} \tag{108}$$

$$\begin{aligned}\frac{D\omega}{Dt} =& \alpha\frac{\omega}{k}P_k - \beta\omega^2 + \frac{\partial}{\partial x_j}\left[\left(\nu + \sigma\nu_t\right)\frac{\partial \omega}{\partial x_j}\right] \\ \alpha =& \frac{1}{\alpha^*}\frac{5}{9}\left(\frac{0.1 + R_t/6}{1 + R_t/6}\right)\end{aligned} \tag{109}$$

With coefficients as:

β	σ^*	σ
0.075	0.5	0.5

Boundary condition for ω is:

$$\omega = \frac{6\nu}{\beta y^2} \tag{110}$$

Pros/Cons:

+ Damping functions based on R_t.

Model Performance:

Channel: Ok.

BFS: Overestimated re-attachment length, and underestimated C_f.

Rib: Underestimation of Nu.

Notes: This model is identical to the HRN version, apart from the added damping functions. Notable is that the WLR-model only improves the prediction for channel flow, with a slight reduction of the agreement for the other two cases.

A.10 Peng-Davidson-Holmberg $k-\omega$

$$\begin{aligned}\nu_t =& C_\mu f_\mu \frac{k}{\omega} \\ f_\mu =& 0.025 + \left[1 - \exp\left\{-\left(\frac{R_t}{10}\right)^{3/4}\right\}\right] \\ & \times \left[0.975 + \frac{0.001}{R_t}\exp\left\{-\left(\frac{R_t}{200}\right)^2\right\}\right]\end{aligned} \tag{111}$$

$$\begin{aligned}\frac{Dk}{Dt} =& P_k - C_k f_k \omega k + \frac{\partial}{\partial x_j}\left[\left(\nu + \frac{\nu_t}{\sigma_k}\right)\frac{\partial k}{\partial x_j}\right] \\ f_k =& 1 - 0.722\exp\left[-\left(\frac{R_t}{10}\right)^4\right]\end{aligned} \tag{112}$$

$$\begin{aligned}\frac{D\omega}{Dt} =& C_{\omega 1} f_\omega \frac{\omega}{k}P_k - C_{\omega 2}\omega^2 + C_\omega \frac{\nu_t}{k}\left(\frac{\partial k}{\partial x_j}\frac{\partial \omega}{\partial x_j}\right) \\ & + \frac{\partial}{\partial x_j}\left[\left(\nu + \frac{\nu_t}{\sigma_\omega}\right)\frac{\partial \omega}{\partial x_j}\right] \\ f_\omega =& 1 + 4.3\exp\left[-\left(\frac{R_t}{1.5}\right)^{1/2}\right]\end{aligned} \tag{113}$$

The boundary conditions for the specific dissipation rate is:

$$\omega = \frac{6\nu}{C_{\omega 2} y^2} \tag{114}$$

The constants in this model are:

C_k	C_μ	$C_{\omega 1}$	$C_{\omega 2}$	C_ω	σ_k	σ_ω
0.09	1.0	0.42	0.075	0.75	0.8	1.35

Pros/Cons:

+ Damping functions based on R_t.

Model Performance:

Channel: Ok, however underestimated U_τ.

BFS: Excellent re-attachment length and C_f.

Rib: Slight underestimation of Nu.

A.11 Bredberg-Peng-Davidson $k-\omega$

$$\begin{aligned}\nu_t =& C_\mu f_\mu \frac{k}{\omega} \\ f_\mu =& 0.09 + \left(0.91 + \frac{1}{R_t^3}\right)\left[1 - \exp\left\{-\left(\frac{R_t}{25}\right)^{2.75}\right\}\right]\end{aligned} \tag{115}$$

$$\frac{Dk}{Dt} = P_k - C_k k\omega + \frac{\partial}{\partial x_j}\left[\left(\nu + \frac{\nu_t}{\sigma_k}\right)\frac{\partial k}{\partial x_j}\right] \tag{116}$$

$$\begin{aligned}\frac{D\omega}{Dt} =& C_{\omega 1}\frac{\omega}{k}P_k - C_{\omega 2}\omega^2 + \\ &+ C_\omega\left(\frac{\nu}{k} + \frac{\nu_t}{k}\right)\frac{\partial k}{\partial x_j}\frac{\partial \omega}{\partial x_j} + \frac{\partial}{\partial x_j}\left[\left(\nu + \frac{\nu_t}{\sigma_\omega}\right)\frac{\partial \omega}{\partial x_j}\right]\end{aligned} \tag{117}$$

The boundary conditions for the specific dissipation rate is:

$$\omega = \frac{2\nu}{C_{\omega 2} y^2} \tag{118}$$

The constants in the model are given as

C_k	C_μ	$C_{\omega 1}$	$C_{\omega 2}$	C_ω	σ_k	σ_ω
0.09	1.0	0.49	0.072	1.1	1.0	1.8

Pros/Cons:

+ Damping functions based on R_t.

+ Only a single damping function

– Slightly less numerically stable than the other $k-\omega$ models, due to the added viscous cross-diffusion term.

Model Performance:

Channel: Good.

BFS: Excellent re-attachment length, however a slight overestimation of C_f in the re-development region.

Rib: Excellent prediction of Nu.

B Test-cases and Performance of EVMs

The listed two-equation EVMs on page 29 have been used to compute three different flows: the fully developed channel flow, the backward-facing-step (BFS) flow and the rib-roughened channel flow.

The computations were made using the incompressible finite-volume method code CALC-BFC, [11]. The code employs the second order bounded differencing scheme van Leer [51] for the convective derivates, and the second order central differencing scheme for the other terms. The SIMPLE-C algorithm is used to deal with the velocity-pressure coupling. CALC-BFC uses Boundary-Fitted-Coordinate, on a non-staggered grid with the Rhie-Chow [42] interpolation to smooth non-physical oscillations.

For all cases only two-dimensional computations were made, to reduce computational costs. The difference between the predicted centerline value using a 3D mesh compared with a 2D mesh is usually negligible. In addition as this is a comparative study for different turbulence models any 3D-effects may be excluded.

B.1 Fully Developed Channel Flow

This flow is a 1D-flow, with a variation only in the wall normal direction. Due to its simplicity this was one of the first cases computed using DNS, and has since then become a standard case for turbulence model comparison. As DNS gives such a wealth of information most designers use these data bases to improve their models. Thus it is not surprising that the accuracy of post-DNS models (from 1990 and later) are significantly higher than those prior to DNS. The DNS used as a comparison here are the data from Moser *et al.* [33], with a Reynolds number based on the channel half width and friction velocity of $Re_\tau = 395$ and $Re_\tau = 590$.

The predicted $U^+ = U/U_\tau$ profiles are compared in Figs. 12 and 13. The difference between the models are only minor, however some models slightly under-predict the friction velocity with a resulting over-prediction of U^+.

Model	YS	AKN	JL	C	LSY	WHR	WLR
U_τ^*	58.1	57.3	54.8	55.0	54.3	57.7	58.5
Nu	40.1	38.9	33.9	35.6	34.9	38.2	40.4

Table 5: Friction velocity and Nusselt number. DNS, $Re_\tau = 395 : U_\tau^* = 1000 \times U_\tau/U_b = 56.9$ and $Nu_{DB} = 41.1$.

Model	RS	HL	PDH	BPD
U_τ^*	49.9	53.4	56.1	54.4
Nu	43.7	50.3	55.3	52.2

Table 6: Friction velocity and Nusselt number. DNS, $Re_\tau = 590 : U_\tau^* = 1000 \times U_\tau/U_b = 53.9$ and $Nu_{DB} = 59.3$.

The normalized friction velocity is listed in tables 5

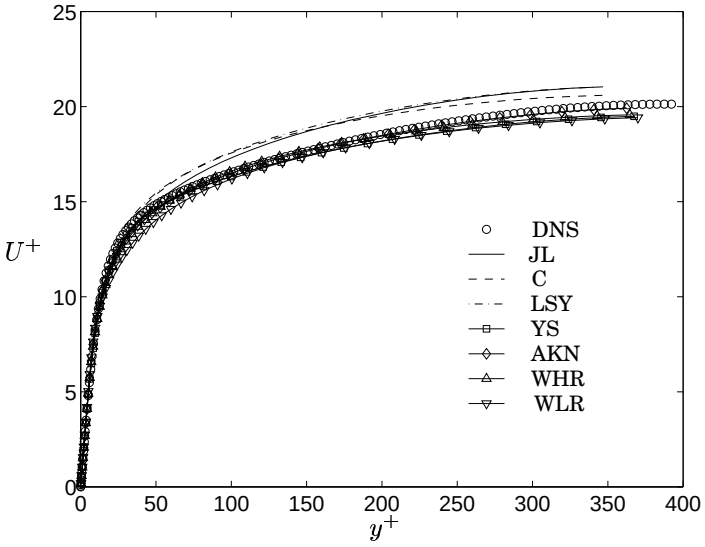

Figure 12: $U^+ = U/U_\tau$. DNS-data, Kim *et al.* [33], $Re_\tau = 395$.

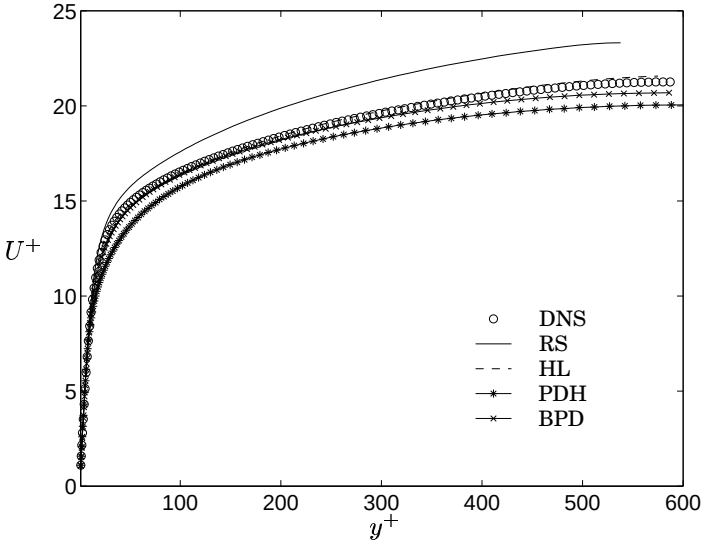

Figure 13: $U^+ = U/U_\tau$. DNS-data, Kim *et al.* [33], $Re_\tau = 590$.

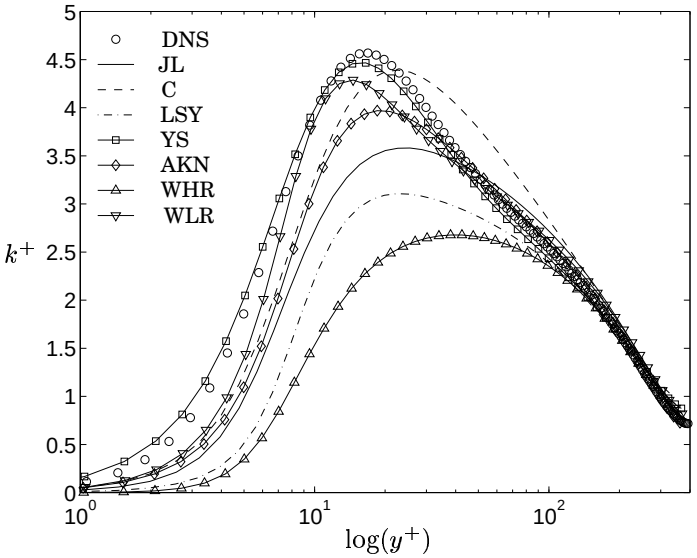

Figure 14: $k^+ = k/U_\tau^2$. DNS-data, Kim *et al.* [33], $Re_\tau = 395$.

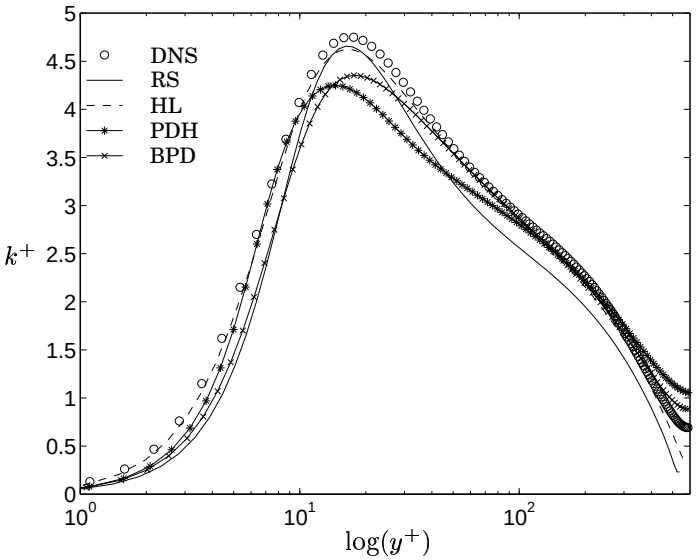

Figure 15: $k^+ = k/U_\tau^2$. DNS-data, Kim *et al.* [33], $Re_\tau = 590$.

and 6 along with the predicted Nusselt number using a constant Prandtl number model. The Nusselt number is not available for the DNS-data and instead the Dittus-Boelter equation [12] is used $Nu_{DB} = 0.023 Re^{0.8} Pr^{0.4}$, as introduced by McAdams [30].

All models predict both the Nusselt number and the friction velocity fairly accurate. The largest deviation for the friction velocity is given by the RS-model which under-predicts U_τ with more than 7%, which is too much for such a simple test-case as the fully developed channel flow. The PDH-model over-predict DNS-data with 4%. The Nusselt number is always under-predicted, with the largest deviation predicted by the RS-model (26%). The WLR-model gives a correct value within 2%.

From these data only the RS-model could be considered as inadequate, which is quite surprising since this model is rather new and could have used DNS-data to more correctly tune damping functions and extra terms.

Progressing to the turbulent kinetic energy, $k^+ = k/U_\tau^2$, the profiles are compared in semi-log plots, Figs. 14 and 15. The spread between the turbulence models is much larger for this quantity than for the velocity profiles. Generally the predictions improve the newer the model is. To quantify the models, the predicted maxima are shown in tables 7 and 8. Only the JL, LSY and WHR-models give k^+ that is too much in error. The closest agreement is given by the HL-model. The WLR-model improves the result substantially compared with the WHR, using the added damping functions. However as noticed later, an improvement in the predicted turbulent kinetic energy don't automatically improve results for other quantities.

The predicted $\varepsilon^+ = \varepsilon\nu/U_\tau^4$-profiles, are shown in Figs. 16 and 17. Note that for the non-ε based models, ε^+ needs to be computed using the relation expressed in the k-equation since it is not explicitly solved. For models

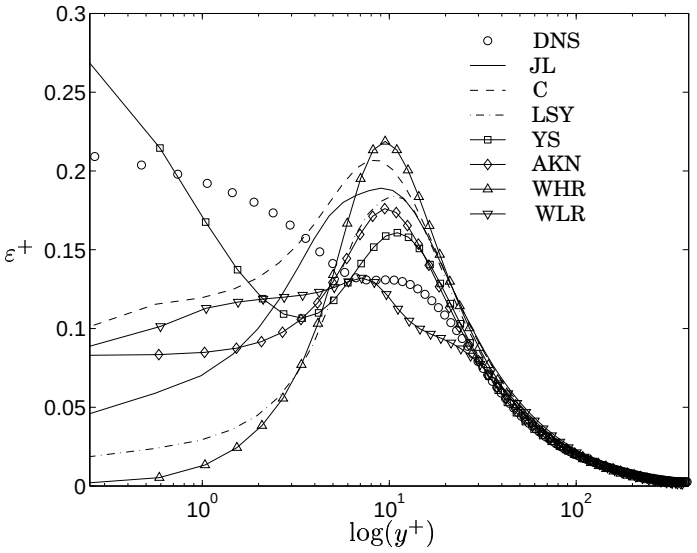

Figure 16: $\varepsilon^+ = \varepsilon\nu/u_\tau^4$. DNS-data, Kim *et al.* [33], $Re_\tau = 395$.

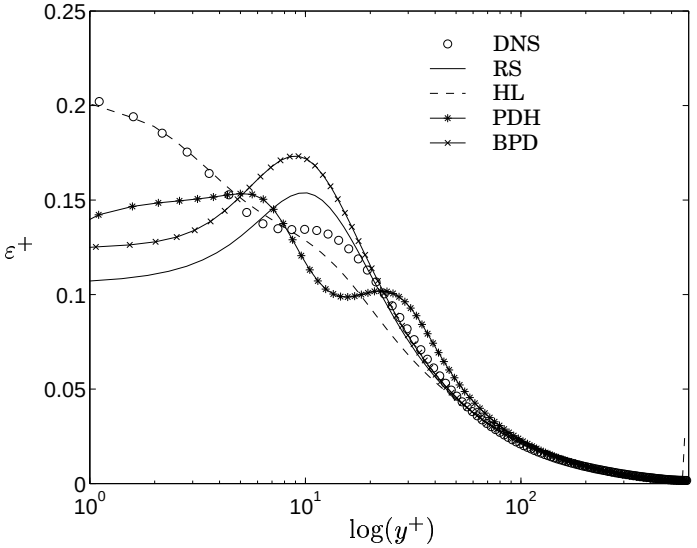

Figure 17: $\varepsilon^+ = \varepsilon\nu/u_\tau^4$. DNS-data, Kim *et al.* [33], $Re_\tau = 590$.

that solve the reduced dissipation rate $\tilde{\varepsilon}$, the boundary value, ε_w, is added in the plots.

The result for ε is considerably worse than any other quantity. Even the variation of ε is generally not captured by the models. DNS-data give the maximum value of ε at the wall which only the YS- and HL-model predict. The other models give the maximum in the buffer-layer. The overall maximum is given in tables 7 and 8. Note however that only for the YS- and HL-model the comparison to the DNS-data is of any value, due to the large discrepancy in the location of the maximum for the other models. In the viscous sub-layer only the HL-model yields prediction in agreement with DNS-data, while for $y^+ > 30$ all models give reasonable results. Indisputable it is the variable Schmidt numbers employed by the HL-model which give the very accurate results for both the k- and ε-profiles. However the importance of capturing these two profiles, especially the dissipation rate, is overrated as the connection between the performance of the

Model	YS	AKN	JL	C	LSY	WHR	WLR
k^+	4.47	3.97	3.58	4.39	3.11	2.68	4.29
ε^+	0.29^w	0.18	0.19	0.21	0.18	0.22	0.13

Table 7: Maximum value of k^+ and ε^+. DNS, $Re_\tau = 395$: $k^+ = 4.57$ and $\varepsilon^+ = 0.22$.

Model	RS	HL	PDH	BPD
k^+	4.66	4.62	4.25	4.35
ε^+	0.15	0.21^w	0.15	0.17

Table 8: Friction velocity and Nusselt number. DNS, $Re_\tau = 590 : k^+ = 4.75$ and $\varepsilon^+ = 0.23$.

model in fully developed channel, and in eg. separated test-cases is weak. The performance of the HL-model is also considerably reduced for the other two test-cases, as noted below.

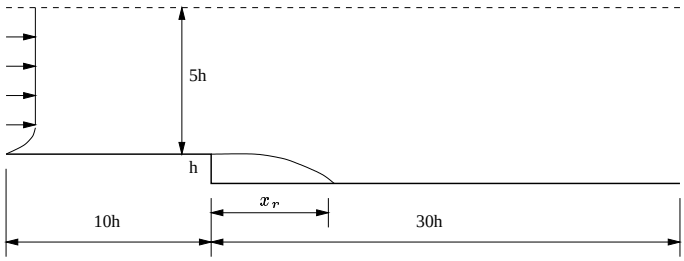

Figure 18: Geometrical conditions, not to scale, BFS-case.

B.2 Backward-facing-step Flow

For the backward-facing step flow, the flow undergoes separation, re-circulation and re-attachment followed by a re-developing boundary layer. In addition, this flow involves a shear-layer mixing process, as well as an adverse pressure, thus the backward-facing step (BFS) is an attractive flow for comparing turbulence models.

The case used here is the one that has been studied using DNS by Lee *et al.* [27], see Fig. 18. This case has a relatively low Reynolds number, $Re_h = 5\,100$, based on the step-height, h. In the present computation the inflow condition was specified using DNS data at $x/h = -10$. Neumann condition was applied for all variables at the outlet located at $x/h = 30$. No-slip condition was used on the walls. The overall calculation domain ranges from $x/h = -10$ to $x/h = 30$, with the step located at $x/h = 0$. The channel height is $5h$ in the inlet section and $6h$ after the step, yielding an expansion ratio of 1.2.

The inlet condition in the BFS-case is crucial for a critical evaluation and comparison. The DNS data of Spalart [45] for the velocity profile and the k-profile, are directly applied at the inlet. The inflow ε or ω was specified in such a way that the model prediction matches the DNS data at $x/h = -3$.

The skin friction coefficient, defined as $C_f = 2\tau_w/(\rho U_\infty^2)$, is shown in Figs. 19 and 20. The predicted friction coefficient varies from very good (PDH) to

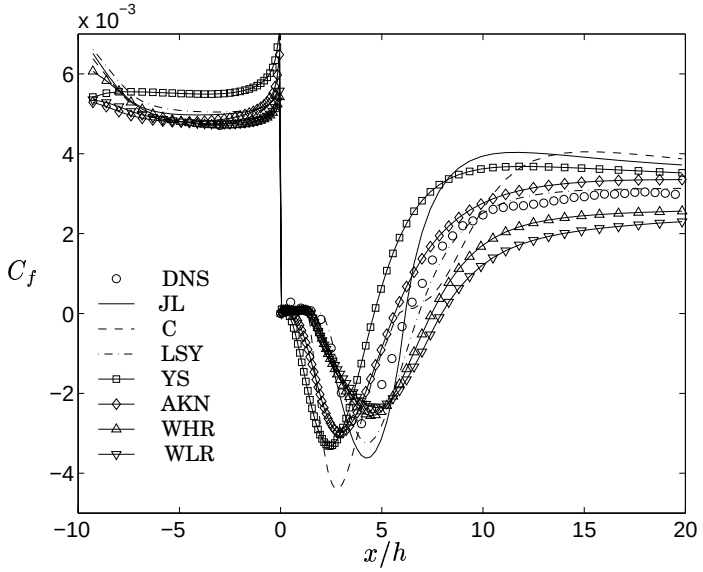

Figure 19: C_f along lower wall. DNS-data, Le *et al.* [27]

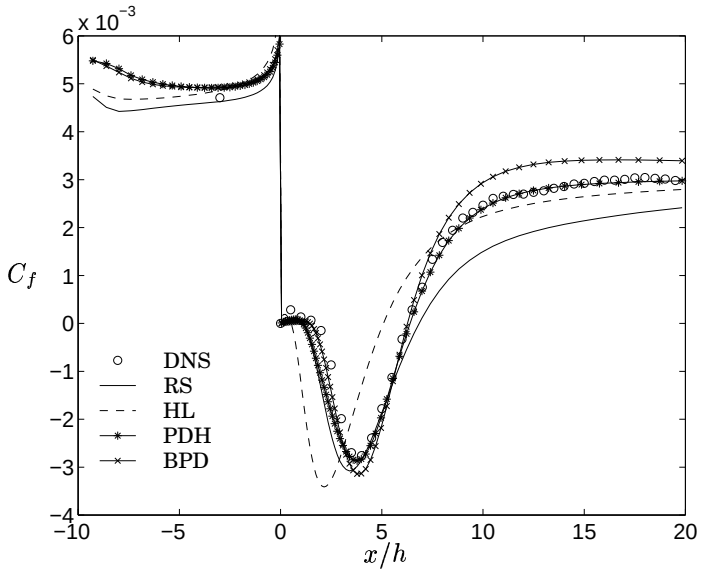

Figure 20: C_f along lower wall. DNS-data, Le *et al.* [27]

rather poor (JL,C,RS). Although hardly discernible, the Chien-model reproduces a highly questionable C_f profile around the re-attachment point. The y^+-based damping functions is the main reason for this spurious behaviour, which also yields erroneous heat transfer in the rib-roughened case.

One of the commonly used quantities to justify the accuracy of a turbulence model in a BFS-case is the re-attachment length of the main separation. Tables 9 and 10 gives the re-attachment length, x_r, using the different models in comparison with DNS data, $x_r/h = 6.28$. The two models which yielded the most favourable values for ε^+ at the wall in the channel flow case, YS and HL, completely fail to capture the re-attachment point in this case. The YS-model under-predicts x_r/h by as much as 26%. The Wilcox $k-\omega$ models (WHR and WLR) don't give very accurate predictions either, with a overestimation of the re-attachment point of 19% and 27% respectively. Notable is that the improved WLR-model

Model	YS	AKN	JL	C	LSY	WHR	WLR
x_r/h	4.62	5.65	6.17	5.86	6.83	7.46	7.96
$C_{f,max}$	3.68	3.35	4.04	4.05	3.13	2.56	2.30

Table 9: Re-attachment point and maximum friction coefficient. DNS: $x_r/h = 6.28$, $1000 \times C_{f,max} = 3.04$.

Model	RS	HL	PDH	BPD
x_r/h	6.85	5.09	6.40	6.27
$C_{f,max}$	2.41	2.79	2.97	3.41

Table 10: Re-attachment point and maximum friction coefficient. DNS: $x_r/h = 6.28$, $1000 \times C_{f,max} = 3.04$.

gives worse result.

When developing the BPD-model it was discovered that the level of skin friction coefficient was highly affected by the diffusion of turbulent kinetic energy, hence the value of σ_k. Using the BPD-model, C_f can be decreased by increasing σ_k, which may explain the significantly lower values retrieved by the WHR and WLR models. However the PDH-model, also a $k-\omega$ model of similar construction, predicts a lower C_f than the BPD-model, even though it employs a lower σ_k. In addition all $k-\varepsilon$ models use $\sigma_k = 1$ and predict markedly different friction coefficients. The coupled behaviour of the different terms in the turbulence models are hence made obvious. Thus adjusting a coefficient based on only a single test-case, is not advised, since the model may then deteriorate for other flows. Furthermore models purely tuned for simple, as the well documented fully developed channel flow test-case, may perform worse than non-tuned model. The HL- and the YS-model may possibly be such models.

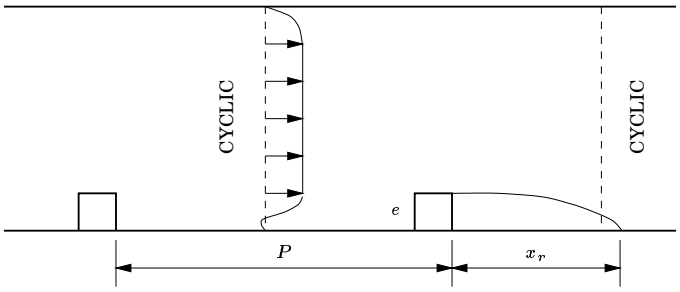

Figure 21: Geometry, RR-case.

B.3 Rib-roughened Channel Flow

The heat transfer performance of the different models is evaluated in the rib-roughened case of Rau *et al.* [41]. The Reynolds number, based on the mean velocity and the channel height was $Re_H = 30\,000$. The height-to-channel hydraulic diameter, e/G, was 0.1, and the pitch-to-rib-height ratio, $P/e = 9$, see Fig. 21.

The experiment provides both flow field and heat transfer measurements, however here only the centerline Nusselt number is used in the comparison. The measured Nusselt numbers were normalized with the

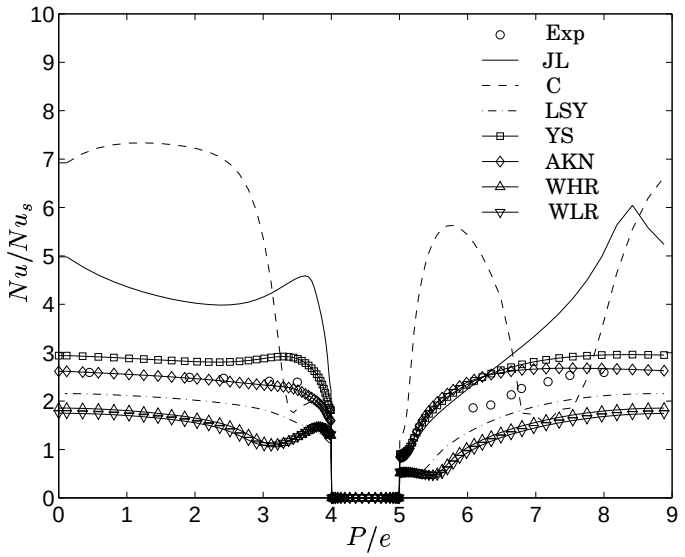

Figure 22: Nu along lower wall. Experiment, Rau *et al.* [41]

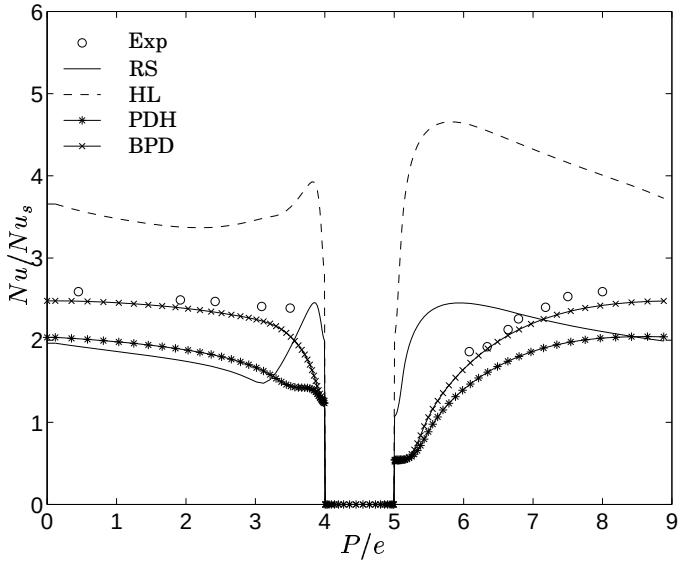

Figure 23: Nu along lower wall. Experiment, Rau *et al.* [41]

Dittus-Boelter equation, [12] as introduced by McAdams [30]:

$$Nu_\infty = 0.023 \cdot Re^{0.8} \cdot Pr^{0.4} \tag{119}$$

The uncertainty in the resulting enhancement factor, Nu/Nu_∞, was estimated to be 5% for the experiment.

The computations were made using periodic boundary condition at the streamwise boundaries, which was verified in the experiment to prevail in the test section. This reduces the uncertainty in the result due to the inlet boundary condition. No-slip condition and constant heat flux were applied at the walls. The rib was, as in the experiment, insulated.

Figs. 22 and 23 compare the Nusselt numbers predicted from the different turbulence models. Two models (AKN, BPD) give accurate predicted Nusselt number, (+6% and -6%, respectively) although the AKN-model yields too high values downstream the rib. The worst

Model	YS	AKN	JL	C	LSY	WHR	WLR
Nu_{max}	227	206	463	546	165	142	133
$\int Nu$	206	185	298	368	137	113	106
%	+18	+6	+71	+111	-21	-35	-39

Table 11: Nusselt number. Experiment: $\int Nu \approx 174$, $Nu_{max} = 198$.

Model	RS	HL	PDH	BPD
Nu_{max}	194	379	156	190
$\int Nu$	158	313	132	163
%	-9	+80	-24	-6

Table 12: Nusselt number. Experiment: $\int Nu \approx 174$, $Nu_{max} = 198$.

results are predicted with the JL, C and HL-models, especially the C-model, with a large over-prediction of the Nusselt number. The Wilcox models (WHR, WLR) under-predict the Nusselt number by a fair margin, while the PDH-model slightly less. The effect of the Yap-correction is apparent, with the LSY-model predicts less than half the Nusselt number as compared with the JL-model. The former is also in better agreement with the experimental data. Similarly the RS-model is an improvement over its predecessor, the C-model, however it still gives an erroneous predicted heat transfer in the re-circulating zones upstream and downstream the rib.

Tables 11 and 12 summaries the predicted Nusselt number. The tables give both the average and the maximum Nusselt number for each model. The comparative values of the experiment is less accurate, especially the averaged value, due to the lack of data around the rib. The value of $\int Nu = 174$ is mostly likely on the higher side. The deviation of turbulence models from the experiment is also listed.

It is of interest to compare the predicted Nusselt number for the rib-roughened with the predicted skin friction in the BFS-case. In tables 9 and 10 the maximum C_f in the re-developing zone, ie. after the re-attachment point is listed. Using Reynolds analogy it is reasonable to believe that models which underestimate the maximum friction coefficient will also underestimate the heat transfer coefficient. The JL- and C-models that severely over-predict the heat transfer in the rib-roughened case also give too large skin friction. The HL-model with a similar large overestimation of the heat transfer, however under-predicts C_f. The models that under-predict Nu (WHR, WLR) also gives low values of skin friction in the backward-facing step case. The RS-model would also follow this identity if it was not for the erroneous behaviour around the rib, which raises the average heat transfer.

C Transformations

C.1 Standard $k-\varepsilon$ model $\Rightarrow$ ω-equation

Following Wilcox, the specific dissipation rate of turbulent kinetic energy, ω, is defined as

$$\omega \equiv \frac{\varepsilon}{C_k k} \tag{120}$$

with $C_k = \beta^* = 0.09$. The ω-equation is now constructed from the k- and ε-equations through dimensional reasoning, and the above definition as:

$$\frac{D\omega}{Dt} = \frac{D}{Dt}\left(\frac{\varepsilon}{C_k k}\right) = \frac{1}{C_k k}\frac{D\varepsilon}{Dt} - \frac{\omega}{k}\frac{Dk}{Dt} \tag{121}$$

Inserting the exact equations for k, and ε, yields:

$$\begin{aligned}\frac{D\omega}{Dt} = &\underbrace{\left[\frac{1}{C_k k}P_\varepsilon - \frac{\omega}{k}P_k\right]}_{\text{Production, } P_\omega} - \underbrace{\left[\frac{1}{C_k k}\Phi_\varepsilon - \frac{\omega}{k}\varepsilon\right]}_{\text{Destruction, } \Phi_\omega} + \\ &+ \underbrace{\left[\frac{1}{C_k k}\Pi_\varepsilon - \frac{\omega}{k}\Pi_k\right]}_{\text{Pressure diffusion, } \Pi_\omega} + \underbrace{\left[\frac{1}{C_k k}D_\varepsilon^T - \frac{\omega}{k}D_k^T\right]}_{\text{Turbulent diffusion, } D_\omega^T} \\ &+ \underbrace{\left[\frac{1}{C_k k}\nu\frac{\partial^2\varepsilon}{\partial x_j^2} + \frac{\omega}{k}\nu\frac{\partial^2 k}{\partial x_j^2}\right]}_{\text{Viscous diffusion, } D_\omega^\nu}\end{aligned} \tag{122}$$

When the standard $k-\varepsilon$ model is used as the transformation basis, the different term in the resulting ω-equation becomes:

C.1.1 Production term

$$\begin{aligned}P_\omega &= \frac{1}{C_k k}P_\varepsilon - \frac{\omega}{k}P_k = \frac{1}{C_k k}C_{\varepsilon 1}\frac{\varepsilon}{k}P_k - \frac{\omega}{k}P_k = \\ &= (C_{\varepsilon 1} - 1)\frac{\omega}{k}P_k\end{aligned} \tag{123}$$

C.1.2 Destruction term

$$\begin{aligned}\Phi_\omega &= \frac{1}{C_k k}\Phi_\varepsilon - \frac{\omega}{k}\Phi_k = \frac{1}{C_k k}C_{\varepsilon 2}\frac{\varepsilon^2}{k} - \frac{\omega}{k}\varepsilon = \\ &= (C_{\varepsilon 2} - 1)C_k k\omega^2\end{aligned} \tag{124}$$

C.1.3 Viscous diffusion term

$$\begin{aligned}D_\omega^\nu =&\frac{1}{C_k k}\nu\frac{\partial^2\varepsilon}{\partial x_j^2} - \frac{\omega}{k}\nu\frac{\partial^2 k}{\partial x_j^2} = \frac{\nu}{k}\frac{\partial^2\omega k}{\partial x_j^2} - \frac{\nu\omega}{k}\frac{\partial^2 k}{\partial x_j^2} = \\ =&\frac{\nu}{k}\left[\frac{\partial}{\partial x_j}\left(\omega\frac{\partial k}{\partial x_j} + k\frac{\partial\omega}{\partial x_j}\right)\right] - \nu\frac{\omega}{k}\frac{\partial^2 k}{\partial x_j^2} = \\ =&\frac{\nu}{k}\left[\frac{\partial\omega}{\partial x_j}\frac{\partial k}{\partial x_j} + \omega\frac{\partial^2 k}{\partial x_j^2} + \frac{\partial k}{\partial x_j}\frac{\partial\omega}{\partial x_j} + k\frac{\partial^2\omega}{\partial x_j^2}\right] - \\ &- \nu\frac{\omega}{k}\frac{\partial^2 k}{\partial x_j^2} = \\ =&\frac{2\nu}{k}\frac{\partial\omega}{\partial x_j}\frac{\partial k}{\partial x_j} + \nu\frac{\omega}{k}\frac{\partial^2 k}{\partial x_j^2} + \nu\frac{\partial^2\omega}{\partial x_j^2} - \nu\frac{\omega}{k}\frac{\partial^2 k}{\partial x_j^2} = \\ =&\frac{2\nu}{k}\frac{\partial\omega}{\partial x_j}\frac{\partial k}{\partial x_j} + \nu\frac{\partial^2\omega}{\partial x_j^2} = \\ =&\frac{2\nu}{k}\frac{\partial\omega}{\partial x_j}\frac{\partial k}{\partial x_j} + \frac{\partial}{\partial x_j}\left(\nu\frac{\partial\omega}{\partial x_j}\right)\end{aligned} \tag{125}$$

C.1.4 Turbulent diffusion term

$$\begin{aligned}D_\omega^T &= \frac{1}{C_k k}\frac{\partial}{\partial x_j}\left(\frac{\nu_t}{\sigma_\varepsilon}\frac{\partial\varepsilon}{\partial x_j}\right) - \frac{\omega}{k}\frac{\partial}{\partial x_j}\left(\frac{\nu_t}{\sigma_k}\frac{\partial k}{\partial x_j}\right) = \\ &= \frac{1}{k}\frac{\partial}{\partial x_j}\left(\frac{\nu_t}{\sigma_\varepsilon}\frac{\partial\omega k}{\partial x_j}\right) - \frac{\omega}{k}\frac{\partial}{\partial x_j}\left(\frac{\nu_t}{\sigma_k}\frac{\partial k}{\partial x_j}\right) =\end{aligned} \tag{126}$$

Assuming constant Schmidt numbers:

$$\begin{aligned}=&\frac{1}{k\sigma_\varepsilon}\frac{\partial}{\partial x_j}\left[\nu_t\left(\omega\frac{\partial k}{\partial x_j} + k\frac{\partial\omega}{\partial x_j}\right)\right] - \frac{\omega}{k\sigma_k}\frac{\partial}{\partial x_j}\left(\nu_t\frac{\partial k}{\partial x_j}\right) \\ =&\frac{1}{k\sigma_\varepsilon}\left(\nu_t\frac{\partial\omega}{\partial x_j}\frac{\partial k}{\partial x_j} + \omega\frac{\partial\nu_t}{\partial x_j}\frac{\partial k}{\partial x_j} + \nu_t\omega\frac{\partial^2 k}{\partial x_j^2}\right) + \\ &+ \frac{1}{k\sigma_\varepsilon}\left(\nu_t\frac{\partial k}{\partial x_j}\frac{\partial\omega}{\partial x_j} + k\frac{\partial\nu_t}{\partial x_j}\frac{\partial\omega}{\partial x_j} + \nu_t k\frac{\partial^2\omega}{\partial x_j^2}\right) - \\ &- \frac{\omega}{k\sigma_k}\left(\frac{\partial\nu_t}{\partial x_j}\frac{\partial k}{\partial x_j} + \nu_t\frac{\partial^2 k}{\partial x_j^2}\right) = \\ =&\frac{2\nu_t}{\sigma_\varepsilon k}\frac{\partial k}{\partial x_j}\frac{\partial\omega}{\partial x_j} + \frac{\omega}{k}\left(\frac{\nu_t}{\sigma_\varepsilon} - \frac{\nu_t}{\sigma_k}\right)\frac{\partial^2 k}{\partial x_j^2} + \\ &+ \frac{\omega}{k}\left(\frac{1}{\sigma_\varepsilon} - \frac{1}{\sigma_k}\right)\frac{\partial\nu_t}{\partial x_j}\frac{\partial k}{\partial x_j} + \frac{1}{\sigma_\varepsilon}\frac{\partial\nu_t}{\partial x_j}\frac{\partial\omega}{\partial x_j} + \frac{\nu_t}{\sigma_\varepsilon}\frac{\partial^2\omega}{\partial x_j^2}\end{aligned} \tag{127}$$

The standard turbulent diffusion term did not appear in the derivation above, however it is there, which can be shown through contracting the two right most terms as:

$$\frac{1}{\sigma_\varepsilon}\frac{\partial\nu_t}{\partial x_j}\frac{\partial\omega}{\partial x_j} + \frac{\nu_t}{\sigma_\varepsilon}\frac{\partial^2\omega}{\partial x_j^2} = \frac{\partial}{\partial x_j}\left(\frac{\nu_t}{\sigma_\varepsilon}\frac{\partial\omega}{\partial x_j}\right) \tag{128}$$

Note that it is necessary to assume a constant σ_ε to make such an operation valid. Furthermore the term with the gradient of turbulent viscosity in Eq. 127 is expanded

using its definition:

$$\begin{aligned}\frac{\omega}{k}\left(\frac{1}{\sigma_\varepsilon}-\frac{1}{\sigma_k}\right)\frac{\partial \nu_t}{\partial x_j}\frac{\partial k}{\partial x_j}=&\left\{\nu_t=C_\mu\frac{k}{\omega}\right\}=\\ =&C_\mu\frac{\omega}{k}\left(\frac{1}{\sigma_\varepsilon}-\frac{1}{\sigma_k}\right)\frac{\partial}{\partial x_j}\left(\frac{k}{\omega}\right)\frac{\partial k}{\partial x_j}=\\ =&C_\mu\frac{\omega}{k}\left(\frac{1}{\sigma_\varepsilon}-\frac{1}{\sigma_k}\right)\left(\frac{1}{\omega}\frac{\partial k}{\partial x_j}-\frac{k}{\omega^2}\frac{\partial \omega}{\partial x_j}\right)\frac{\partial k}{\partial x_j}=\\ =&\frac{\nu_t\omega}{k^2}\left(\frac{1}{\sigma_\varepsilon}-\frac{1}{\sigma_k}\right)\left(\frac{\partial k}{\partial x_j}\right)^2-\\ &-\frac{\nu_t}{k}\left(\frac{1}{\sigma_\varepsilon}-\frac{1}{\sigma_k}\right)\frac{\partial k}{\partial x_j}\frac{\partial \omega}{\partial x_j}\end{aligned} \tag{129}$$

Note that no damping function was used for ν_t as these are normally dependent on the wall-distance. Thus the turbulent diffusion term in the ω-equation is:

$$\begin{aligned}D_\omega^T=&\frac{\nu_t}{k}\left(\frac{1}{\sigma_\varepsilon}+\frac{1}{\sigma_k}\right)\frac{\partial k}{\partial x_j}\frac{\partial \omega}{\partial x_j}+\frac{\omega}{k}\left(\frac{\nu_t}{\sigma_\varepsilon}-\frac{\nu_t}{\sigma_k}\right)\frac{\partial^2 k}{\partial x_j^2}+\\ &+\frac{\omega}{k^2}\left(\frac{\nu_t}{\sigma_\varepsilon}-\frac{\nu_t}{\sigma_k}\right)\left(\frac{\partial k}{\partial x_j}\right)^2+\frac{\partial}{\partial x_j}\left(\frac{\nu_t}{\sigma_\varepsilon}\frac{\partial \omega}{\partial x_j}\right)\end{aligned} \tag{130}$$

C.1.5 Total

The ω-equation now becomes:

$$\begin{aligned}\frac{D\omega}{Dt}=&\left(C_{\varepsilon 1}-1\right)\frac{\omega}{k}\nu_t\left(\frac{\partial U_i}{\partial x_j}+\frac{\partial U_i}{\partial x_j}\right)\frac{\partial U_i}{\partial x_j}-\\ &-\left(C_{\varepsilon 2}-1\right)C_k\omega^2+\frac{1}{k}\left(2\nu+\frac{\nu_t}{\sigma_\varepsilon}+\frac{\nu_t}{\sigma_k}\right)\frac{\partial k}{\partial x_j}\frac{\partial \omega}{\partial x_j}\\ &+\frac{\omega}{k}\left(\frac{\nu_t}{\sigma_\varepsilon}-\frac{\nu_t}{\sigma_k}\right)\frac{\partial^2 k}{\partial x_j^2}+\frac{\omega}{k^2}\left(\frac{\nu_t}{\sigma_\varepsilon}-\frac{\nu_t}{\sigma_k}\right)\left(\frac{\partial k}{\partial x_j}\right)^2\\ &+\frac{\partial}{\partial x_j}\left[\left(\nu+\frac{\nu_t}{\sigma_\varepsilon}\right)\frac{\partial \omega}{\partial x_j}\right]\end{aligned} \tag{131}$$

C.2 $k-\omega$ model (with Cross-diffusion Term) $\Rightarrow$ ε-equation

The ε-equation could be constructed through the same method as for the ω-equation. Using a $k-\omega$ model the ε-equation is:

$$\frac{D\varepsilon}{Dt}=\frac{D}{Dt}\left(C_k\omega k\right)=C_k k\frac{D\omega}{Dt}+C_k\omega\frac{Dk}{Dt} \tag{132}$$

with the different terms as:

C.2.1 Production term

$$\begin{aligned}P_\varepsilon=&C_k\left(\omega P_k+kP_\omega\right)=C_k\left(\frac{\varepsilon}{C_k k}P_k+kC_{\omega 1}\frac{\omega}{k}P_k\right)=\\ =&\left(C_{\omega 1}+1\right)\frac{\varepsilon}{k}P_k\end{aligned} \tag{133}$$

C.2.2 Destruction term

$$\begin{aligned}\Phi_\varepsilon=&C_k\left(\omega\Phi_k+k\Phi_\omega\right)=C_k\left(\omega C_k k\omega+kC_{\omega 2}\omega^2\right)=\\ =&\left(1+\frac{C_{\omega 2}}{C_k}\right)C_k^2k\omega^2=\left(1+\frac{C_{\omega 2}}{C_k}\right)\frac{\varepsilon^2}{k}\end{aligned} \tag{134}$$

C.2.3 Viscous diffusion term

$$\begin{aligned}D_\varepsilon^\nu=&C_k\left(\omega\nu\frac{\partial^2 k}{\partial x_j^2}+k\nu\frac{\partial^2 \omega}{\partial x_j^2}\right)=\\ =&\nu\frac{\varepsilon}{k}\frac{\partial^2 k}{\partial x_j^2}+k\nu\frac{\partial^2}{\partial x_j^2}\left(\frac{\varepsilon}{k}\right)=\\ =&\nu\frac{\varepsilon}{k}\frac{\partial^2 k}{\partial x_j^2}+k\nu\left[\frac{\partial}{\partial x_j}\left(\frac{1}{k}\frac{\partial \varepsilon}{\partial x_j}-\frac{\varepsilon}{k^2}\frac{\partial k}{\partial x_j}\right)\right]=\\ =&\nu\frac{\varepsilon}{k}\frac{\partial^2 k}{\partial x_j^2}+k\nu\times\left[-\frac{1}{k^2}\frac{\partial k}{\partial x_j}\frac{\partial \varepsilon}{\partial x_j}+\right.\\ &\left.+\frac{1}{k}\frac{\partial^2 \varepsilon}{\partial x_j^2}-\frac{\partial}{\partial x_j}\left(\frac{\varepsilon}{k^2}\right)\frac{\partial k}{\partial x_j}-\frac{\varepsilon}{k^2}\frac{\partial^2 k}{\partial x_j^2}\right]=\\ =&\nu\frac{\varepsilon}{k}\frac{\partial^2 k}{\partial x_j^2}-\frac{\nu}{k}\frac{\partial k}{\partial x_j}\frac{\partial \varepsilon}{\partial x_j}+\nu\frac{\partial^2 \varepsilon}{\partial x_j^2}-\\ &-k\nu\left[\frac{1}{k^2}\frac{\partial \varepsilon}{\partial x_j}\frac{\partial k}{\partial x_j}-\frac{2\varepsilon}{k^3}\left(\frac{\partial k}{\partial x_j}\right)^2\right]-\nu\frac{\varepsilon}{k}\frac{\partial^2 k}{\partial x_j^2}=\\ =&-\frac{2\nu}{k}\frac{\partial k}{\partial x_j}\frac{\partial \varepsilon}{\partial x_j}+\frac{2\nu\varepsilon}{k^2}\left(\frac{\partial k}{\partial x_j}\right)^2+\nu\frac{\partial^2 \varepsilon}{\partial x_j^2}=\\ =&-\frac{2\nu}{k}\frac{\partial k}{\partial x_j}\frac{\partial \varepsilon}{\partial x_j}+\frac{2\nu\varepsilon}{k^2}\left(\frac{\partial k}{\partial x_j}\right)^2+\frac{\partial}{\partial x_j}\left(\nu\frac{\partial \varepsilon}{\partial x_j}\right)\end{aligned} \tag{135}$$

C.2.4 Turbulent diffusion term

$$\begin{aligned}D_\varepsilon^T=&C_k\left[\omega\frac{\partial}{\partial x_j}\left(\frac{\nu_t}{\sigma_k}\frac{\partial k}{\partial x_j}\right)+k\frac{\partial}{\partial x_j}\left(\frac{\nu_t}{\sigma_\omega}\frac{\partial \omega}{\partial x_j}\right)\right]=\\ =&C_k\left[\frac{\varepsilon}{C_k k}\frac{\partial}{\partial x_j}\left(\frac{\nu_t}{\sigma_k}\frac{\partial k}{\partial x_j}\right)+\right.\\ &\left.+k\frac{\partial}{\partial x_j}\left(\frac{\nu_t}{\sigma_\omega}\frac{\partial}{\partial x_j}\left(\frac{\varepsilon}{C_k k}\right)\right)\right]\end{aligned} \tag{136}$$

Here again it is necessary to assume constant Schmidt numbers:

$$
\begin{aligned}
=&\frac{\varepsilon}{\sigma_k k}\left(\frac{\partial \nu_t}{\partial x_j}\frac{\partial k}{\partial x_j}+\nu_t\frac{\partial^2 k}{\partial x_j^2}\right)+\\
&+\frac{k}{\sigma_\omega}\frac{\partial}{\partial x_j}\left[\nu_t\left(\frac{1}{k}\frac{\partial \varepsilon}{\partial x_j}-\frac{\varepsilon}{k^2}\frac{\partial k}{\partial x_j}\right)\right]=\\
=&\frac{\varepsilon}{\sigma_k k}\left(\frac{\partial \nu_t}{\partial x_j}\frac{\partial k}{\partial x_j}+\nu_t\frac{\partial^2 k}{\partial x_j^2}\right)+\\
&+\frac{k}{\sigma_\omega}\left(\frac{1}{k}\frac{\partial \nu_t}{\partial x_j}\frac{\partial \varepsilon}{\partial x_j}-\frac{\nu_t}{k^2}\frac{\partial k}{\partial x_j}\frac{\partial \varepsilon}{\partial x_j}+\frac{\nu_t}{k}\frac{\partial^2 \varepsilon}{\partial x_j^2}\right)+\\
&+\frac{k}{\sigma_\omega}\left(-\frac{\varepsilon}{k^2}\frac{\partial \nu_t}{\partial x_j}\frac{\partial k}{\partial x_j}-\frac{\nu_t}{k^2}\frac{\partial \varepsilon}{\partial x_j}\frac{\partial k}{\partial x_j}\right)+\\
&+\frac{k}{\sigma_\omega}\left(\frac{2\varepsilon\nu_t}{k^3}\frac{\partial k}{\partial x_j}\frac{\partial k}{\partial x_j}-\frac{\varepsilon\nu_t}{k^2}\frac{\partial^2 k}{\partial x_j^2}\right)=\\
=&-\frac{2\nu_t}{\sigma_\omega k}\frac{\partial k}{\partial x_j}\frac{\partial \varepsilon}{\partial x_j}+\frac{\varepsilon}{k}\left(\frac{\nu_t}{\sigma_k}-\frac{\nu_t}{\sigma_\omega}\right)\frac{\partial^2 k}{\partial x_j^2}+\\
&+\frac{\varepsilon}{k}\left(\frac{1}{\sigma_k}-\frac{1}{\sigma_\omega}\right)\frac{\partial \nu_t}{\partial x_j}\frac{\partial k}{\partial x_j}+\frac{2\varepsilon\nu_t}{\sigma_\omega k^2}\left(\frac{\partial k}{\partial x_j}\right)^2+\\
&+\frac{1}{\sigma_\omega}\frac{\partial \nu_t}{\partial x_j}\frac{\partial \varepsilon}{\partial x_j}+\frac{\nu_t}{\sigma_\omega}\frac{\partial^2 \varepsilon}{\partial x_j^2}
\end{aligned}
\tag{137}
$$

Two terms are re-arranged:

$$
\frac{\nu_t}{\sigma_\omega}\frac{\partial^2 \varepsilon}{\partial x_j^2}+\frac{1}{\sigma_\omega}\frac{\partial \nu_t}{\partial x_j}\frac{\partial \varepsilon}{\partial x_j}=\frac{\partial}{\partial x_j}\left(\frac{\nu_t}{\sigma_\omega}\frac{\partial \varepsilon}{\partial x_j}\right)
\tag{138}
$$

and the term with the gradient of turbulent viscosity is expanded assuming a HRN-model for ν_t:

$$
\begin{aligned}
&\frac{\varepsilon}{k}\left(\frac{1}{\sigma_k}-\frac{1}{\sigma_\omega}\right)\frac{\partial \nu_t}{\partial x_j}\frac{\partial k}{\partial x_j}=\left\{\nu_t=C_\mu\frac{k^2}{\varepsilon}\right\}=\\
=&C_\mu\frac{\varepsilon}{k}\left(\frac{1}{\sigma_k}-\frac{1}{\sigma_\omega}\right)\frac{\partial}{\partial x_j}\left(\frac{k^2}{\varepsilon}\right)\frac{\partial k}{\partial x_j}=\\
=&C_\mu\frac{\varepsilon}{k}\left(\frac{1}{\sigma_k}-\frac{1}{\sigma_\omega}\right)\left(\frac{2k}{\varepsilon}\frac{\partial k}{\partial x_j}-\frac{k^2}{\varepsilon^2}\frac{\partial \varepsilon}{\partial x_j}\right)\frac{\partial k}{\partial x_j}=\\
=&\frac{\nu_t\varepsilon}{k^2}\left(\frac{1}{\sigma_k}-\frac{1}{\sigma_\omega}\right)\left(\frac{\partial k}{\partial x_j}\right)^2-\\
&-\frac{\nu_t}{k}\left(\frac{1}{\sigma_k}-\frac{1}{\sigma_\omega}\right)\frac{\partial k}{\partial x_j}\frac{\partial \varepsilon}{\partial x_j}
\end{aligned}
\tag{139}
$$

and hence the turbulent diffusion term becomes:

$$
\begin{aligned}
D_\varepsilon^T=&-\frac{\nu_t}{k}\left(\frac{1}{\sigma_\omega}+\frac{1}{\sigma_k}\right)\frac{\partial k}{\partial x_j}\frac{\partial \varepsilon}{\partial x_j}+\frac{\varepsilon}{k}\left(\frac{\nu_t}{\sigma_k}-\frac{\nu_t}{\sigma_\omega}\right)\frac{\partial^2 k}{\partial x_j^2}\\
&+\frac{\varepsilon}{k^2}\left(\frac{\nu_t}{\sigma_k}+\frac{\nu_t}{\sigma_\omega}\right)\left(\frac{\partial k}{\partial x_j}\right)^2+\frac{\partial}{\partial x_j}\left(\frac{\nu_t}{\sigma_\omega}\frac{\partial \varepsilon}{\partial x_j}\right)
\end{aligned}
\tag{140}
$$

C.2.5 Cross-diffusion term

Now dealing with the cross-diffusion term from the ω-equation:

$$
\begin{aligned}
D_\varepsilon^{CD}=C_k k D_\omega^{CD}&=C_k k\left(C_1\frac{\nu}{k}+C_2\frac{\nu_t}{k}\right)\frac{\partial k}{\partial x_j}\frac{\partial \omega}{\partial x_j}=\\
&=C_k\left(C_1\nu+C_2\nu_t\right)\frac{\partial k}{\partial x_j}\frac{\partial}{\partial x_j}\left(\frac{\varepsilon}{C_k k}\right)=\\
&=\left(C_1\nu+C_2\nu_t\right)\frac{\partial k}{\partial x_j}\left(\frac{1}{k}\frac{\partial \varepsilon}{\partial x_j}-\frac{\varepsilon}{k^2}\frac{\partial k}{\partial x_j}\right)=\\
&=\left(C_1\frac{\nu}{k}+C_2\frac{\nu_t}{k}\right)\left[\frac{\partial k}{\partial x_j}\frac{\partial \varepsilon}{\partial x_j}-\frac{\varepsilon}{k}\left(\frac{\partial k}{\partial x_j}\right)^2\right]
\end{aligned}
\tag{141}
$$

C.2.6 Total

Adding it all up, the ε-equation from the cross-diffusion modelled $k-\omega$ becomes:

$$
\begin{aligned}
\frac{D\varepsilon}{Dt}=&\left(1+C_{\omega 1}\right)\frac{\varepsilon}{k}\nu_t\left(\frac{\partial U_i}{\partial x_j}+\frac{\partial U_i}{\partial x_j}\right)\frac{\partial U_i}{\partial x_j}-\\
&-\left(1+\frac{C_{\omega 2}}{C_k}\right)\frac{\varepsilon^2}{k}-\\
&-\left[\left(2-C_1\right)\frac{\nu}{k}+\left(\frac{1}{\sigma_\omega}+\frac{1}{\sigma_k}-C_2\right)\frac{\nu_t}{k}\right]\frac{\partial k}{\partial x_j}\frac{\partial \varepsilon}{\partial x_j}\\
&+\frac{\varepsilon}{k}\left[\left(2-C_1\right)\frac{\nu}{k}+\left(\frac{1}{\sigma_\omega}+\frac{1}{\sigma_k}-C_2\right)\frac{\nu_t}{k}\right]\left(\frac{\partial k}{\partial x_j}\right)^2\\
&+\frac{\varepsilon}{k}\left(\frac{\nu_t}{\sigma_k}-\frac{\nu_t}{\sigma_\omega}\right)\frac{\partial^2 k}{\partial x_j^2}+\frac{\partial}{\partial x_j}\left[\left(\nu+\frac{\nu_t}{\sigma_\omega}\right)\frac{\partial \varepsilon}{\partial x_j}\right]
\end{aligned}
\tag{142}
$$

For a model without cross-diffusion term (WHR,WLR) C_1 (the viscous term) and C_2 (the turbulent term) is set to zero. For the two cross-diffusion $k-\omega$ models treated here, the coefficients is $C_1=0$, $C_2=0.75$ (PDH) and $C_1=C_2=1.1$ (BPD).

D Secondary equation

A comparison between the used secondary quantities could be made by solving a transport equation for the variable, $\phi = k^m/l^n$. In the logarithmic region, the convective term and the viscous diffusion could be neglected, hence the transport equation for the secondary quantity is reduced to "production – dissipation equal to the diffusion" as:

$$\underbrace{C_{\phi 1}\nu_t \frac{k^{m-1}}{l^n}\left(\frac{\partial U}{\partial y}\right)^2}_{\text{Production}} - \underbrace{C_{\phi 2}\frac{k^{m+1/2}}{l^{n+1}}}_{\text{Destruction}} = \underbrace{\frac{\partial}{\partial y}\left[\frac{\nu_t}{\sigma_\phi}\frac{\partial (k^m/l^n)}{\partial y}\right]}_{\text{Diffusion}} \tag{143}$$

where only gradients normal to the wall are retained for simplicity. Furthermore in order to compare the secondary quantities, relations for the involved variable need to established. Here, similarly to Launder and Spalding [26] the law of the wall for the velocity, turbulent kinetic energy, turbulent length-scale, and the turbulent viscosity are used:

$$\begin{aligned} \frac{U}{U_\tau} &= \frac{1}{\kappa}\ln(y^+) + B \\ k &= \frac{U_\tau^2}{\sqrt{C_\mu}} \\ l &= \frac{\kappa y}{C_\mu^{3/4}} \\ \nu_t &= C_\mu \sqrt{k} l \end{aligned} \tag{144}$$

Using the above relations the production term can be simplified to:

$$C_{\phi 1}\nu_t \frac{k^{m-1}}{l^n}\left(\frac{\partial U}{\partial y}\right)^2 = C_{\phi 1} C_\mu \frac{k^{m-1/2}}{l^{n-1}}\left(\frac{U_\tau}{\kappa y}\right)^2 = C_{\phi 1}\frac{k^{m+1/2}}{l^{n+1}} \tag{145}$$

The same approach is used for the diffusion term:

$$\frac{\partial}{\partial y}\left[\frac{\nu_t}{\sigma_\phi}\frac{\partial (k^m/l^n)}{\partial y}\right] = \frac{\partial}{\partial y}\left[\frac{\nu_t}{\sigma_\phi}\left(\frac{l^n \partial k^m/\partial y - k^m \partial l^n/\partial y}{l^{2n}}\right)\right] \tag{146}$$

Assuming that the law of the wall holds, the derivate of k is zero, and hence:

$$= -\frac{\partial}{\partial y}\left(\frac{\nu_t}{\sigma_\phi}\frac{k^m}{l^{2n}}\frac{\partial l^n}{\partial y}\right) \tag{147}$$

Inserting the relation for the turbulent viscosity with a constant Schmidt number gives:

$$= -\frac{C_\mu}{\sigma_\phi}\frac{\partial}{\partial y}\left(\frac{k^{m+1/2}}{l^{2n-1}}\frac{\partial l^n}{\partial y}\right) = -\frac{nC_\mu}{\sigma_\phi}\frac{\partial}{\partial y}\left(\frac{k^{m+1/2}}{l^n}\frac{\partial l}{\partial y}\right) \tag{148}$$

Continuing to expand the derivate gives:

$$\begin{aligned} &= -\frac{nC_\mu}{\sigma_\phi}\frac{1}{l^{2n}}\left(l^n\frac{\partial k^{m+1/2}}{\partial y} - k^{m+1/2}\frac{\partial l^n}{\partial y}\right)\frac{\partial l}{\partial y} - \\ &\quad -\frac{nC_\mu}{\sigma_\phi}\frac{k^{m+1/2}}{l^n}\frac{\partial^2 l}{\partial y^2} \end{aligned} \tag{149}$$

Assuming a linear variation of the turbulent length-scale the second derivate is zero, and with the derivate of k equals to zero, the diffusion term becomes:

$$= \frac{n^2 C_\mu}{\sigma_\phi}\frac{k^{m+1/2}}{l^{n+1}}\left(\frac{\partial l}{\partial y}\right)^2 = \frac{n^2\kappa^2}{\sqrt{C_\mu}\sigma_\phi}\frac{k^{m+1/2}}{l^{n+1}} \tag{150}$$

In summation the transport equation for the secondary quantity is:

$$\begin{aligned} &\frac{k^{m+1/2}}{l^{n+1}}\left(C_{\phi 1} + \frac{n^2\kappa^2}{\sqrt{C_\mu}\sigma_\phi}\right) = \frac{k^{m+1/2}}{l^{n+1}}C_{\phi 2} \qquad \Rightarrow \\ &\frac{\sqrt{C_\mu}}{\kappa^2}(C_{\phi 2} - C_{\phi 1}) = \frac{n^2}{\sigma_\phi} \end{aligned} \tag{151}$$

where n takes the value according to the used secondary variable. For the EVM-types referred to in this report the following values for n are obtained:

$$\begin{aligned} &k-\varepsilon:\ n = 1 \\ &k-\omega:\ n = 1 \\ &k-\tau:\ n = -1 \\ &k-l:\ n = -1 \end{aligned}$$

In conclusion all the studied two-equation models thus need to fulfill the following relation for the Schmidt number in the logarithmic region:

$$\sigma_\phi = \frac{\kappa^2}{\sqrt{C_\mu}(C_{\phi 2} - C_{\phi 1})} \tag{152}$$

Different values may however be applicable through the tuning of the coefficients, $C_{\phi 1}$ and $C_{\phi 2}$.